

ENGINEERED PRESENTATION OF NEURAL CELL ADHESION MOLECULES FOR DIRECTED

NEURAL AND NEURAL STEM CELL BEHAVIORS

By

JOCIE FATIMA CHERRY

A dissertation submitted to the

Graduate School-New Brunswick

Rutgers, The State University of New Jersey

and

The Graduate School of Biomedical Sciences

University of Medicine and Dentistry of New Jersey

in partial fulfillment of the requirements

for the degree of

Doctor of Philosophy

Graduate Program in Biomedical Engineering

written under the direction of

Prabhas V. Moghe, PhD

and approved by

New Brunswick, New Jersey

October 2013

ABSTRACT OF THE DISSERTATION

ENGINEERED PRESENTATION OF NEURAL CELL ADHESION MOLECULES FOR DIRECTED NEURAL AND NEURAL STEM CELL BEHAVIORS

By JOCIE FATIMA CHERRY

Dissertation Director:

Prabhas V. Moghe

Neurotraumatic injuries result in an irreplaceable cell loss and concomitant deficit in motor and sensory functions. Cell transplantation therapies could potentially address the deficit of neuronal tissues, but remain challenged by limited survival, organization, and integration of transplanted cells. Substrates designed to present specific neurotrophic cues, in precise configurations are candidates for maintaining cell differentiation *in vitro* and enhancing integration and survival of transplanted cells *in vivo*. The goal of this dissertation was to design biologically active interfaces based on key developmental neural cell adhesion molecules previously shown to promote neuritogenesis, neuronal differentiation, and survival of neural cells. Specifically, this thesis focuses on modulating the display of protein fragments derived from L1 cell adhesion molecule and N-cadherin and examining cellular responses.

We investigated the efficacy of L1-derived peptide sequences displayed via non-permissive human albumin nanoparticles, which elicited modest neuronal adhesion and neurite outgrowth of primary neurons. In contrast, substrate-bound L1-Fc chimera promoted enhanced neuronal responses. Following this result, we utilized protein A to maximize L1-Fc effectiveness and yield a systematically oriented, multivalent presentation compared to passive adsorption methods. Protein A-presented L1-Fc, displayed from polymeric substrates, greatly improved neurite outgrowth of spinal cord and cerebellar neurons and neuronal differentiation

of human embryonic stem cell-derived neural stem cells (hESC-NSCs), compared to L1-Fc presented from the cationic polymer, poly-D-lysine. Next, we sought to address limitations of L1 functionalized substrates, namely, inadequate L1-mediated cell adhesion and limited lineage restriction of hESC-NSCs. To this end, we investigated the effects of presenting N-cadherin-Fc and L1-Fc on differentiation, neurite outgrowth, and survival of hESC-NSCs. Low density N-cadherin substrates promoted greater neuronal differentiation and survival of hESC-NSCs. Enhanced neurite outgrowth and neuronal differentiation was observed in hESC-NSCs cultured on N-cadherin-/L1-Fc substrates, demonstrating the synergistic effect of these two fragments. Findings from this thesis support the paradigm of designing stem cell-bioactive materials by fine-tuning surface concentrations and microscale organization of ligands that regulate different stages of neural development. Such materials could be candidates for recapitulating the microenvironment in the context of biomimetic materials for neural developmental models as well as transplantation devices for neural tissue engineering.

ACKNOWLEDGEMENTS

Wow...the completion of my graduate school journey is FINALLY upon me and it is so surreal. I have had an immeasurable amount of support over the years, which has allowed this thesis to come to fruition. I would first like to thank my advisor, Dr. Prabhas V. Moghe, for your guidance and support, as well as for giving me the freedom to explore different research directions for my project. You taught me to be both pragmatic and systematic in my approach to science. Thank you for giving me the tools and confidence to reach my full potential as a scientist.

Dr. Moghe has always said that it takes a village to raise and develop a scientist and with that I would like to thank my “village”. It is with immense gratitude that I thank my co-advisor, Dr. Melitta Schachner. Thank you for your immeasurable input as well as the opportunity to conduct research at your laboratory in Hamburg. My experiences in Hamburg lead to the rebirth of my project. Thank you Dr. Gabriele Loers (Schachner Lab) for taking me under your wing while I was in Hamburg and providing an enriching experience for me. Thank you Dr. David I. Shreiber for your candid advice and for making it clear that your door was always open for me. I would also like to thank Dr. Martin Grumet for your advice about the possible directions for my project and considerations for moving this work forward for *in vivo* studies.

I owe my deepest gratitude to Dr. Evelyn S. Erenrich. You assisted me before my journey even began by granting me the opportunity and honor of becoming the inaugural Northeast Alliance Bridge fellow at Rutgers University. This thesis would not have become a reality had it not been for this wonderful opportunity and I am forever grateful. I extend many thanks to the BME staff (Larry, Linda, Robin, and Stratos) for your help and ears for various situations over the years.

To my lab mates, the “Mogheicans” past (Dr. Rebecca Moore, Dr. Nicole Plourde, Dr. Aaron Carlson, Jing Xu, Dr. Adam York, Dr. Craig Griffith) and present (Sebastián Vega, Joe Kim, Dr. Latrisha Petersen, Adriana Martin, Daniel Lewis, Margot Zevon, George Dorfman, Maria Qadri) as well as collaborating laboratories, thank you for your scientific and emotional support. We became a family and shared in each other’s failures and triumphs and I will truly remain grateful for the encouragement you all gave me along the way. I would especially like to thank Dr. Dominik Naczynski - Dr. Lavanya Peddada - Dr. Jeffery Barminko (the “peeps”), Dr. Melinda Kutzing, Lauren Lacagnino, and Dr. Maria Pia Rossi. I will always cherish the time we spent inside and outside of the BME building. We formed a friendship and a bond that will be everlasting. I am indebted to my previous student, Farah Benarba, for your dedication and enthusiasm about the work we did together. Thank you for voluntarily staying in the lab and playing an instrumental role in the progression of my work during my leave of absence.

Thank you, Dr. Shirley Masand, for extending your support and friendship to me. Dr. Aina Andrianarijaona, thank you for keeping me calm and sane during the last steps of this process.

Before my journey at Rutgers began, I had an incredible support system in place that always encouraged me to pursue my dreams. I want to thank Kellee Rouse. We have known each other since the 4th grade and have shared every possible life event together. Words cannot express how much I appreciate all that you have done with and for me throughout the years. I want to thank the Mulumba family (Kiilu, Shelleye, Mama and Daddy Mulumba, and Joan) for being my family away from home and taking me in as one of your own from day one. To my brother, Demond Cherry, thank you for all of your support and the much needed comedy that came along with it! My sister Nicole “Nikki” Bolden, I am forever grateful for you not only for being an amazing sister, but a wonderful friend. You were extremely encouraging in all that I ever pursued and you always tried to instill in me the confidence needed to achieve what I set out to do and to do it well. To my incredible mother, Doreen Williams, I know this might sound cliché, but the mold was broken with you. I could not have asked for a better role model in a woman or in a mother. You have a sense of confidence, balance, and a way with people that I still aspire to have. If I can be half of the woman, the person, and the mother that you are, I will be just fine. Words

cannot accurately or truly express how much I appreciate all that you have done and been for me.

Finally, I want to thank my husband Iya and my daughter Suraiya. Iya, you have been by my side for the majority of this journey and I thank you. I thank you for your tough love, your encouragement, and for you always wanting the best for me. You have been an incredible source of support. Suraiya, thank you for the motivation through your cries, smiles, and laughter. The capacity my heart has to love was realized when you were placed into my arms.

DEDICATION

To my wonderful husband Iya and my sweet, sweet Suraiya – We did it! Thank you for the motivation, strength, and courage when I thought I had none. Thank you for your patience and encouragement through this journey. I share this dissertation with you as my accomplishments are your accomplishments.

TABLE OF CONTENTS

ABSTRACT OF THE DISSERTATION	ii
ACKNOWLEDGEMENTS.....	iv
DEDICATION	viii
TABLE OF CONTENTS.....	ix
LIST OF FIGURES	xii
CHAPTER 1: INTRODUCTION.....	1
1.1 Spinal Cord Injury	1
1.2 Stem Cells: A Source for Cell Replacement Therapy in Neural Tissue Engineering	3
1.2.1 Neural Stem Cells.....	4
1.2.2 Human Embryonic Stem Cell-Derived Neural Stem Cells.....	4
1.3 Biomaterial Scaffolds for Neural Tissue Engineering	6
1.4 Biofunctionalized Biomaterials for Engineered Neural Stem Cell Microenvironments.	7
1.5 Cell Adhesion Molecules.....	8
1.5.1 L1 Cell Adhesion Molecule.....	9
1.5.2 N-cadherin.....	11
1.6 Thesis Overview.....	12
1.7 References.....	14
CHAPTER 2: EFFECTS OF L1-PEPTIDE FUNCTIONALIZED ALBUMIN NANOPARTICLES ON ADHESION AND NEURITE OUTGROWTH OF PRIMARY MOTOR NEURONS, CEREBELLAR NEURONS, AND DORSAL ROOT GANGLION CELLS.	23
Abstract.....	23
2.1 Introduction.....	24
2.2 Materials and Methods.....	27
2.2.1 Synthesis of Albumin Nanoparticles.....	27
2.2.2 Albumin Nanoparticle Characterization	27
2.2.3 Fabrication of L1 Peptide Albumin Nanoparticles.....	28
2.2.4 Quantification of L1 peptide Loading Efficiency.....	29
2.2.5 L1 Peptide ELISA.....	30
2.2.6 Substrate Preparation for Cell Studies.....	31
2.2.7 Neuronal Cell Cultures.....	31
2.2.8 Cell Adhesion to Biofunctionalized ANP Substrates.	32
2.2.9 Neurite Outgrowth on Biofunctionalized Substrates.	33
2.3 Results.....	33
2.3.1 Morphology and Size of ANPs.....	33

2.3.2 L1 Peptide Conjugated to ANPs Maintains Functionality and Accessibility for Antibody Binding	34
2.3.3 L1p-ANP Effects on Adhesion and Neurite Outgrowth of Cerebellar and Motor Neurons.....	36
2.3.4 Dorsal Root Ganglion Explants Extend Neurites on L1p-ANP Substrates in the Presence of Serum.....	40
2.4 Discussion.....	41
2.5 References.....	44

CHAPTER 3: ORIENTED, MULTIMERIC BIOINTERFACES OF THE L1 CELL ADHESION MOLECULE: AN APPROACH TO ENHANCE NEURONAL AND NEURAL STEM CELL FUNCTION ON 2-D AND 3-D POLYMER SUBSTRATES..... 48

Abstract.....	48
3.1 Introduction.....	49
3.2 Materials and Methods.....	52
3.2.1 Biointerfaces on Polymer Thin Films.....	52
3.2.2 Verification of L1-Fc Functionality.....	52
3.2.3 Quantification of Protein Layer on Polymer Thin Films.....	53
3.2.4 AFM Analysis of Biointerfaces on Thin Films.....	54
3.2.5 Fibrous Polymer Scaffold Fabrication and Characterization.....	54
3.2.6 Primary Neuronal Cell cultures.....	55
3.2.7 Quantification of Neurite Outgrowth.....	56
3.2.8 Functional Blocking Assays of Cell Adhesion and Neurite Outgrowth.....	56
3.2.9 hESC-Derived Neural Progenitor Cell Culture and Differentiation.....	57
3.2.10 Immunocytochemistry of Neuronal Phenotypes.....	57
3.2.11 Statistical Analysis.....	58
3.3 Results.....	58
3.3.1 Protein A Coated Polymer Films Support Increased Surface Adsorption of L1-Fc.....	58
3.3.2 Spatial Distribution of L1-Fc when Presented on PDL and Protein A.....	60
3.3.3 Multimeric L1 Presentation Enhances Neurite Outgrowth of Cultured Neurons on 2-D Films.....	63
3.3.4 Multimeric L1 Presentation Enhances Neurite Outgrowth of Cultured Neurons in 3-D, Fibrous Substrates.....	64
3.3.5 Role of L1-L1 Homophilic Cell-Substrate Adhesion Underlying Neurite Outgrowth on Multimeric Films.....	66
3.3.6 Multimeric L1 Films Support RGD Peptide-Sensitive Integrin Mediated Cell Adhesion and Neurite Outgrowth.....	68
3.3.7 L1 Films Promote Neuronal Differentiation of Human Neural Progenitor Cells but Oriented Presentation is Not Necessary in 2D.....	69
3.3.8 Oriented, Multimeric L1 Presentation Triggers Enhanced Neuronal Differentiation of Human Progenitor Cells in 3-D Fibrous Scaffolds.....	72
3.4 Discussion.....	73
3.6 Acknowledgments.....	78
3.7 References.....	78

CHAPTER 4: N-CADHERIN AND L1 BIOMIMETIC SUBSTRATES MODULATE DIFFERENTIATION AND NEURITE EXTENSION OF HUMAN EMBRYONIC STEM CELL-DERIVED NEURAL STEM CELLS..... 83

Abstract..... 83

4.1 Introduction..... 85

4.2 Materials and Methods..... 89

4.2.1 Fabrication of Polymer Thin Films and Electrospun Scaffolds..... 90

4.2.2 Preparation of N-cadherin- and L1-Fc Substrates..... 90

4.2.3 Detection of Substrate Bound N-cadherin and L1-Fc..... 90

4.2.4 H9-NSC Neural Stem Cell Culture..... 91

4.2.5 Immunocytochemistry of H9-NSCs..... 92

4.2.6 Quantification of Neurite Outgrowth and Neuronal Differentiation..... 92

4.2.7 Antibody Blocking of Cellular N-cadherin..... 93

4.2.8 Fibroblast Growth Factor Receptor Inhibition Assay..... 93

4.2.9 Oxidative Stress Survival Assay..... 94

4.3 Results..... 94

4.3.1 N-cad-Fc and L1-Fc Functionalized 2-D Films.....

4.3.2 N-cad-/L1-Fc Substrates Promote H9-NSC Attachment..... 95

4.3.3 Surface N-cad-Fc Induces Differential Localization of Cellular N-cadherin..... 95

4.3.4 N-cad-Fc Combined with L1-Fc Influences Neuritogenesis and Neurite Outgrowth..... 98

4.3.5 Surface Presented N-cad-Fc Combined with L1-Fc Enhances Neuronal Differentiation..... 100

4.3.6 Interruption of Cell-Substrate N-cadherin Engagement Leads to Improved Neurite Outgrowth, But No Change in Neuronal Differentiation..... 103

4.3.7 Inhibition of Fibroblast Growth Factor Receptor Modulates Neuronal Differentiation..... 105

4.3.8 Combined Display of N-cadherin- and L1-Fc has Synergistic Outcomes in NSCs Cultured in Fibrous 3-D Scaffolds..... 107

4.3.9 Low N-cad-Fc Presenting 2-D Films and Scaffolds Promote H9-NSC Survival..... 109

4.4 Discussion..... 113

4.5 Summary and Conclusions..... 122

4.6 Supplemental Data..... 124

4.7 References..... 127

CHAPTER 5: DISSERTATION SUMMARY AND FUTURE DIRECTIONS..... 134

5.1 Dissertation Summary..... 134

5.2 Future Directions..... 136

5.2.1 Identifying the Molecular Basis of L1/N-cadherin Functionalized Substrates in Modulating NSC Behaviors..... 136

5.2.2 Improvement in Neuronal Yield and Alternative Cell Sources for Cell Transplantation..... 137

5.2.3 Alternative Approach for Tethering L1-Fc and N-cadherin-Fc..... 140

5.2.4 L1 and N-cadherin-Derived Peptide Biofunctionalized Substrates for Neural Tissue Engineering..... 141

5.2.5 Transplantation of H9-NSCs within L1-/N-cadherin-Fc Functionalized Scaffolds for <i>in vivo</i> Models.....	142
5.3 References.....	143

TABLE OF FIGURES

1.1 Schematic of L1 cell adhesion molecule.....	10
1.2 Illustration of N-cadherin	12
2.1 Schematic for covalent linkage of L1p to ANPs.....	29
2.2 Size and morphology of ANPs	35
2.3 L1p is functional following conjugation to ANPs	36
2.4 Morphology, adhesion, and neuritogenesis of cerebellar neurons in the presence of L1p-ANPs	38
2.5 Response of cerebellar neurons to soluble L1p-ANPs.....	39
2.6 Neurite extension of DRGs cultured on L1p-ANPs	41
3.1 Presentation of L1-Fc by protein A results in enhanced L1 adsorption and improved directed presentation of L1-Fc.....	60
3.3 Protein A presentation of L1-Fc enhances neurite outgrowth in spinal cord and cerebellar neurons	65
3.4 Protein A-presented L1-Fc increases neurite outgrowth in aligned, polymeric scaffolds	67
3.5 Anti-L1 antibody and cyclic RGD treatment reduces cell attachment and neurite outgrowth	70
3.6 L1-Fc supports neuronal differentiation and neuritogenesis of neural progenitor cells.....	72
3.7 L1-Fc supports neuronal differentiation and neuritogenesis of neural progenitor cells within aligned scaffolds	74
4.1 H9-NSC attachment and N-cadherin localization in response to N-cad-Fc 2-D Films.....	97
4.2 N-cad- and L1-Fc combined influence neuritogenesis and neurite outgrowth of H9-NSCs on 2-D substrates.....	100
4.3 Neuronal differentiation of neural stem cells in response to N-cadherin-Fc and L1-Fc presenting 2-D substrates.....	102
4.4 Interruption of N-cadherin interactions improves neurite outgrowth on 2-D substrates.....	104
4.5 Inhibition of FGFR improves neuronal differentiation of H9-NSCs when cultured on high N-cad-Fc 2-D films.....	106
4.6 N-cad-/L1-Fc presenting scaffolds affect neuritogenesis and neuronal differentiation	111
4.7 Low levels of N-cad-Fc promotes increased H9-NSC survival in the presence of hydrogen peroxide.....	112
4.8 Proposed model for N-cadherin and L1-mediated H9-NSC behaviors	119
4.S1 Co-localization of N-cadherin and β -catenin in H9-NSCs cultured on N-cad-Fc substrates.....	124
4.S2 Isotype control treatment of H9-NSCs for the N-cadherin antibody blocking studies	125

4.S3 MAP2 expression and morphology of H9-NSCs cultured on N-cad-Fc substrates after 2 weeks on 2-D films	126
4.S4 Ki67 expression of H9-NSCs in response to N-cad-Fc substrates.....	127

Chapter 1

Introduction

1.1. Spinal Cord Injury

Traumatic injury to the spinal cord or brain is highly prevalent, yet there is still a severe lack of effective treatments that have the ability to preserve or restore motor and cognitive functions. An estimated 11,000 Americans suffer from spinal cord injuries (SCI) and 1.5 million people sustain brain trauma^[1]. Medical treatment for these conditions is extremely costly, with SCI treatment estimated to be \$11 billion and brain trauma treatment estimated to be over \$56 billion^[1]. Available treatments do not stimulate neurogenesis, myelination, repair of damaged neurons, and guided axonal growth following injury within the CNS. Instead, clinical treatments seek to mitigate the severity of secondary damage or inflammation caused by macrophages and activated astrocytes, which leads to formation of the glial scar^[2]. For example, the steroid methylprednisolone administered systemically, at high doses, immediately following injury in order to attenuate the inflammatory response that occurs immediately following injury^[2]. While methylprednisolone modestly suppresses severe inflammation, administration within 8 hours of injury is required and it does not stimulate tissue regeneration or neurogenesis, myelination of axons, nor restore function of damaged neurons. Furthermore, the required high doses of methylprednisolone, due to systemic delivery, lead to adverse side effects^[3]. The lack of effective SCI treatments represents a significant gap in the field, and motivates extensive research into new approaches to treat traumatic CNS injuries.

The body's response to SCI is complex and consists of both acute and chronic phases. The primary response or acute phase of SCI involves the damage and death of

neurons, astrocytes, and oligodendrocytes, which leads to demyelinated axons. Traumatic spinal cord injuries resulting from crushed or severed axon processes rarely result in the regeneration of damaged structures and functional restoration, ultimately leading to permanent structural and functional impairment. One major barrier of CNS regeneration lies in neuronal death^[4] and the inability of projection neurons to reconnect with their targets due to demyelination, the lack of protective, guidance cues, and the presence of inhibitory factors^[5]. Following injury to the spinal cord, studies observed that severed axons do begin to sprout within six hours of injury after which growth cones develop at the nerve endings^[6]. However, the sprouts extend only a short distance before growth is aborted and the new sprouts are resorbed^[4]. Therefore, an environment that promotes survival of remaining neural tissue is necessary for recovery to occur.

The secondary response to SCI includes the inflammatory response and glial scar formation, which proceeds from several hours to several weeks following initial damage. The glial scar consists of macrophages or microglia, astrocytes, meningeal cells, as well as several inhibitory molecules and extracellular matrix molecules^[7]. The glial scar creates a physical barrier against axonal re-growth and results in an environment that limits tissue regeneration by blocking re-growth of severed axons to their target sites^[4,8], while inhibitory molecules pose a chemical barrier that prevents axonal regrowth and extension. In order for damaged or severed neurons to regenerate, a permissive environment that provides survival and guided growth promoting cues must be established.

Current research into new therapeutic interventions for SCI typically focus on several key goals: 1) replace neurons and glia lost during the acute injury phase, 2) neutralize axonal growth-inhibiting molecules, 3) promote regeneration of axons into and beyond the injury site, and 4) re-establish neuronal circuitry to restore functional connections^[9]. Extensive research is currently underway to address one or more of these

therapeutic targets and new approaches to SCI treatment have shown great promise^[10,11]. In particular, one area that has gained much attention is cell replacement therapy, particularly with the recent emergence of new sources of clinically relevant, human cell sources for transplantation. Due to cell loss and nerve tissue degeneration following SCI, cell replacement therapy represents a promising approach for SCI treatment, as well as treatment of traumatic brain injury and neurodegenerative diseases.

1.2. Stem Cells: A Source for Cell Replacement Therapy in Neural Tissue Engineering

Cell replacement therapy has become an area of great interest as a potential treatment for SCI and neurodegenerative diseases^[11-13]. Cell replacement therapy or cell transplantation involves replacing damaged tissue with an exogenous cell source to re-establish damaged neuronal circuitry and promote functional recovery^[14]. Stem cell biology advances have garnered considerable interest in regeneration-based treatment of CNS injuries, using stem cells. Cell transplantation therapy has been widely investigated as a therapeutic option for the treatment of SCI and other traumatic CNS injuries^[5,15-23]. Current research aims to design and develop treatments for SCI that the use of stem cells for cell transplantation therapy. Several cell types have been investigated as potential candidates for cell replacement therapy for treatment of SCI in animal models such as mesenchymal stem cells, olfactory ensheathing cells, Schwann cells, and neural stem cells^[24,25]. Each of these cell types has a specific functional purpose in mind, which can include replacement of neuronal cells to restore functional neuronal circuitry, replacement of glial cells to promote axonal regeneration and remyelination, or incorporation of cells that secrete anti-inflammatory or neurotrophic factors to promote cell survival and mediate the immune response to injury. Neural stem cells are especially promising due to their ability to

differentiate to multiple neural cell types while providing trophic support that can encourage endogenous cell survival^[14,26].

1.2.1. Neural Stem Cells

Neural stem cells (NSCs) are multipotent cells, which possess the ability to self-renew or differentiate into neurons, oligodendrocytes, and astrocytes^[27-29]. During CNS development, NSCs are present in many regions of the brain such as the hippocampus, cerebellum, ganglionic eminence, and the spinal cord^[28]. While adult primary NSCs are present within the adult brain^[30,31] and the central canal of the spinal cord^[32], including difficulty isolating these cells, scarcity, the propensity to differentiate into glial cells versus neurons, and cell senescence during long term culture^[33], prevent these cells from becoming a viable option for therapeutic use. Other stem cell sources have been explored for generating NSCs, such as fetal brain-derived NSCs^[34,35], human embryonic stem cells and human induced pluripotent stem^[36,37]. This thesis will focus on the use of NSCs derived from human embryonic stem cells due to their capacity for extensive expansion and differentiation to neural lineages.

1.2.2. Human Embryonic Stem Cell-Derived Neural Stem Cells

Derived from the inner cell mass of a pre-implantation blastocyst, human embryonic stem cells (hESCs) are represent a promising source for cell replacement therapies as they have the ability to self-renew, thus providing an unlimited cell source, and can give rise to most somatic cell lineages^[33,38-41]. Directed differentiation of hESCs towards the neural lineage or neural stem cells has been achieved by various protocols, including those that use soluble factors, artificial extracellular matrices, co-cultures, or a combination thereof^[37,42-50]. Moreover, several approaches have been used to direct hESCs towards specific types of neural cells such as neurons^[51], oligodendrocytes^[23], dopaminergic neurons^[52], motor

neurons^[53], and other neuronal subtypes^[54-56]. Directed neural differentiation is typically achieved by supplementing the media with growth factors and their antagonists. Neuroectodermal cells have been generated through Noggin supplementation^[57], while FGF2, FGF8, and sonic hedgehog (SHH) treatment yielded hESC-derived forebrain and midbrain neurons^[53,58], and oligodendrocytes have been produced by combining bFGF, epidermal growth factor (EGF), and retinoic acid treatment^[23]. Although protocols utilized to generate specific types of neural cells from hESCs are varied, they are also consistent in the sense that they rely on exposing cells to specific proteins, morphogens, and growth factors that mimic signals cells encounter during embryonic development and neuronal specification. Therefore, it would be advantageous to use molecules in engineering neurogenic microenvironments, inspired by their key roles in neural development for directed neural phenotypes.

Transplantation studies of NSCs for treatment of SCI have shown varying degrees of success. A recent, extensive review highlighted several preclinical studies where NSCs were transplanted into the injured spinal cord^[25]. In the studies where no improvement in functional behavior was observed, poor NSC survival^[59,60] and neuropathic pain, which may have been the result of significant glial differentiation, were observed^[61]. Poor engraftment following transplantation of NSCs into the injury site of spinal cord is a common observation^[62]. Additionally, the harsh microenvironment of the injury site is not amenable to neuronal differentiation of transplanted NSCs, as uncommitted transplanted cells tend to differentiate into glia^[61,63,64]. Researchers aim to improve the outcome of NSC transplantation into SCI lesions through neural tissue engineering and biomaterial approaches, which allow for better control of the local microenvironment of the transplanted cells^[12].

1.3. Biomaterial Scaffolds for Neural Tissue Engineering

During tissue repair, cells must receive the appropriate cues from the surrounding environment in order to function properly. Given that the natural cell environment is three-dimensional in geometry and with organized biological cues at the micro/nanoscale; implantable constructs must mimic these features for proper cellular functions. The importance of an appropriate scaffolding matrix for cell therapies is evidenced by the poor engraftment efficiency of direct cell seeding (in the absence of scaffolding/matrix) at the site of injury^[65]. Studies have demonstrated that less than 10% of cells engraft, following direct injection of stem cells into the injury site ^[62,66,67]. Poor engraftment efficiency might be caused by cell death due to the absence of an appropriate ECM or scaffold that provides adequate and proper physical interactions essential for survival and functional integration of transplanted NSCs^[65,68]. Biomaterial scaffolds represent a favorable approach for neural tissue engineering as they have the ability to simulate specific parameters found in the native microenvironment that support adhesion, proliferation, differentiation, and survival of NSCs *in vitro* and following *in vivo* transplantation^[68,69]. Fabricated from both natural and synthetic materials, a diverse array of scaffold configurations has been investigated for neural tissue engineering, including hydrogels, guidance conduits, and fibrous scaffolds ^[12,62,70-72]. The use of fibrous scaffolds as delivery vehicles for cell transplantation has gained considerable interest as fibrous scaffolds possess an architecture that closely mimics the native ECM^[70]. The work in this thesis focuses on fibrous scaffolds fabricated from synthetic polymers via electrospinning.

Electrospinning, a method used to fabricate 3-D scaffolds, allows for fine tuning of specific parameters in order to mimic cellular microenvironments found *in vivo*^[73]. Due to

the ability finely control fiber diameter, alignment, as well as inter-fiber spacing, electrospun scaffolds are capable of recapitulating local tissue environments, supporting newly transplanted and host cells, and maintaining endogenous architecture at the site of injury^[70,73]. Scaffolds that result from electrospinning can result in fibers that are on the nano-scale (tens of nanometers in size), or micro-sized fibers that are few microns in diameter^[74], resulting in structures similar to that of endogenous ECM^[70,73,75]. In designing three-dimensional (3-D) scaffolds, the fiber size, fiber orientation, and porosity play a crucial role in scaffold function for cell-cell interactions and cell-ECM interactions. Electrospun fibrous scaffolds fabricated from natural and synthetic polymers have been investigated for neural tissue engineering^[12,62,70,72,76,77]. Synthetic polymers are commonly used because they have better mechanical properties, are more consistent, and they afford the ease of tuning various parameters compared to natural polymers^[71], but they usually lack bioactive cues and therefore require biofunctionalization^[12,71].

1.4. Biofunctionalized Biomaterials for Engineered Neural Stem Cell Microenvironments

Biomaterials offer a support structure and the ability to design microenvironments, *in vitro*, that mimic those found *in vivo*. Engineering microenvironments for directing neural stem cell behavior requires the modification of materials with specific biomolecules, as many synthetic materials do not provided appropriate biological cues. Several approaches have been investigated for the presentation of biomolecules for neural tissue engineering applications including physical adsorption, covalent linking, and blending^[78].

The manner in which a biomolecule, whether a protein fragment, peptide, or growth factor is presented from the biomaterial surface greatly influences the efficacy of the biomolecule. For example, laminin was covalently linked or adsorbed onto the surface of

electrospun PLLA scaffolds, or mixed into the polymer solution prior to electrospinning, and PC12 cells were cultured on these substrates^[79]. Scaffolds in which laminin electrospun along with PLLA promoted longer neurite lengths compared to surface immobilized or adsorbed laminin^[79]. The presentation strategy growth of factors has also been shown to modulate the bioactivity of tethered or immobilized growth factors. Immobilized BDNF^[80], EGF^[81], GDNF^[82] promoted enhanced neuronal differentiation and neurite outgrowth compared to the soluble form. Additionally, immobilized EGF activated a different signaling pathway compared to soluble EGF^[81], further highlighting the role of surface biofunctionalization of materials for neural tissue engineering. Immobilizing bioactive molecules to biomaterials is advantageous, as immobilization can not only sustain the long-term stability of the bioactive cues, but also render higher local concentrations compared to soluble administration and promote multivalency^[83]. Numerous biological molecules have been investigated for their ability to elicit desired cellular responses for neural tissue engineering such as neurotrophins^[84,85], proteins or protein-derived fragments found in the native ECM such as laminin, collagen, and fibronectin^[76,86], and ECM protein-derived peptides^[87,88]. Neural cell adhesion molecules also represent promising candidates for the design of biomaterials for neural tissue engineering applications. Neural cell adhesion molecules are expressed throughout CNS development as well as the adult nervous system and are critical to the normal function of the central nervous system. This thesis research focuses on two major classes of cell adhesion molecules. As such, the biology and surface functionalization of cell adhesion molecules is reviewed further next.

1.5. Cell Adhesion Molecules

Cell adhesion molecules are cell surface proteins that mediate cell-cell interactions as well as cell-ECM interactions^[89]. They are composed of an extracellular domain that

binds in a homophilic manner or heterophilic manner with other cell adhesion proteins or with the ECM, a transmembrane region, and an intracellular domain, which mediates binding between the cell adhesion molecule and proteins of the cytoskeleton^[89]. There are four major classes of cell adhesion molecules such as selectins, integrins, cell adhesion molecules from the immunoglobulin superfamily, and cadherins, which are all present during different stages of neural development^[90]. The work performed for this dissertation was focused on engineered presentation of two key neural proteins involved in nervous system development, L1, a member of the immunoglobulin superfamily, and a member of the cadherin family, N-cadherin, and they are discussed in more detail.

1.5.1. L1 Cell Adhesion Molecule

L1 is a neural cell adhesion, transmembrane, glycoprotein expressed on the surface of post-mitotic neurons in the CNS, on Schwann cells in the peripheral nervous system, and on growth cones of axon^[91-93]. L1 acts through homophilic or L1-L1 interactions and through heterophilic interactions with other cell adhesion proteins such as NCAM and contractin, as well as ECM proteins such as laminin and tenascin^[92,94,95]. A member of the immunoglobulin superfamily, the extracellular region of L1 is composed of six Ig-like domains and five fibronectin type III repeats (Figure 1.1) and these domains contain important binding sites for adhesion, neurite outgrowth, and survival^[96-99]. The intracellular domain of L1 contains a highly conserved sequence, which binds to ankyrin, an adaptor protein that links L1 to the actin cytoskeleton via spectrin^[92,100]. L1 is a key adhesion ligand for promoting neuronal survival, differentiation, neuritogenesis, adhesion, and migration of neural cells both *in vitro* and *in vivo*^[93,96-99,101-103], as well as fasciculation^[104,105], and subcellular synapse organization^[106]. Soluble L1 is capable of promoting recovery of motor function in adult rats that endured a contusion induced spinal

cord injury^[102,107-109] and regenerative growth of Purkinje cell axons^[110]. L1-transfected mouse embryonic stem cells (mESCs), injected into the site of a spinal cord lesion, maintained integrity, were migratory, and enhanced functional recovery in comparison to non-transfected mESCs^[111]. More recently, mESCs engineered to secrete an L1 trimer, while expressing full length L1 at the cell membrane, were promoted superior locomotor recovery, reduced glial scar volume, and enhanced regrowth, sprouting, and remyelination compared to mESCs only expressing full length L1 and parental cells, in a contusion spinal cord injury model^[112].

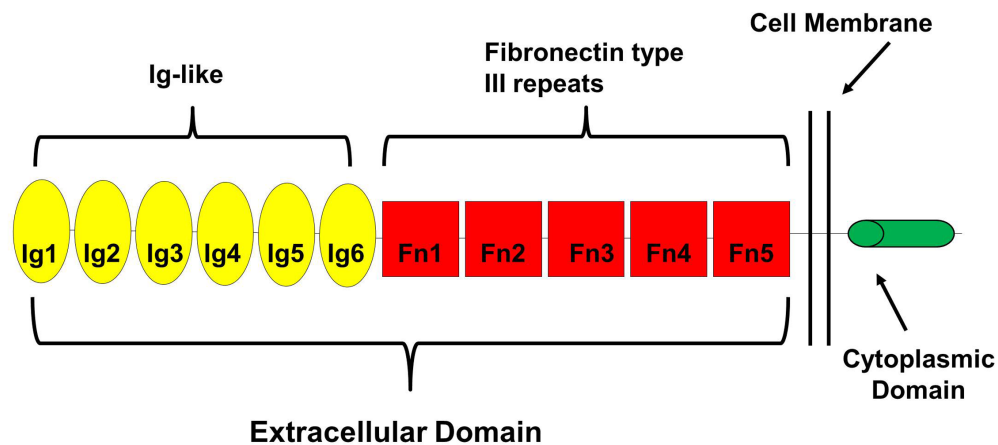


Figure 1.1. Schematic of L1 cell adhesion molecule. L1 cell adhesion molecule is composed of six immunoglobulin-like (Ig-like) domains, five Fibronectin type III repeats, a transmembrane region, which links L1 to the cytoskeleton via adaptor proteins.

L1 has been reported to play a role in proliferation and differentiation behaviors of NSCs. Surface-bound L1 reduced inhibited proliferation, while increasing neuronal differentiation and accelerated the production of GABAergic neurons and decreasing astrocyte differentiation of primary mouse neural stem cells^[113]. Overexpression of L1 in mESC-derived neural precursors resulted in reduced proliferation and astrocytic differentiation, in addition to increased neuronal differentiation and inhibiting astrocytic differentiation^[102,111,114]. Due to the beneficial effects of L1 on both neurons and neural stem

cells *in vitro*, as well as its ability to promote functional recovery in rodent SCI *in vivo* models, combined with its crucial role in neural development, L1 holds great promise for use as a biomimetic in designing bioactive biomaterials for treatment of SCI and other traumatic nervous system injuries.

1.5.2. N-cadherin

N-cadherin is a part of the classical cadherin family, containing five extracellular domains (Figure 1.2) that mediate cis and trans homophilic and heterophilic interactions^[115]. The conserved intracellular domain of N-cadherin binds to β -catenin and p120-catenin, following homophilic interactions of N-cadherin, and this N-cadherin- β -catenin complex is ultimately coupled to actin by interactions with α -catenin, forming adherens junctions that mediate cell-cell signaling^[116,117]. N-cadherin is highly expressed in neuroepithelial cells during early embryonic and neonatal development, and in neuroanatomical connections during late embryonic stages and early postnatal development^[118]. N-cadherin expression and function is required for several phases of neuronal development such as synaptogenesis, axonal and dendritic morphogenesis and synaptic plasticity^[119-122]. Cell-cell contact mediated by N-cadherin plays a dynamic role during neural development in the balance between self-renewal, migration, and differentiation of neural stem cells^[116,123]. For example, during development, high expression of N-cadherin-mediated cell-cell contacts promote neural stem cell maintenance and self-renewal, while decreased N-cadherin expression allows neural stem cells to dissociate and migrate to their proper microenvironment to differentiate further^[123].

This same phenomenon has been observed *in vitro*, and demonstrates that the influence of N-cadherin on neural stem cell behavior translates to *in vitro* culture systems. The ability of N-cadherin to promote self-renewal and maintenance of neural stem cells and

neuronal differentiation, when presented as an artificial extracellular matrix, has been demonstrated in immortalized, embryonic mouse forebrains-derived NSCs^[124]. Furthermore, E-cadherin-/N-cadherin-Fc co-presenting poly-styrene substrates, supported self-renewal and neuronal differentiation of mouse embryonic stem cells and mouse induced pluripotent stem cells^[125]. Other groups have demonstrated the ability surface adsorbed N-cadherin to promote or enhance neurite outgrowth, survival, and functionality of primary neurons isolated from different regions of murine or rat CNS^[126-129]. These studies, combined with the emergent understanding of N-cadherin's role during neural development, point to N-cadherin as a promising candidate for designing biomimetic biomaterials for neural tissue engineering applications.

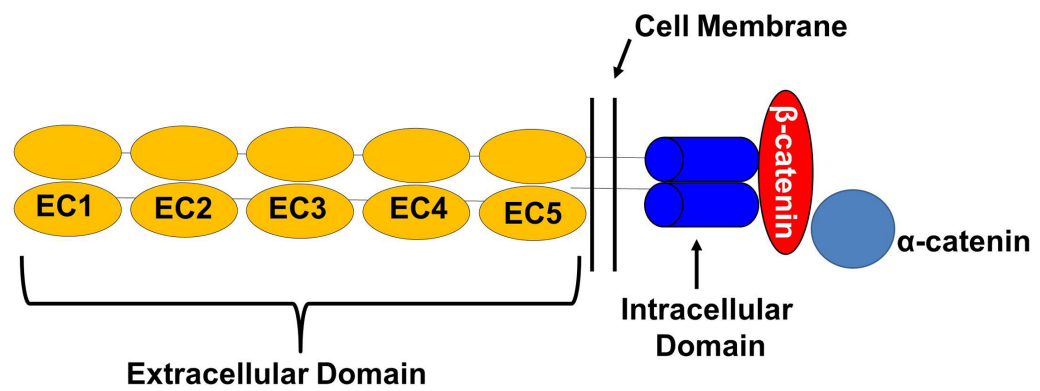


Figure 1.2. Illustration of N-cadherin. N-cadherin, a calcium dependent adhesion protein that mediates cell-cell contacts through cis- and trans-interactions. The intracellular domain of N-cadherin interacts with the cytoplasmic protein, β -catenin, which links N-cadherin to the cytoskeleton via α -catenin, following N-cadherin-N-cadherin binding.

1.6. Thesis Overview

The goal of this dissertation was to investigate substrate modification approaches to create “biomimetic”, neurogenic scaffolds and to elucidate the biointerfacial responsiveness of such substrates to human neural stem cells or hESC derived neurons, for potential application to SCI treatment. Several problems associated with regeneration following

spinal cord injury and current research avenues that are being explored in the field of neural tissue engineering. However, there is an unmet need for the development of bioactive biomaterials for neural cell transplantation. In Chapter 2, we explored a minimal approach for directing neural cell behavior by presenting neural adhesion molecules from nanoscale substrates. Specifically, we investigated the feasibility of using human albumin nanoparticles to present an L1 cell adhesion molecule-derived peptide, in order to promote high efficacy and spatial control of bioactivity of the peptide. The L1 peptide is derived from a region of L1 that was shown to mediate neurite outgrowth^[130]. The idea of presenting L1 peptide from nanoparticles was to enhance the effectiveness of the peptide by increasing peptide exposure and binding activity. Previous work from our laboratory demonstrated the advantage of using the albumin nanoparticle system to present the cell adhesion domain of fibronectin₉₋₁₀ to primary keratinocytes and fibroblasts^[131-133]. Therefore, we hypothesized that albumin nanoparticle system would improve L1 peptide efficacy, over presenting the peptide alone, in promoting enhance neural cell behaviors. Before delving into the complex system of hESC derived neural stem cells and testing how L1 peptide nanoparticles influenced neuronal differentiation and neurite extension, we opted to test our L1 peptide-albumin nanoparticle system on model, primary neuronal cells in order to determine which parameters (e.g. L1 peptide concentration and albumin nanoparticle size) would promote enhanced neurite outgrowth compared to presenting the peptide alone, with the aim of translating the use of this system to hESC-NSCs. We observed that the L1 peptide-nanoparticle system promoted only modest adhesion and process extension of murine cerebellar neurons, motor neurons, and Schwann cells compared to the peptide alone. However, we did observe the larger derivative of L1, which enhanced neurite outgrowth.

In chapter 3, we shifted our focus toward aimed to investigate a different approach for designing bioactive biomaterials for neural tissue engineering. Instead of moving further with the L1 peptide nanoparticle system for controlling hESC derived NSC behaviors, we decided to use a larger, more inclusive fragment of L1. The results from our studies in Chapter 2 prompted us to use L1-Fc as a candidate for the design of our biomaterials. However, since the neurite outgrowth promoting effects of this region has been shown before, we sought to develop a design that would improve the effectiveness of L1 compared to the conventional presentation of L1. Therefore, we selected protein A to present L1-Fc in a multimeric fashion from two dimensional surfaces and polymeric electrospun scaffolds, whereby this presentation would mimic the physiological orientation of L1 to primary neurons and hESC-NSCs. We postulated that this presentation strategy would maximize L1-Fc function and enhance neurite outgrowth and neuronal differentiation. In Chapter 4, a similar presentation design based on protein A was used to investigate the differential presentation of N-cadherin-Fc to hESC-derived NSCs alone or in combination with L1-Fc. Here, we sought to investigate the effects of varying concentrations of N-cadherin on neuronal differentiation of hESC-NSCs, as N-cadherin is expressed early during neural development and involved in key neuronal developmental events. Additionally, we examined the optimal configurations for combining N-cadherin-Fc and L1-Fc that would promote enhanced neuronal differentiation and neurite outgrowth, as both proteins elicit different responses from neuronal cells. Chapter 5, summarizes the findings and implications of this dissertation and outlines potential future applications that could further our understanding of how neural cell adhesion biomimetic scaffolds promote neuronal development, with the goal of adapting these constructs to models of SCI.

1.7. References

1. Zhang N, HH Yan and XJ Wen. (2005). Tissue-engineering approaches for axonal guidance. *Brain Research Reviews* 49:48-64.
2. McKerracher L. (2001). Spinal cord repair: Strategies to promote axon regeneration. *Neurobiology of Disease* 8:11-18.
3. Chvatal SA, YT Kim, AM Bratt-Leal, H Lee and RV Bellamkonda. (2008). Spatial distribution and acute anti-inflammatory effects of Methylprednisolone after sustained local delivery to the contused spinal cord. *Biomaterials* 29:1967-75.
4. Zhang N, H Yan and X Wen. (2005). Tissue-engineering approaches for axonal guidance. *Brain Res Brain Res Rev* 49:48-64.
5. Zhang SC. (2003). Embryonic stem cells for neural replacement therapy: Prospects and challenges. *Journal of Hematotherapy & Stem Cell Research* 12:625-634.
6. Schwab ME and D Bartholdi. (1996). Degeneration and regeneration of axons in the lesioned spinal cord. *Physiol Rev* 76:319-70.
7. Rolls A, R Shechter and M Schwartz. (2009). The bright side of the glial scar in CNS repair. *Nature reviews. Neuroscience* 10:235-41.
8. Fitch MT and J Silver. (2008). CNS injury, glial scars, and inflammation: Inhibitory extracellular matrices and regeneration failure. *Experimental neurology* 209:294-301.
9. Thuret S, LD Moon and FH Gage. (2006). Therapeutic interventions after spinal cord injury. *Nature reviews. Neuroscience* 7:628-43.
10. Harrop JS, R Hashimoto, D Norvell, A Raich, B Aarabi, RG Grossman, JD Guest, CH Tator, J Chapman and MG Fehlings. (2012). Evaluation of clinical experience using cell-based therapies in patients with spinal cord injury: a systematic review. *J Neurosurg Spine* 17:230-46.
11. Kim BG, DH Hwang, SI Lee, EJ Kim and SU Kim. (2007). Stem cell-based cell therapy for spinal cord injury. *Cell transplantation* 16:355-64.
12. Kim H, MJ Cooke and MS Shoichet. (2012). Creating permissive microenvironments for stem cell transplantation into the central nervous system. *Trends in Biotechnology* 30:55-63.
13. Kim SU, HJ Lee and YB Kim. (2013). Neural stem cell-based treatment for neurodegenerative diseases. *Neuropathology : official journal of the Japanese Society of Neuropathology*.
14. Ormerod BK, TD Palmer and MA Caldwell. (2008). Neurodegeneration and cell replacement. *Philosophical transactions of the Royal Society of London. Series B, Biological sciences* 363:153-70.
15. Cao Q, XM Xu, WH Devries, GU Enzmann, P Ping, P Tsoulfas, PM Wood, MB Bunge and SR Whittemore. (2005). Functional recovery in traumatic spinal cord injury after transplantation of multineurotrophin-expressing glial-restricted precursor cells. *J Neurosci* 25:6947-57.
16. Cao QL, RM Howard, JB Dennison and SR Whittemore. (2002). Differentiation of engrafted neuronal-restricted precursor cells is inhibited in the traumatically injured spinal cord. *Exp Neurol* 177:349-59.
17. Cao QL, YP Zhang, RM Howard, WM Walters, P Tsoulfas and SR Whittemore. (2001). Pluripotent stem cells engrafted into the normal or lesioned adult rat spinal cord are restricted to a glial lineage. *Exp Neurol* 167:48-58.
18. Cloutier F, MM Siegenthaler, G Nistor and HS Keirstead. (2006). Transplantation of human embryonic stem cell-derived oligodendrocyte progenitors into rat spinal cord injuries does not cause harm. *Regen Med* 1:469-79.

19. Cummings BJ, N Uchida, SJ Tamaki, DL Salazar, M Hooshmand, R Summers, FH Gage and AJ Anderson. (2005). Human neural stem cells differentiate and promote locomotor recovery in spinal cord-injured mice. *Proc Natl Acad Sci U S A* 102:14069-74.
20. Keirstead HS, T Ben-Hur, B Rogister, MT O'Leary, M Dubois-Dalcq and WF Blakemore. (1999). Polysialylated neural cell adhesion molecule-positive CNS precursors generate both oligodendrocytes and Schwann cells to remyelinate the CNS after transplantation. *J Neurosci* 19:7529-36.
21. Keirstead HS, G Nistor, G Bernal, M Totoiu, F Cloutier, K Sharp and O Steward. (2005). Human embryonic stem cell-derived oligodendrocyte progenitor cell transplants remyelinate and restore locomotion after spinal cord injury. *J Neurosci* 25:4694-705.
22. Mitsui T, JS Shumsky, AC Lepore, M Murray and I Fischer. (2005). Transplantation of neuronal and glial restricted precursors into contused spinal cord improves bladder and motor functions, decreases thermal hypersensitivity, and modifies intraspinal circuitry. *J Neurosci* 25:9624-36.
23. Nistor GI, MO Totoiu, N Haque, MK Carpenter and HS Keirstead. (2005). Human embryonic stem cells differentiate into oligodendrocytes in high purity and myelinate after spinal cord transplantation. *Glia* 49:385-96.
24. Ruff CA, JT Wilcox and MG Fehlings. (2012). Cell-based transplantation strategies to promote plasticity following spinal cord injury. *Experimental neurology* 235:78-90.
25. Tetzlaff W, EB Okon, S Karimi-Abdolrezaee, CE Hill, JS Sparling, JR Plemel, WT Plunet, EC Tsai, D Baptiste, LJ Smithson, MD Kawaja, MG Fehlings and BK Kwon. (2011). A systematic review of cellular transplantation therapies for spinal cord injury. *Journal of neurotrauma* 28:1611-82.
26. Lu P, LL Jones, EY Snyder and MH Tuszynski. (2003). Neural stem cells constitutively secrete neurotrophic factors and promote extensive host axonal growth after spinal cord injury. *Experimental neurology* 181:115-29.
27. Alvarez-Buylla A, JM Garcia-Verdugo and AD Tramontin. (2001). A unified hypothesis on the lineage of neural stem cells. *Nature reviews. Neuroscience* 2:287-93.
28. Temple S. (2001). The development of neural stem cells. *Nature* 414:112-7.
29. Gotz M and WB Huttner. (2005). The cell biology of neurogenesis. *Nature reviews. Molecular cell biology* 6:777-88.
30. Kukekov VG, ED Laywell, O Suslov, K Davies, B Scheffler, LB Thomas, TF O'Brien, M Kusakabe and DA Steindler. (1999). Multipotent stem/progenitor cells with similar properties arise from two neurogenic regions of adult human brain. *Experimental neurology* 156:333-44.
31. Gage FH. (2000). Mammalian neural stem cells. *Science* 287:1433-8.
32. Weiss S, C Dunne, J Hewson, C Wohl, M Wheatley, AC Peterson and BA Reynolds. (1996). Multipotent CNS stem cells are present in the adult mammalian spinal cord and ventricular neuroaxis. *The Journal of neuroscience : the official journal of the Society for Neuroscience* 16:7599-609.
33. Hibaoui Y and A Feki. (2012). Human pluripotent stem cells: applications and challenges in neurological diseases. *Front Physiol* 3:267.
34. Svendsen CN, MA Caldwell, J Shen, MG ter Borg, AE Rosser, P Tyers, S Karmioli and SB Dunnett. (1997). Long-term survival of human central nervous system progenitor cells transplanted into a rat model of Parkinson's disease. *Exp Neurol* 148:135-46.

35. Svendsen CN, MG ter Borg, RJ Armstrong, AE Rosser, S Chandran, T Ostenfeld and MA Caldwell. (1998). A new method for the rapid and long term growth of human neural precursor cells. *Journal of neuroscience methods* 85:141-52.
36. Nemati S, M Hatami, S Kiani, K Hemmesi, H Gourabi, N Masoudi, S Alaei and H Baharvand. (2011). Long-term self-renewable feeder-free human induced pluripotent stem cell-derived neural progenitors. *Stem cells and development* 20:503-14.
37. Solozobova V, N Wyvekens and J Pruszk. (2012). Lessons from the embryonic neural stem cell niche for neural lineage differentiation of pluripotent stem cells. *Stem cell reviews* 8:813-29.
38. Hoffman LM and MK Carpenter. (2005). Characterization and culture of human embryonic stem cells. *Nat Biotechnol* 23:699-708.
39. Liew CG, H Moore, L Ruban, N Shah, K Cosgrove, M Dunne and P Andrews. (2005). Human embryonic stem cells: possibilities for human cell transplantation. *Ann Med* 37:521-32.
40. Reubinoff BE, MF Pera, CY Fong, A Trounson and A Bongso. (2000). Embryonic stem cell lines from human blastocysts: somatic differentiation in vitro. *Nat Biotechnol* 18:399-404.
41. Thomson JA, J Itskovitz-Eldor, SS Shapiro, MA Waknitz, JJ Swiergiel, VS Marshall and JM Jones. (1998). Embryonic stem cell lines derived from human blastocysts. *Science* 282:1145-7.
42. Carpenter MK, MS Inokuma, J Denham, T Mujtaba, CP Chiu and MS Rao. (2001). Enrichment of neurons and neural precursors from human embryonic stem cells. *Experimental neurology* 172:383-97.
43. Elkabetz Y, G Panagiotakos, G Al Shamy, ND Socci, V Tabar and L Studer. (2008). Human ES cell-derived neural rosettes reveal a functionally distinct early neural stem cell stage. *Genes & development* 22:152-65.
44. Nat R, M Nilbratt, S Narkilahti, B Winblad, O Hovatta and A Nordberg. (2007). Neurogenic neuroepithelial and radial glial cells generated from six human embryonic stem cell lines in serum-free suspension and adherent cultures. *Glia* 55:385-99.
45. Perrier AL, V Tabar, T Barberi, ME Rubio, J Bruses, N Topf, NL Harrison and L Studer. (2004). Derivation of midbrain dopamine neurons from human embryonic stem cells. *Proceedings of the National Academy of Sciences of the United States of America* 101:12543-8.
46. Shin S, M Mitalipova, S Noggle, D Tibbitts, A Venable, R Rao and SL Stice. (2006). Long-term proliferation of human embryonic stem cell-derived neuroepithelial cells using defined adherent culture conditions. *Stem Cells* 24:125-38.
47. Zhang SC, M Wernig, ID Duncan, O Brustle and JA Thomson. (2001). In vitro differentiation of transplantable neural precursors from human embryonic stem cells. *Nature biotechnology* 19:1129-33.
48. Ma W, T Tavakoli, E Derby, Y Serebryakova, MS Rao and MP Mattson. (2008). Cell-extracellular matrix interactions regulate neural differentiation of human embryonic stem cells. *BMC Dev Biol* 8:90.
49. Chambers SM, CA Fasano, EP Papapetrou, M Tomishima, M Sadelain and L Studer. (2009). Highly efficient neural conversion of human ES and iPS cells by dual inhibition of SMAD signaling. *Nature biotechnology* 27:275-80.
50. Hu BY and SC Zhang. (2010). Directed differentiation of neural-stem cells and subtype-specific neurons from hESCs. *Methods Mol Biol* 636:123-37.

51. Carpenter MK, MS Inokuma, J Denham, T Mujtaba, CP Chiu and MS Rao. (2001). Enrichment of neurons and neural precursors from human embryonic stem cells. *Exp Neurol* 172:383-97.
52. Park S, KS Lee, YJ Lee, HA Shin, HY Cho, KC Wang, YS Kim, HT Lee, KS Chung, EY Kim and J Lim. (2004). Generation of dopaminergic neurons in vitro from human embryonic stem cells treated with neurotrophic factors. *Neurosci Lett* 359:99-103.
53. Perrier AL, V Tabar, T Barberi, ME Rubio, J Bruses, N Topf, NL Harrison and L Studer. (2004). Derivation of midbrain dopamine neurons from human embryonic stem cells. *Proc Natl Acad Sci U S A* 101:12543-8.
54. Bissonnette CJ, L Lyass, BJ Bhattacharyya, A Belmadani, RJ Miller and JA Kessler. (2011). The controlled generation of functional basal forebrain cholinergic neurons from human embryonic stem cells. *Stem Cells* 29:802-11.
55. Vanderhaeghen P. (2012). Generation of cortical neurons from pluripotent stem cells. *Prog Brain Res* 201:183-95.
56. Zeng H, M Guo, K Martins-Taylor, X Wang, Z Zhang, JW Park, S Zhan, MS Kronenberg, A Lichtler, HX Liu, FP Chen, L Yue, XJ Li and RH Xu. (2010). Specification of region-specific neurons including forebrain glutamatergic neurons from human induced pluripotent stem cells. *PloS one* 5:e11853.
57. Pera MF, J Andrade, S Houssami, B Reubinoff, A Trounson, EG Stanley, D Ward-van Oostwaard and C Mummery. (2004). Regulation of human embryonic stem cell differentiation by BMP-2 and its antagonist noggin. *J Cell Sci* 117:1269-80.
58. Yan Y, D Yang, ED Zarnowska, Z Du, B Werbel, C Valliere, RA Pearce, JA Thomson and SC Zhang. (2005). Directed differentiation of dopaminergic neuronal subtypes from human embryonic stem cells. *Stem Cells* 23:781-90.
59. Parr AM, I Kulbatski and CH Tator. (2007). Transplantation of adult rat spinal cord stem/progenitor cells for spinal cord injury. *J Neurotrauma* 24:835-45.
60. Tarasenko YI, J Gao, L Nie, KM Johnson, JJ Grady, CE Hulsebosch, DJ McAdoo and P Wu. (2007). Human fetal neural stem cells grafted into contusion-injured rat spinal cords improve behavior. *J Neurosci Res* 85:47-57.
61. Macias MY, MB Syring, MA Pizzi, MJ Crowe, AR Alexanian and SN Kurpad. (2006). Pain with no gain: Allodynia following neural stem cell transplantation in spinal cord injury. *Experimental Neurology* 201:335-348.
62. Cooke MJ, K Vulic and MS Shoichet. (2010). Design of biomaterials to enhance stem cell survival when transplanted into the damaged central nervous system. *Soft Matter* 6:4988-4998.
63. Cao QL, RM Howard, JB Dennison and SR Whittemore. (2002). Differentiation of engrafted neuronal-restricted precursor cells is inhibited in the traumatically injured spinal cord. *Experimental neurology* 177:349-59.
64. Cao QL, YP Zhang, RM Howard, WM Walters, P Tsoulfas and SR Whittemore. (2001). Pluripotent stem cells engrafted into the normal or lesioned adult rat spinal cord are restricted to a glial lineage. *Experimental neurology* 167:48-58.
65. Ferreira L, JM Karp, L Nobre and R Langer. (2008). New opportunities: the use of nanotechnologies to manipulate and track stem cells. *Cell Stem Cell* 3:136-46.
66. Laflamme MA and CE Murry. (2005). Regenerating the heart. *Nat Biotechnol* 23:845-56.
67. Mooney DJ and H Vandenburgh. (2008). Cell delivery mechanisms for tissue repair. *Cell Stem Cell* 2:205-13.

68. Potter W, RE Kalil and WJ Kao. (2008). Biomimetic material systems for neural progenitor cell-based therapy. *Frontiers in bioscience : a journal and virtual library* 13:806-21.
69. Delcroix GJR, PC Schiller, JP Benoit and CN Montero-Menei. (2010). Adult cell therapy for brain neuronal damages and the role of tissue engineering. *Biomaterials* 31:2105-2120.
70. Lee YS and TL Arinzeh. (2011). Electrospun Nanofibrous Materials for Neural Tissue Engineering. *Polymers* 3:413-426.
71. Wang TY, JS Forsythe, CL Parish and DR Nisbet. (2012). Biofunctionalisation of polymeric scaffolds for neural tissue engineering. *Journal of biomaterials applications* 27:369-90.
72. Owen SC and MS Shoichet. (2010). Design of three-dimensional biomimetic scaffolds. *J Biomed Mater Res A* 94:1321-31.
73. Sill TJ and HA von Recum. (2008). Electrospinning: applications in drug delivery and tissue engineering. *Biomaterials* 29:1989-2006.
74. Murugan R and S Ramakrishna. (2006). Nano-featured scaffolds for tissue engineering: a review of spinning methodologies. *Tissue engineering* 12:435-47.
75. Li D and YN Xia. (2004). Electrospinning of nanofibers: Reinventing the wheel? *Advanced Materials* 16:1151-1170.
76. Khaing ZZ and CE Schmidt. (2012). Advances in natural biomaterials for nerve tissue repair. *Neurosci Lett* 519:103-14.
77. McCreedy DA and SE Sakiyama-Elbert. (2012). Combination therapies in the CNS: engineering the environment. *Neurosci Lett* 519:115-21.
78. Wang TY, JS Forsythe, CL Parish and DR Nisbet. (2012). Biofunctionalisation of polymeric scaffolds for neural tissue engineering. *J Biomater Appl* 27:369-90.
79. Koh HS, T Yong, CK Chan and S Ramakrishna. (2008). Enhancement of neurite outgrowth using nano-structured scaffolds coupled with laminin. *Biomaterials* 29:3574-82.
80. Horne MK, DR Nisbet, JS Forsythe and CL Parish. (2010). Three-dimensional nanofibrous scaffolds incorporating immobilized BDNF promote proliferation and differentiation of cortical neural stem cells. *Stem Cells Dev* 19:843-52.
81. Ito Y, G Chen, Y Imanishi, T Morooka, E Nishida, Y Okabayashi and M Kasuga. (2001). Differential control of cellular gene expression by diffusible and non-diffusible EGF. *J Biochem* 129:733-7.
82. Wang TY, JS Forsythe, DR Nisbet and CL Parish. (2012). Promoting engraftment of transplanted neural stem cells/progenitors using biofunctionalised electrospun scaffolds. *Biomaterials* 33:9188-97.
83. Ito Y. (2008). Covalently immobilized biosignal molecule materials for tissue engineering. *Soft Matter* 4:46-56.
84. Chew SY, R Mi, A Hoke and KW Leong. (2007). Aligned Protein-Polymer Composite Fibers Enhance Nerve Regeneration: A Potential Tissue-Engineering Platform. *Advanced functional materials* 17:1288-1296.
85. Mohtaram NK, A Montgomery and SM Willerth. (2013). Biomaterial-based drug delivery systems for the controlled release of neurotrophic factors. *Biomedical materials* 8:022001.
86. Tate CC, DA Shear, MC Tate, DR Archer, DG Stein and MC LaPlaca. (2009). Laminin and fibronectin scaffolds enhance neural stem cell transplantation into the injured brain. *Journal of tissue engineering and regenerative medicine* 3:208-17.

87. Tysseling-Mattiace VM, V Sahni, KL Niece, D Birch, C Czeisler, MG Fehlings, SI Stupp and JA Kessler. (2008). Self-assembling nanofibers inhibit glial scar formation and promote axon elongation after spinal cord injury. *J Neurosci* 28:3814-23.
88. Cooke MJ, T Zahir, SR Phillips, DS Shah, D Athey, JH Lakey, MS Shoichet and SA Przyborski. (2010). Neural differentiation regulated by biomimetic surfaces presenting motifs of extracellular matrix proteins. *Journal of biomedical materials research. Part A* 93:824-32.
89. Bian S. (2013). Cell Adhesion Molecules in Neural Stem Cell and Stem Cell-Based Therapy for Neural Disorders. In: *Neural Stem Cells - New Perspectives*. Bonfanti L ed. InTech. pp 349-380.
90. Shapiro L, J Love and DR Colman. (2007). Adhesion molecules in the nervous system: structural insights into function and diversity. *Annu Rev Neurosci* 30:451-74.
91. Appel F, J Holm, JF Conscience and M Schachner. (1993). Several extracellular domains of the neural cell adhesion molecule L1 are involved in neurite outgrowth and cell body adhesion. *J Neurosci* 13:4764-75.
92. Maness PF and M Schachner. (2007). Neural recognition molecules of the immunoglobulin superfamily: signaling transducers of axon guidance and neuronal migration. *Nat Neurosci* 10:19-26.
93. Moos M, R Tacke, H Scherer, D Teplow, K Fruh and M Schachner. (1988). Neural adhesion molecule L1 as a member of the immunoglobulin superfamily with binding domains similar to fibronectin. *Nature* 334:701-3.
94. Grumet M, DR Friedlander and GM Edelman. (1993). Evidence for the binding of Ng-CAM to laminin. *Cell Adhes Commun* 1:177-90.
95. Kadmon G, A Kowitz, P Altevogt and M Schachner. (1990). Functional cooperation between the neural adhesion molecules L1 and N-CAM is carbohydrate dependent. *The Journal of cell biology* 110:209-18.
96. Mechtersheimer S, P Gutwein, N Agmon-Levin, A Stoeck, M Oleszewski, S Riedle, R Postina, F Fahrenholz, M Fogel, V Lemmon and P Altevogt. (2001). Ectodomain shedding of L1 adhesion molecule promotes cell migration by autocrine binding to integrins. *J Cell Biol* 155:661-73.
97. Silletti S, F Mei, D Sheppard and AM Montgomery. (2000). Plasmin-sensitive dibasic sequences in the third fibronectin-like domain of L1-cell adhesion molecule (CAM) facilitate homomultimerization and concomitant integrin recruitment. *J Cell Biol* 149:1485-502.
98. Stallcup WB. (2000). The third fibronectin type III repeat is required for L1 to serve as an optimal substratum for neurite extension. *J Neurosci Res* 61:33-43.
99. Thelen K, V Kedar, AK Panicker, RS Schmid, BR Midkiff and PF Maness. (2002). The neural cell adhesion molecule L1 potentiates integrin-dependent cell migration to extracellular matrix proteins. *J Neurosci* 22:4918-31.
100. Bennett V and AJ Baines. (2001). Spectrin and ankyrin-based pathways: metazoan inventions for integrating cells into tissues. *Physiol Rev* 81:1353-92.
101. Loers G, SZ Chen, M Grumet and M Schachner. (2005). Signal transduction pathways implicated in neural recognition molecule L1 triggered neuroprotection and neuritogenesis. *Journal of neurochemistry* 92:1463-1476.
102. Bernreuther C, M Dihne, V Johann, J Schiefer, Y Cui, G Hargus, JS Schmid, J Xu, CM Kosinski and M Schachner. (2006). Neural cell adhesion molecule L1-transfected embryonic stem cells promote functional recovery after excitotoxic lesion of the mouse striatum. *J Neurosci* 26:11532-9.

103. Nishimune H, C Bernreuther, P Carroll, S Chen, M Schachner and CE Henderson. (2005). Neural adhesion molecules L1 and CHL1 are survival factors for motoneurons. *J Neurosci Res* 80:593-9.
104. Rathjen FG, JM Wolff, R Frank, F Bonhoeffer and U Rutishauser. (1987). Membrane glycoproteins involved in neurite fasciculation. *The Journal of cell biology* 104:343-53.
105. Weiland UM, H Ott, M Bastmeyer, H Schaden, S Giordano and CA Stuermer. (1997). Expression of an L1-related cell adhesion molecule on developing CNS fiber tracts in zebrafish and its functional contribution to axon fasciculation. *Molecular and cellular neurosciences* 9:77-89.
106. Huang ZJ. (2006). Subcellular organization of GABAergic synapses: role of ankyrins and L1 cell adhesion molecules. *Nat Neurosci* 9:163-6.
107. Chen J, C Bernreuther, M Dihne and M Schachner. (2005). Cell adhesion molecule L1-transfected embryonic stem cells with enhanced survival support regrowth of corticospinal tract axons in mice after spinal cord injury. *J. Neurotrauma* 22:896-906.
108. Chen J, J Wu, I Apostolova, M Skup, A Irintchev, S Kugler and M Schachner. (2007). Adeno-associated virus-mediated L1 expression promotes functional recovery after spinal cord injury. *Brain* 130:954-69.
109. Lavdas AA, J Chen, F Papastefanaki, S Chen, M Schachner, R Matsas and D Thomaidou. (2010). Schwann cells engineered to express the cell adhesion molecule L1 accelerate myelination and motor recovery after spinal cord injury. *Exp Neurol* 221:206-16.
110. Zhang Y, X Zhang, J Yeh, P Richardson and X Bo. (2007). Engineered expression of polysialic acid enhances Purkinje cell axonal regeneration in L1/GAP-43 double transgenic mice. *Eur J Neurosci* 25:351-61.
111. Cui YF, JC Xu, G Hargus, I Jakovcevski, M Schachner and C Bernreuther. (2011). Embryonic stem cell-derived L1 overexpressing neural aggregates enhance recovery after spinal cord injury in mice. *PloS one* 6:e17126.
112. He X, M Knepper, C Ding, J Li, S Castro, M Siddiqui and M Schachner. (2012). Promotion of spinal cord regeneration by neural stem cell-secreted trimerized cell adhesion molecule L1. *PloS one* 7:e46223.
113. Dihne M, C Bernreuther, M Sibbe, W Paulus and M Schachner. (2003). A new role for the cell adhesion molecule L1 in neural precursor cell proliferation, differentiation, and transmitter-specific subtype generation. *J Neurosci* 23:6638-50.
114. Cui YF, G Hargus, JC Xu, JS Schmid, YQ Shen, M Glatzel, M Schachner and C Bernreuther. (2010). Embryonic stem cell-derived L1 overexpressing neural aggregates enhance recovery in Parkinsonian mice. *Brain* 133:189-204.
115. Zhang Y, S Sivasankar, WJ Nelson and S Chu. (2009). Resolving cadherin interactions and binding cooperativity at the single-molecule level. *Proc Natl Acad Sci U S A* 106:109-14.
116. Tepass U, K Truong, D Godt, M Ikura and M Peifer. (2000). Cadherins in embryonic and neural morphogenesis. *Nature reviews. Molecular cell biology* 1:91-100.
117. Wheelock MJ and KR Johnson. (2003). Cadherin-mediated cellular signaling. *Curr Opin Cell Biol* 15:509-14.
118. Redies C and M Takeichi. (1993). Expression of N-cadherin mRNA during development of the mouse brain. *Dev Dyn* 197:26-39.
119. Benson DL and H Tanaka. (1998). N-cadherin redistribution during synaptogenesis in hippocampal neurons. *J Neurosci* 18:6892-904.

120. Arikath J and LF Reichardt. (2008). Cadherins and catenins at synapses: roles in synaptogenesis and synaptic plasticity. *Trends Neurosci* 31:487-94.
121. Salinas PC and SR Price. (2005). Cadherins and catenins in synapse development. *Curr Opin Neurobiol* 15:73-80.
122. Ye B and YN Jan. (2005). The cadherin superfamily and dendrite development. *Trends Cell Biol* 15:64-7.
123. Rouso DL, CA Pearson, ZB Gaber, A Miquelajauregui, S Li, C Portera-Cailliau, EE Morrissey and BG Novitch. (2012). Foxp-mediated suppression of N-cadherin regulates neuroepithelial character and progenitor maintenance in the CNS. *Neuron* 74:314-30.
124. Yue XS, Y Murakami, T Tamai, M Nagaoka, CS Cho, Y Ito and T Akaike. (2010). A fusion protein N-cadherin-Fc as an artificial extracellular matrix surface for maintenance of stem cell features. *Biomaterials* 31:5287-96.
125. Haque A, XS Yue, A Motazedian, Y Tagawa and T Akaike. (2012). Characterization and neural differentiation of mouse embryonic and induced pluripotent stem cells on cadherin-based substrata. *Biomaterials* 33:5094-106.
126. Shi P, K Shen and LC Kam. (2007). Local presentation of L1 and N-cadherin in multicomponent, microscale patterns differentially direct neuron function in vitro. *Dev Neurobiol* 67:1765-76.
127. Williams EJ, G Williams, FV Howell, SD Skaper, FS Walsh and P Doherty. (2001). Identification of an N-cadherin motif that can interact with the fibroblast growth factor receptor and is required for axonal growth. *J Biol Chem* 276:43879-86.
128. Doherty P and FS Walsh. (1996). CAM-FGF Receptor Interactions: A Model for Axonal Growth. *Molecular and cellular neurosciences* 8:99-111.
129. Williams EJ, J Furness, FS Walsh and P Doherty. (1994). Activation of the FGF receptor underlies neurite outgrowth stimulated by L1, N-CAM, and N-cadherin. *Neuron* 13:583-94.
130. Appel F, J Holm, JF Conscience, F von Bohlen und Halbach, A Faissner, P James and M Schachner. (1995). Identification of the border between fibronectin type III homologous repeats 2 and 3 of the neural cell adhesion molecule L1 as a neurite outgrowth promoting and signal transducing domain. *J Neurobiol* 28:297-312.
131. Pereira M, RI Sharma, R Penkala, TA Gentzel, JE Schwarzbauer and PV Moghe. (2007). Engineered cell-adhesive nanoparticles nucleate extracellular matrix assembly. *Tissue Eng* 13:567-78.
132. Sharma RI, M Pereira, JE Schwarzbauer and PV Moghe. (2006). Albumin-derived nanocarriers: substrates for enhanced cell adhesive ligand display and cell motility. *Biomaterials* 27:3589-98.
133. Sharma RI, DI Shreiber and PV Moghe. (2008). Nanoscale variation of bioadhesive substrates as a tool for engineering of cell matrix assembly. *Tissue Eng Part A* 14:1237-50.

Chapter 2

Effects of L1-peptide Functionalized Albumin Nanoparticles on Adhesion and Neurite Outgrowth of Primary Motor Neurons, Cerebellar Neurons, and Dorsal Root Ganglion Cells

Abstract

The overall goal of this study was to investigate the potential of albumin nanoparticles (ANPs) to maximize the efficacy of an L1 cell adhesion molecule-derived peptide (L1p) in promoting enhanced adhesion and neurite outgrowth of primary neurons. The use of the ligand-ANP system as a tool to control neuronal cell behavior was inspired by previous studies in which fibronectin fragment III₉₋₁₀ (Fnf) conjugated to ANPs promoted a more motile phenotype in keratinocytes compared to those cultured on Fnf-only substrates. An increase in endocytosis and a clustered ligand display, which induced integrin clustering, were responsible for the enhanced keratinocyte response. This study used a similar platform, testing the ability of ANPs to improve L1p-mediated responses in comparison to L1p and ANPs. L1 peptide was successfully tethered to ANPs and remained functional and accessible for cell binding, but L1p-ANPs promoted only modest adhesion or outgrowth compared to L1p alone, when presented as a physisorbed substrate or as a soluble cue to dissociated primary neurons. In contrast, dorsal root ganglion cells (DRGs) adhered to L1p-ANPs and appeared to have a denser network of neurites compared to an ANP-treated substrate, in the presence of serum. Although L1p is neuritogenic, conjugating this small ligand to a relatively large, non-permissive albumin nanoparticle seemingly obstructed L1p effects when presented to dissociated neurons, under serum-free conditions. Provision of adhesion promoting serum proteins allowed cells to interact with L1p-ANPs and extend neurites along the surface, suggesting that combining L1p-ANPs with a factor that

encourages adhesion is necessary to elucidate the full potential of ANP-presented L1p. Further modifications to the ANP system are required in order for it to be an optimal presentation platform of neural peptides for neural tissue engineering applications.

2.1. Introduction

Traumatic central nervous system (CNS) injuries rarely result in the regeneration of damaged structures and functions. Ultimately, permanent structural and functional impairment is the outcome due to the limited ability of the CNS to self-repair and regenerate^[1-3]. Existing treatments aim to reduce secondary damage caused by macrophages that migrate to the injury site and activated astrocytes^[2], but fail to promote regeneration of damaged neuronal cells. In order to promote restoration of motor functions, damaged tissues require external cues to encourage axonal regeneration and lost cells need to be replaced with functional, exogenous cell source. Current research efforts seek to combine biomaterials, exogenous cell sources, and biological cues to design treatments to support and promote axonal regeneration^[3-5]. Derivatives of proteins and growth factors native to the neuronal microenvironment, such as laminin, brain derived neurotrophic factor (BDNF), and the cell adhesion molecule, L1 have been investigated, in combination with biomaterials and cell sources, for stimulating neuritogenesis^[6-8].

L1 is a key transmembrane glycoprotein that plays a critical role in neurite outgrowth and adhesion^[9-11], neuronal survival^[12,13], , and migration^[14-16] of neuronal cells, in addition to differentiation of stem cells^[11,17,18]. Here we evaluated the ability of an L1 derived peptide, presented from albumin nanoparticles, to enhance adhesion and neurite outgrowth of motor neurons, cerebellar neurons, and dorsal root ganglion. The ligand-ANP system has been shown by the Moghe laboratory to increase exposure and binding activity as well as endocytosis kinetics of ligands^[19,20]. The nanoscale presentation of adhesion

ligands could also be coupled with nanoparticles of different inertial mass (sizes), which could in turn regulate specific cell response^[21,22]. This study aimed to use a similar platform for presenting peptides derived from L1. The peptide selected is based on previous research that demonstrated the effectiveness of this motif on adhesion and neurite outgrowth of neural cells^[23]. Studies performed in the laboratory of Dr. Melitta Schachner also showed the ability of the peptide to promote enhanced survival of cerebellar neurons in the presence of oxidative stress (unpublished data). When presented in a substrate-physisorbed configuration, the ligand-ANP system also has the benefit of facilitating rapid internalization of the peptide, which plays a role in L1-mediated outgrowth and migration^[24]. We hypothesized the ANP based L1p presentation would modulate the kinetics of adhesion and neurite outgrowth neuronal cells. The use of ANPs to present the ligands could potentially be exploited to (a) further enhance its "exposure"; and (b) accelerate the endocytosis of the peptide within neurons, hypothesized to emulate the L1 effect on increased neurite outgrowth. Presenting the peptides in a clustered manner mediates receptor clustering^[25-28], which increases exposure and binding activity between the peptides and their receptors, and resulting in increased endocytosis, steps critical to accelerate significant neurite outgrowth neuronal cells.

Engineered substrates that present spatially controlled biological cues may be relevant for the development of cell-based tissue regenerative therapies. Several studies have shown that the control and regulation of cellular adhesion, growth, and cell function can be modulated significantly by presenting biological molecules in a manner that enhances ligand-receptor interactions^[27-33]. For example, Maheshwari et al. investigated the effects of clustered RGD peptides on cell adhesion and motility and discerned, following growth factor stimulation, a high-ligand density display increased adhesion, while clustered

RGD reduced the ligand density needed to increase migration speeds^[27]. Mannix et al. also demonstrated the benefits of ligand-clustering using 30 nm, superparamagnetic beads functionalized with N1-2, 4-dinitrophenyl-L-lysine (DNP-Lys)^[28]. Clustering of DNP-Lys was promoted by applying an electromagnetic field, which caused the beads to be attracted to one another and inducing integrin clustering. An increase in calcium signaling, which plays a role in cellular responses, was observed as a result of integrin clustering^[28]. While that system can turn cell responses on and off, the use of superparamagnetic beads for therapy is not ideal as cytotoxicity is a likely issue.

Our group previously demonstrated that substrates based on biofunctionalized albumin nanoparticles (ANPs) promoted ligand exposure and cell binding as well as epithelial cell motility and connective tissue matrix assembly^[19,20]. Specifically, ANPs functionalized with III₉₋₁₀ fibronectin fragment (Fnf) significantly enhanced cell motility in keratinocytes compared to Fnf alone^[20]. The ligand-ANP system has been shown to increase exposure and binding activity as well as endocytosis kinetics of ligands, which is hypothesized to play a role in migration^[19,20,34]. Due to the nanoscale presentation of cell adhesion molecules and possible receptor-based endocytotic fates, the substrates based on ANPs functionalized with neural adhesion molecules like L1 offer a method to target neural cell motility and functions. We investigated different concentrations of L1 peptide tethered to ANPs; using adsorbed and soluble presentations of L1 peptide functionalized albumin nanoparticles. To assess the effects of L1 peptide albumin nanoparticles on cellular adhesion and neurite outgrowth cerebellar neurons and motor neurons were used in the studies, as well as dorsal root ganglion.

2.2. Materials and Methods

2.2.1. Synthesis of Albumin Nanoparticles

Albumin nanoparticles (ANPs) were synthesized from recombinant human serum albumin (HSA) utilizing the coacervation method previously described^[35,36]. Some fabrication steps were modified as described by Naczynski et al.^[36]. Briefly, HSA powder was dissolved to 10% (w/v) in 2.5 mM NaCl and the pH was adjusted to 8.5. The albumin nanoparticles (ANPs) were formed by the continuous addition of 2 ml of ethanol, using a syringe pump (Harvard Apparatus PHD 2000, Holliston, MA) at a rate of 1.5 ml/min, to 500 μ l of the HSA solution. During the addition of ethanol, the HSA solution was stirred the entire time (700 rpm), at room temperature. Immediately following the addition of the ethanol, 5.85 μ l of 8% glutaraldehyde was added to crosslink the nanoparticles. Additionally, crosslinking the nanoparticles results in the autofluorescence of the ANPs. The crosslinking reaction was performed under stirring for 18 h at room temperature. Following the crosslinking step, the ANPs were purified by three rounds of centrifugation at 16,100 g, for 8 min each time at 4°C, followed by resuspension by sonication (15 min) in 2 ml of sterile PBS without Ca²⁺ and Mg²⁺.

2.2.2. Albumin Nanoparticle Characterization

The size and morphology of the ANPs were determined using dynamic light scattering (DLS) and scanning electron microscopy (SEM), respectively. The Malvern Zetasizer Nano (Zen 3690, Malvern Instruments Ltd, Malvern, Worcestershire, UK) was used to determine the size and polydispersity index (PDI) of the ANPs. The samples were diluted 1:50 in deionized water and measured at 37°C at a scattering angle of 90° and scanned three times. SEM was used to visualize ANP morphology. ANP samples were adsorbed onto an aluminum stub overnight at 4°C and washed two times with PBS and two

times with water in order to remove free ANPs and residual salts. The ANPs were air dried, sputtered coated with gold-palladium, and imaged at 20 kV acceleration potential. Samples for SEM imaging were dried under vacuum and sputter-coated with gold-palladium^[37].

2.2.3. Fabrication of L1 Peptide Albumin Nanoparticles

The L1 peptide (L1p), ELEGIEILNSSAVLVKWRPVDC (Genscript, Piscataway, NJ), was conjugated to the ANPs using the heterobifunctional crosslinker Sulfo-LC-SPDP (Pierce), as previously described^[36]. The schematic depicting the first step of the functionalization process is shown in Figure 2.1A. The ANPs were re-dispersed in PBS-EDTA (PBS containing 1 mM EDTA and 0.02% sodium azide, at pH 7.5). 1 mM of SPDP was added to 2 mg of ANPs for 30 min at room temperature, while rocking, and unreacted SPDP was removed by dialysis overnight, at room temperature. The SPDP-activated ANPs were reacted with L1p, which was covalently linked to ANPs through the formation of a disulfide bond between the thiol group (-SH), located on the cysteine of L1p, and the pyridyldithiol group (PD) located on the free end of the SPDP (Figure 2.1B). Free L1p was removed using overnight dialysis.

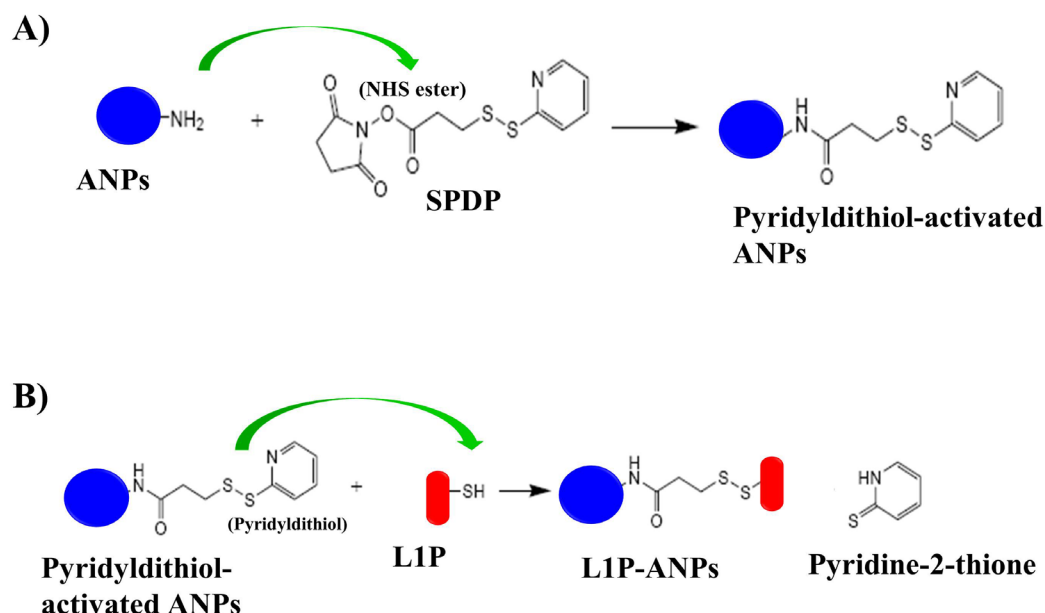


Figure 2.1. Schematic for covalent linkage of L1p to ANPs. A) ANPs were reacted with the heterobifunctional crosslinker, SPDP, in which the NHS ester of SPDP reacted with primary amines of ANPs, resulting in an active ANP. Following dialysis, the activated ANPs were mixed with the sulfhydryl containing L1p, in which pyridyldithiol reacted with the sulfhydryl group on the peptide, forming a disulfide bond and resulting in L1p-ANPs, as well as the production of the byproduct, pyridine-2-thione. ANPs: albumin nanoparticles, L1p: L1 peptide. Schematic adapted from <http://www.piercenet.com/instructions/2160279.pdf>

2.2.4. Quantification of L1peptide Loading Efficiency

The byproduct, Pyridine-2-Thione was used to determine the L1p loading efficiency onto ANPs. Pyridine-2-Thione (py2SH) is released once the free end of SPDP, 2-pyridyldithiol (PD), reacts with a thiol group (Figure 2.1B) and py2SH is detectable at an absorbance of 343 nm. Prior to functionalizing reacting L1p with the ANPs, the concentration of free PD groups, which would indicate the maximum amount of L1p to be conjugated to the ANPs, was determined by reacting activated ANPs with dithiothreitol (DTT). DTT is thiol containing compound that would react with free PD groups of activated ANPs. The supernatant concentration of reaction by product, py2SH was determined by absorbance measurements at 343 nm. A standard curve of β -mercaptothione (Sigma),

ranging from 0 – 20 $\mu\text{g/ml}$, was used to determine the levels py2SH generated. To ensure the maximum number of L1p was conjugated to the ANPs, a 3-fold concentration of L1p was reacted with the ANPs. The release of py2SH corresponds with the conjugation of L1p to the free end of SPDP, therefore every mole of py2SH detected was calculated to equal a mole of L1p conjugated to ANPs. After the reaction of L1p with ANPs, L1p-ANPs were diluted 1:10 in PBS-EDTA and the absorbance of the sample was read at 343 nm. A standard curve of β -mercaptothione (Sigma), ranging from 0 – 20 $\mu\text{g/ml}$, was used to determine the levels py2SH generated from the L1p-ANP reaction.

2.2.5. L1 Peptide ELISA

In addition to using the py2SH assay to quantify the loading efficiency of L1p onto ANPs, enzyme linked immunosorbant assay (ELISA) was used to detect the presence of L1p as well as to determine that the peptide was functional. L1p-ANPs were adsorbed onto maxisorb, 96 well plates overnight at 4°C. The wells were washed with PBS once, for 2 minutes and treated with a blocking buffer, composed of 1% bovine serum albumin (BSA, Sigma Aldrich, St. Louis, MO, USA) in PBS, for 1.5 hours at room temperature. After one wash for 2 minutes in PBS, the samples were incubated for 1.5 hours with a monoclonal rat anti-L1 557 antibody (kindly provided by Dr. Melitta Schachner, Hamburg, Germany), which recognizes the sequence within L1 that corresponds to L1p^[23] The wells were washed three times for 5 minutes each with PBS containing 0.05% Tween-20 (PBST) and subsequently treated with the secondary antibody, horseradish peroxidase conjugated-goat anti-rat IgG antibody (1:1000) (Sigma-Aldrich) for 1.5 hours at room temperature. Following three, 5 minute washes with PBST, 0.5 mg/ml of OPD (Sigma-Aldrich) was added to each well and allowed to react with the samples for up to 30 minutes in the dark at room temperature. The reaction was stopped with 2.5 N H_2SO_4 and absorbance was read on an absorbance

plate reader at 490 nm. The absorbance readings were used to assess the presence and accessibility L1p on the ANPs, compared to the respective controls.

2.2.6. Substrate Preparation for Cell Studies

Tissue culture polystyrene (TCPS) well plates or glass coverslips were coated with 100 µg/ml of poly-L-lysine (Sigma) for 1 hour and washed three times with phosphate buffered saline (PBS). Next, PLL surfaces were treated with the following with the following: L1p-ANPs (50 and 100 µg/ml of L1p), ANPs alone, L1p alone (50 and 100 µg/ml), or L1-Fc (10 µg/ml), or PBS (for the PLL control). The concentration of the ANP control was based on the resulting ANP concentration used for L1p-ANPs to achieve a final concentration of 50 µg/ml or 100 µg/ml of L1p. After coating overnight at 4°C, each surface was washed three times with PBS and neuronal cells were plated onto the surfaces immediately. In the case where ANPs were introduced as a soluble cue, the cells were allowed to attach for two hours onto surfaces treated with 10 µg/ml of PLL and L1p-ANPs were added to the media at 1, 10, and 100 µg/ml based on the L1p concentration. The concentration of ANPs added to the medium corresponded to the ANP concentration of L1p-ANPs.

2.2.7. Neuronal Cell Cultures

Cerebellar granule neurons were isolated from cerebella of P6-P8 C57BL/6J mice and dissociated with 0.025% trypsin (Lonza) and plated at 3.3×10^4 cells/cm². The cells were cultured in serum-free, chemically defined medium composed of Neurobasal-A media (Life Technologies) supplemented 1 mg/ml BSA, 12.5 µg/ml insulin (Sigma), 100 µg/ml transferrin (Calbiochem), 30 nM sodium selenite (Sigma), 1% penicillin/streptomycin (pen/strep) (Lonza), 2 mM L-glutamine (Life Technologies), 4 nM thyroxine (Sigma), and 1x B27 supplement (Life Technologies)

Motor neurons were isolated from spinal cords of e13 – e15 C57BL/6J mouse embryos and dissociated with 0.01% Collagenase (Life Technologies) and 0.025% trypsin. Following two purifying, gradient spins with 25%/50% Opti-prep (Axis Shields) followed by 3% BSA, motor neurons were plated onto substrates at 3.3×10^4 cells/cm². Motor neurons were cultured in serum-free, DMEM/F/12 (1:1) (Life Technologies) supplemented with the following: 30 nM sodium selenite, 8 ng/ml hydrocortisone (Sigma), 20 nM progesterone (Sigma), 29 µg/ml putrescine (Sigma), 9 µg/ml insulin, 5 µg/ml transferrin, 9 µg/ml BSA, 1% Pen/Strep, 1x B27, and 2 mM L-glutamine.

Chick dorsal root ganglion explants (DRGs) (Charles River Laboratories, Wilmington, MA) were isolated from E8 chick embryos, following a protocol previously described^[38]. In brief, chick embryos were incubated in a chamber at 37°C for 8 days. Using sterilized, fine forceps, the DRGs were removed from the vertebral column and transferred to cold Hanks' Balanced Salt Solution (HBSS) without Ca₂⁺ or Mg₂⁺ (Lonza) and kept on ice until seeded onto the culture surface. DRGs were cultured in media composed of 88% DMEM (Cellgro), 10% FBS (Life Technologies), 2 mM glutamine, 1% pen/strep, and 100 ng/ml of nerve growth factor (NGF) (R&D Systems).

2.2.8. Cell Adhesion to Biofunctionalized ANP substrates

To examine adhesion of cerebellar and motor neurons to substrates coated with L1p, L1p-ANPs, ANPs, L1-Fc and poly-L-lysine (PLL), each cell type was plated onto well plates treated with L1p, L1p-ANPs, ANPs, L1-Fc, and PLL. After 4 hours, the cells were fixed with 2.5% glutaraldehyde, and stained with 1% toluidine blue/1% methylene blue in 1% borax (Sigma). 10 images were taken for each condition and the total number of cells were counted using ImageJ (<http://rsb.info.nih.gov/ij/>).

2.2.9. Neurite Outgrowth on Biofunctionalized ANP substrates

To examine neurite outgrowth of cerebellar neuron and motor neurons, the cells were fixed with 2.5% glutaraldehyde, and stained with 1% toluidine blue/1% methylene blue in 1% borax after 24 hours. The samples were visualized using the KS image analysis system (Kontron, Zeiss, München, Germany). To examine neurite outgrowth from DRGs, after 3 days, DRGs were fixed with 4% paraformaldehyde, permeabilized with 0.1% Triton-X (Sigma), and blocked with 5% normal goat serum (MP Biomedicals) in PBS for 1 hour. Following blocking, DRGs were immunolabeled with anti-neurofilament-200 (Sigma) overnight at 4°C. Next, DRGs were washed three times with PBS and immunostained with goat anti-mouse IgG-594, for 1 hour, and washed three times with PBS, and visualized using a Nikon epifluorescence microscope (Nikon).

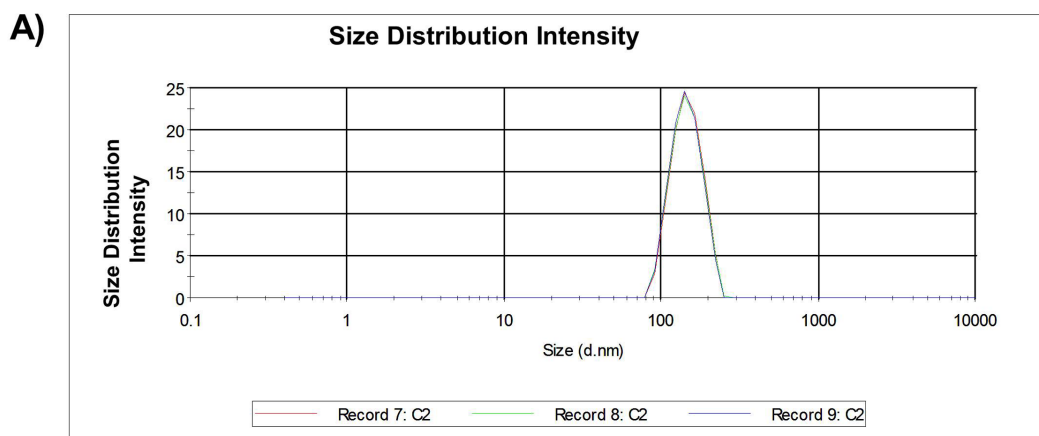
2.3. Results

2.3.1. Morphology and Size of ANPs

A representative plot of the size distribution intensity generated DLS is shown in Figure 2.2A. For each sample measured, three measurements were taken and each time a single peak was observed, indicating the uniformity of the ANPs. DLS measurements showed that the average size of ANPs was 150 ± 1.5 nm and the particles were very monodisperse as shown by the low PDI of 0.041 ± 0.02 (Figure 2.2B) SEM images showed the spherical morphology of ANPs and confirmed the DLS results showing ANPs that were uniform in size. (Figure 2.2C) Following conjugation to L1p, the size of the ANPs increased to by 30 nm to 182 ± 4.4 nm. L1p-ANPs had a higher PDI of $0.119 \pm .01$, compared to unconjugated ANPs, but still low, suggesting that L1p-ANPs remained monodisperse.

2.3.2. L1 Peptide Conjugated to ANPs Maintains Functionality and Accessibility for Antibody Binding

An ELISA was used to detect the presence of the peptide conjugated to the nanoparticles, as well as to determine the accessibility of the conjugated peptide. The antibody used, 557, was raised against the specific region of L1 that contains the sequence of the L1p^[23]. The results of the ELISA verified that L1p was both present and accessible for antibody binding as shown by increases in absorbance with an increase in adsorbed L1p-ANPs (Figure 2.3). The 1000 ng L1p-ANP absorbance reading was much greater compared to ANPs adsorbed at the same albumin nanoparticle concentration. The results of the ELISA, combined with the results of the py2SH assay, indicate that L1p was successfully conjugated to ANPs and peptide functionality was maintained.



B)

Nanoparticle Type	Size (nm)	Polydispersity Index (PDI)
ANPs	150 ± 1.5	0.041 ± 0.02
L1p-ANPs	182 ± 4.4	0.119 ± 0.01

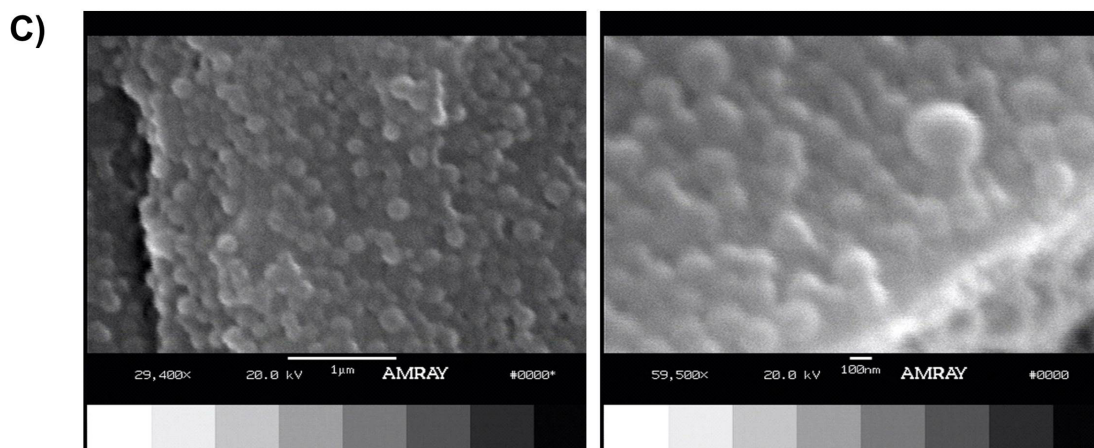


Figure 2.2. Size and morphology of ANPs A) The size distribution intensity plot generated using DLS indicates that ANPs are over 100 nm and uniform in size. B) The average sizes and PDIs of ANPs and L1p-ANPs. L1p-ANPs were about 20% larger than ANPs and not as uniform in size as ANPs. C) SEM images show that ANPs are spherical and uniform in size. ANPs: albumin nanoparticles, L1p: L1 peptide, DLS: dynamic light scattering, PDI: polydispersity index

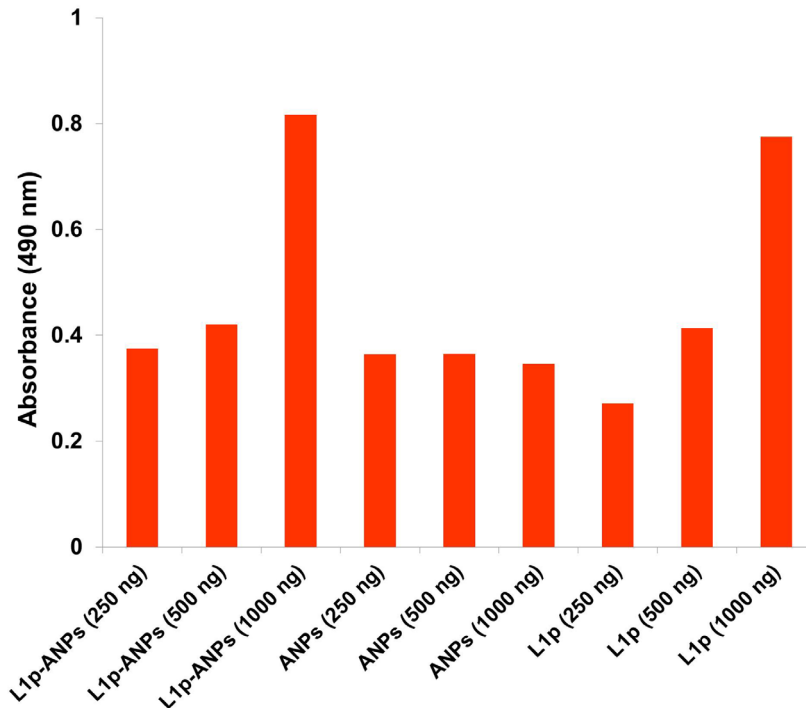


Figure 2.3. L1p is functional following conjugation to ANPs. ELISA was used to detect the presence and the accessibility for binding after L1p was tethered to ANPs. The absorbance readings increased as the mass of L1p-ANPs increased, similar to L1p, and in contrast to ANPs. L1p-ANPs: L1 peptide albumin nanoparticles, ANPs: albumin nanoparticles, L1p: L1 peptide

2.3.3. L1p-ANP Effects on Adhesion and Neurite Outgrowth of Cerebellar and Motor Neurons

Once the presence and functionality of L1p to ANPs had been established, the next step was to test the ability of L1p functionalized-ANPs to improve the neurite outgrowth promoting effects of L1p. Cerebellar neurons derived from P7 mouse pups were used in these studies, as previous work has shown the effectiveness of both L1-Fc and an antibody against the sequence of L1p in promoting neurite outgrowth of cerebellar neurons^[23]. Two concentrations of L1p-ANPs were examined and compared to L1p alone, L1-Fc, ANPs alone,

and PLL. To assess adhesion, neurons were observed after 4 hours and after 24 hours in culture for neurite outgrowth. Cell attachment was greatly impaired in CGNs cultured on substrates treated with L1p-ANPs, at both concentrations, as well as ANPs (Figure 2.4B). While the degree of adhesion was marginally better with L1p-ANPs presenting 100 $\mu\text{g}/\text{ml}$ of L1p, compared to ANPs alone, adhesion was much less than that observed on L1p alone and PLL. Cerebellar neuron morphology after 24 hours (Figure 2.4A) showed that in addition to low cell attachment on L1p-ANP and ANP substrates, only a small percentage of cells that did attach extended neurites (red arrows). Additionally, cerebellar neurons cultured on ANPs appeared clumped together compared to cerebellar neurons cultured on other surfaces. Quantification of the percent of cells that extended neurites further confirmed only a small percentage of cells extended neurites when grown on L1p-ANPs and ANPs (Figure 2.4C).

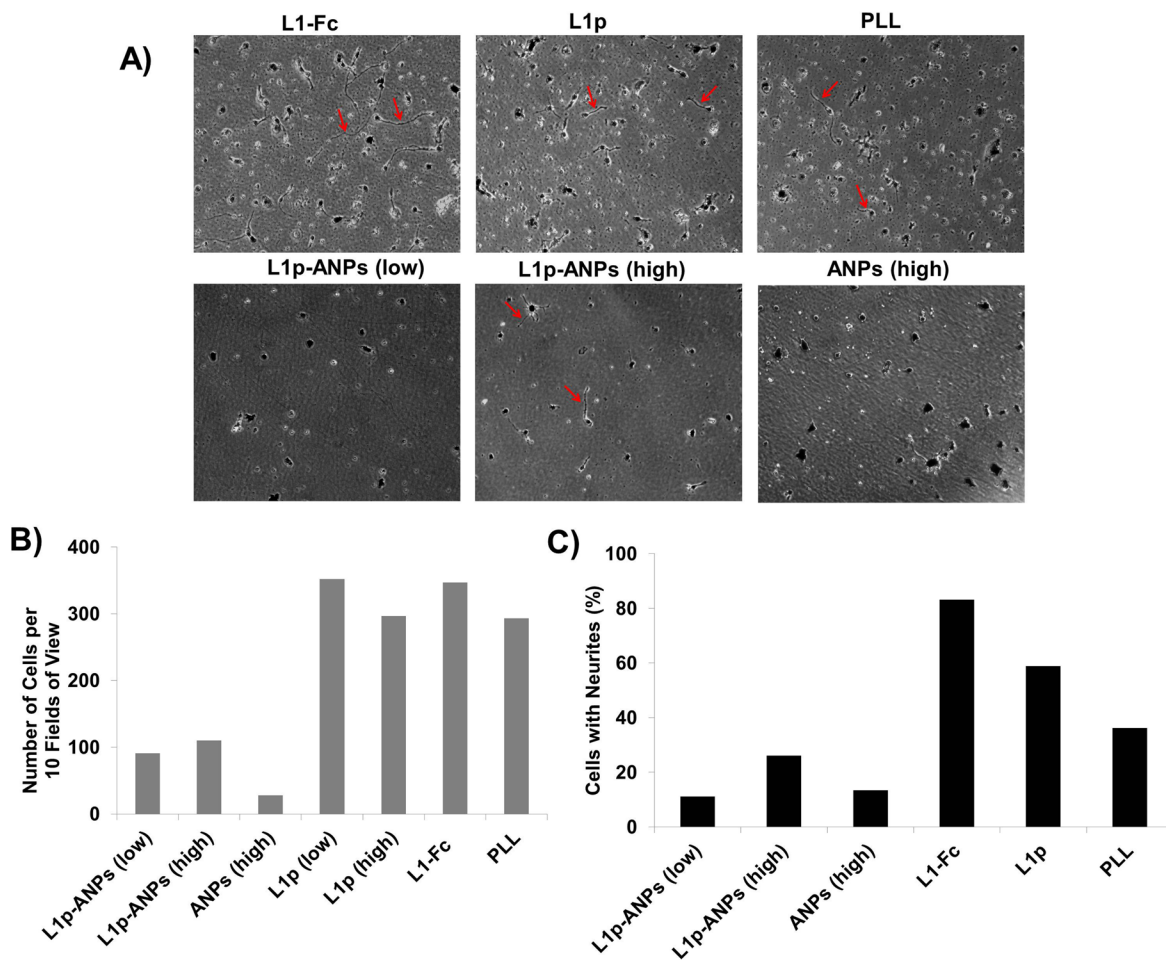


Figure 2.4. Morphology, adhesion, and neuritogenesis of cerebellar neurons in the presence of L1p-ANPs. A) Cerebellar neurons after 24 hours on glass coverslips coated with PLL (100 $\mu\text{g/ml}$) followed by L1-Fc (10 $\mu\text{g/ml}$), L1p (100 $\mu\text{g/ml}$), L1p-ANPs (low - 50 $\mu\text{g/ml}$) or L1p-ANPs (high - 100 $\mu\text{g/ml}$), or ANPs, which had an equivalent albumin concentration to that in high L1p-ANPs. Neurite extension is indicated by red arrows. B) After 4 hours, adhesion of cerebellar neurons was examined with the fewest cells adhering to ANPs alone. L1p-ANPs, both high and low, promoted a slight increase in attachment over ANPs, but much less than the background treatment of PLL. C) L1p-ANPs (low and high L1p concentrations) promoted little neurite extension compared to L1p and PLL.

Since adhesion was greatly reduced when L1p-ANPs were presented adsorbed to the surface of PLL coated coverslips, we were curious if the soluble presentation of L1p-ANPs would have a positive effect on neurite outgrowth, as soluble L1 has been reported to be effective in promoting neurite outgrowth as well as nanoparticles^[39]. Two hours after cerebellar neurons were plated onto PLL-coated coverslips, low, medium, and high L1p-

ANPs (1, 10, 100 $\mu\text{g}/\text{ml}$ of L1p, respectively) was added to the culture media. The same mass of ANPs matching that of L1p-ANPs was added as a soluble cue as well. Similarly to that observed in cerebellar neurons cultured on physisorbed L1p-ANPs, the percentage of cells that extended neurites in the presence of soluble L1p-ANPs, at all concentrations, was much less than the percent of cells that extended neurites on L1p alone (Figure 2.5A-B). In comparison to neurons treated with ANPs, a higher percentage of neurons did extend neurites following treatment with 1 $\mu\text{g}/\text{ml}$ (low), 10 $\mu\text{g}/\text{ml}$ (med), and 100 $\mu\text{g}/\text{ml}$ (high) of L1p-ANPs.

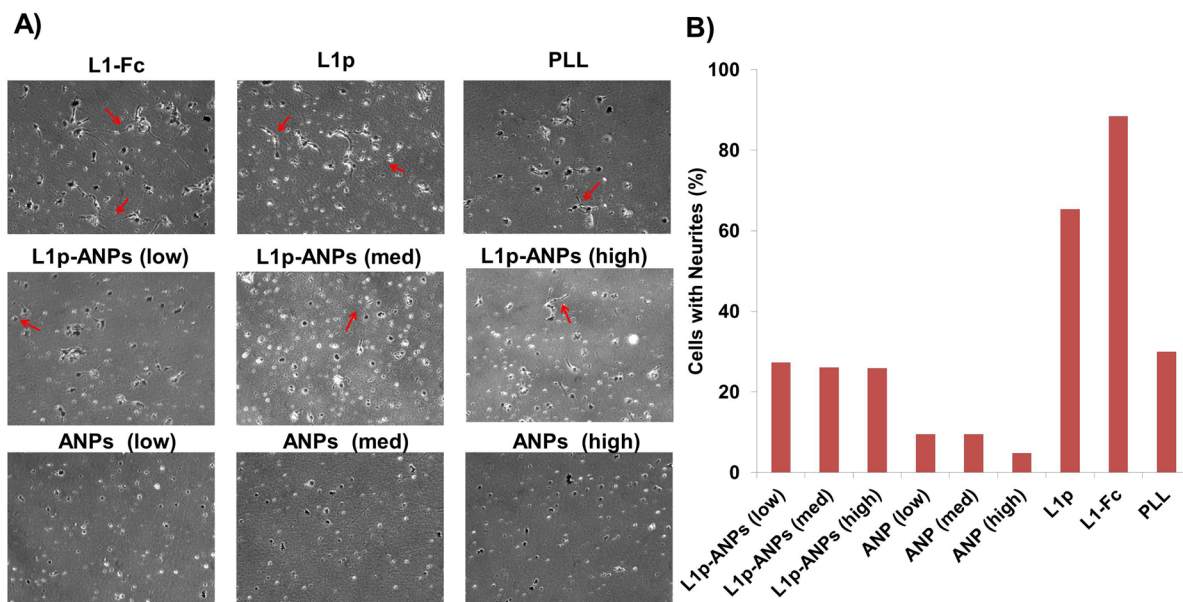


Figure 2.5. Response of cerebellar neurons to soluble L1p-ANPs. A) After 2 hours, cerebellar neurons, plated on a 100 $\mu\text{g}/\text{ml}$ of PLL, were treated with varying concentrations of soluble L1p-ANPs [low (1 $\mu\text{g}/\text{ml}$ L1p), medium (10 $\mu\text{g}/\text{ml}$) or high (100 $\mu\text{g}/\text{ml}$)] or corresponding concentrations of ANPs. Adsorbed L1p (100 $\mu\text{g}/\text{ml}$) and L1-Fc (10 $\mu\text{g}/\text{ml}$) and PLL alone were used as controls. The red arrows indicate cells that extended neurites for each condition. B) Quantification of the percentage of neurons that extended neurites. L1p-ANPs had a higher percentage of cells that extended neurites, compared to ANPs alone, but not greater than that observed on PLL.

2.3.4. Dorsal Root Ganglion Explants Extend Neurites on L1p-ANP Substrates in the Presence of Serum

In addition to testing the L1p-ANPs in promoting neurite outgrowth of dissociated cerebellar and motor neurons, we also examined how DRGs would respond to L1p-ANPs. DRG explants are commonly used as a model cell type for studies examining neurite outgrowth. DRGs mimic more closely how cells might behave *in vivo* as they were not dissociated and were left intact with supportive cells, such as Schwann cells. In the previous experiments, we used serum free media that was supplemented with B27 (<http://www.patentgenius.com/patent/6506576.html>), as those culture conditions have been optimized for those cell types and the presence of serum may have confounded observations of cell responses. We found that L1p-ANPs promoted very little cell adhesion of dissociated neurons. Therefore, DRGs were cultured in serum containing media, as the serum proteins might assist in promoting cell attachment on substrates treated with ANPs and allow the cells to come in contact with L1p presented from ANPs. Prior to coating the surface with L1p-ANPs or ANPs, glass coverslips were treated with oxygen plasma to facilitate serum protein adsorption as well as ANP adsorption, as no PLL was used for these studies. DRGs were plated onto substrates coated with L1p-ANPs, ANPs, or plasma treated glass. Neurite extension was observed in DRGs for each condition. However, a qualitative difference in the distance of outgrowth and the density of neurites between DRGs cultured on L1p-ANPs and ANPs alone (Figure 2.6), demonstrating the neuritogenic effects L1p-ANPs. While the distance of neurite extension appeared to be similar between DRGs cultured on plasma treated glass only and L1p-ANPs, L1p-ANPs substrates appeared to generate denser neurite network. These results point to the need to combine adhesion promoting factors with L1p-ANPs in order elucidate the ability of this presentation strategy to enhance L1p effectiveness.

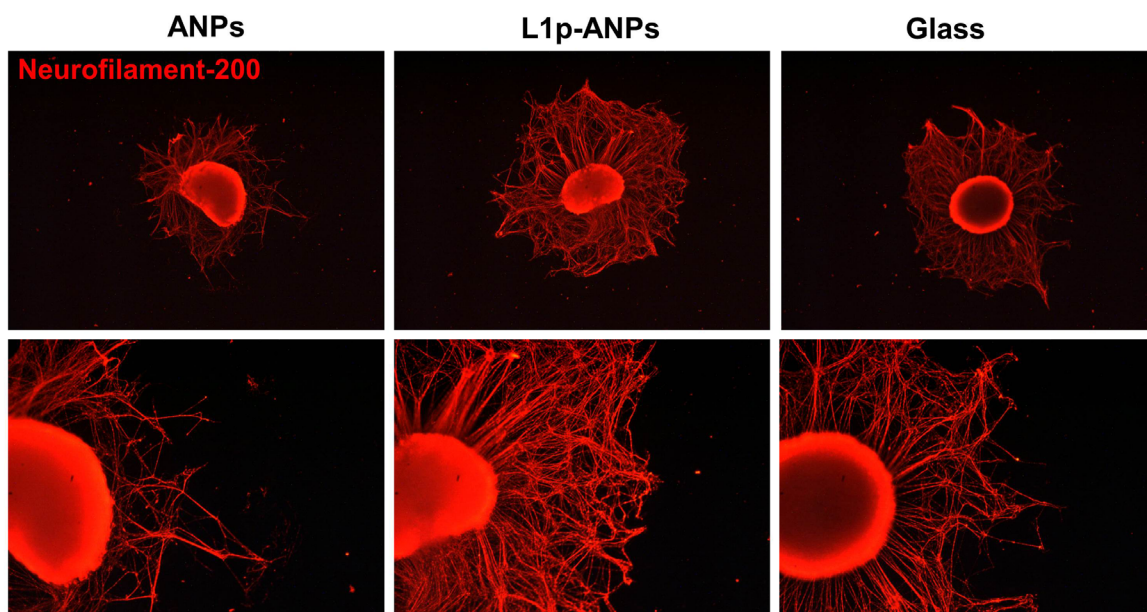


Figure 2.6. Neurite extension of DRGs cultured on L1p-ANPs. Glass coverslips were oxygen-plasma treated and L1p-ANPs (100 $\mu\text{g}/\text{ml}$ L1p), ANPs were adsorbed overnight at 4°C. DRGs were plated onto each substrate, cultured for 3 days in serum containing media, and immunolabeled with neurofilament-200 (red). Neurites extending from DRGs cultured on L1p-ANPs appeared to be longer and denser compared to DRGs cultured on ANPs, demonstrating the ability of L1p-ANPs to promote neurite outgrowth.

2.4. Discussion

The overall goal of these studies was to engineer a delivery system for L1 peptide that would improve the peptide efficacy and promote enhanced cellular behaviors of neuronal cells such as neurite outgrowth. Albumin is an ideal material for nanoparticle applications because it is a naturally occurring protein, therefore biocompatible, and albumin nanoparticles have recently been approved by the FDA as a drug delivery system for cancer therapeutics^[40]. While studies have demonstrated the usefulness of albumin nanoparticles in modulating cell behavior as both an adsorbed substrate^[19,20,34,37] and soluble cue^[41], the results of our studies demonstrate that neural cells, specifically

dissociated, murine cerebellar and motor neurons do not respond favorably. In contrast, dorsal root ganglion showed improved outgrowth on L1p-ANPs compared to ANPs alone, in the presence of serum proteins. Perhaps the result here was due to the presence of supportive cells and cell-cell contacts not present in dissociated cultures, as well as the serum proteins aiding cell attachment to the surface.

Albumin nanoparticles are composed of groups of monomeric albumin that come together to form nanoparticles that reach sizes that are over 100 nm, in contrast to monomeric albumin, which is only 6 nm. Plausibly, conjugating L1p to albumin monomers versus nanoparticles would attenuate the degree of non-permissiveness of the L1p-albumin system, as the ratio of L1p to albumin would be higher compared to L1p conjugated to a much larger albumin nanoparticle. Another possible approach for converting ANPs into a more permissive system for neural cell attachment is to add a cationic coating to ANPs. Poly-L-lysine (PLL) or poly-D-lysine (PDL) is commonly used as surface coatings that encourage the adhesion of neurons to various surfaces^[42,43]. Treating ANPs with PDL or PLL prior to conjugating L1p to ANPs could possibly attenuate the anti-adhesive effect of albumin. Park et al. used PDL coated, growth factor loaded nanoparticles in combination with PGLA scaffolds to promote neuronal differentiation of PC12 cells^[44]. The positive charge provided by PDL was pivotal in promoting PC12 adhesion. Another study by Nojehdehian et al. used PLL to coat retinoic acid-loaded PLGA microspheres for nerve tissue engineering and observed an increase in cell adhesion with the PLL coating compared to uncoated microspheres^[45], and the increase in surface area as a result of coating with PLL improved cell attachment and expansion^[46]. An additional advantage to using PLL or PDL to coat the nanoparticles is the presence of several amine groups, which could also be used for the conjugation of L1p to the particles and might result in enhanced conjugation efficiency

of the peptide. Studies have been underway in our laboratory to assess the effects treating ANPs with (PDL). Preliminary work demonstrated that PDL treatment of ANPs reduced the formation of ANP aggregates, which formed following functionalization of ANPs with the peptide growth factor sequestering peptide, P14^[47]. It is plausible that some degree of aggregation of L1p-ANPs occurred, as the polydispersity index increased close to a full order of magnitude over ANPs alone, which would increase the effective surface area of non-permissive albumin, further reducing the effectiveness of L1p. Thus, PDL treatment would serve to promote cell adhesion and as an aid for maintaining a uniformity of ANPs.

Our studies show that L1-Fc promotes significantly better adhesion and outgrowth compared L1p with and without ANPs. The data suggests that larger protein fragments of L1 are better suited for promoting adhesion and outgrowth of the neural cells tested within our system. Our initial goal aimed to determine the minimal effects of neural cell adhesion molecules, such as L1, presented from non-permissive substrates previously shown to maximize ligand function. However, we observed that L1p-ANPs were significantly less effective in promoting neuronal adhesion, despite the presence of PLL, in contrast to L1-Fc. As a result, we shifted our efforts to using protein fragments and focused on multimeric presentation larger fragments. To this end, the remaining work described within this thesis utilized L1-Fc, which is a fusion protein composed of the extracellular domain of human L1 and the Fc region of human IgG1. L1-Fc contains several sequences involved in L1-mediated cell attachment, neurite outgrowth, and survival in contrast to the peptide. Co-conjugation of L1p with other, more adhesive peptides could also prove to be beneficial in overcoming the non-permissiveness of albumin nanoparticles. Peptides such as RGD or fragments such as fibronectin type III 9-10, which bind to $\alpha_5\beta_1$ integrins, have been shown

to promote cell adhesion, onto non-permissive substrates, when coated with fibronectin type III 9-10 alone or conjugated to albumin nanoparticles^[37].

In summary, albumin nanoparticles functionalized with L1-derived peptides were investigated for their ability to promote enhanced neurite outgrowth of neuronal cells, with the intention of translating the system for use with human embryonic stem cell-derived neural stem cells. Albumin nanoparticles were selected as the carrier of L1 peptides as a way to present the peptides in a clustered manner, which was hypothesized to enhance the exposure of L1 peptides to further increase peptide-receptor binding, leading to enhanced cells responses such as neurite outgrowth. Based on results from several *in vitro* experiments, the albumin nanoparticle system is not the ideal approach for presenting L1 peptides to neuronal cells. Both cell attachment and neurite outgrowth of dissociated primary neurons were greatly reduced when cultured on L1p-ANPs. In contrast, larger L1 derivative, L1-Fc, promoted enhanced neurite outgrowth, indicating the need to display large fragments of L1 from alternative substrates. Because small nanoparticles are not ideally suited to display such large protein fragments (MW of L1-Fc is 200 kDa), an alternative approach for presenting L1 was explored and is discussed in Chapter 3 of this dissertation.

2.5. References

1. Zhang SC. (2003). Embryonic stem cells for neural replacement therapy: Prospects and challenges. *Journal of Hematotherapy & Stem Cell Research* 12:625-634.
2. McKerracher L. (2001). Spinal cord repair: Strategies to promote axon regeneration. *Neurobiology of Disease* 8:11-18.
3. Zhang N, H Yan and X Wen. (2005). Tissue-engineering approaches for axonal guidance. *Brain Res Brain Res Rev* 49:48-64.
4. Jain KK. (2009). Cell therapy for CNS trauma. *Mol Biotechnol* 42:367-76.
5. McCreedy DA and SE Sakiyama-Elbert. (2012). Combination therapies in the CNS: engineering the environment. *Neurosci Lett* 519:115-21.
6. Koh HS, T Yong, CK Chan and S Ramakrishna. (2008). Enhancement of neurite outgrowth using nano-structured scaffolds coupled with laminin. *Biomaterials* 29:3574-82.

7. Horne MK, DR Nisbet, JS Forsythe and CL Parish. (2010). Three-dimensional nanofibrous scaffolds incorporating immobilized BDNF promote proliferation and differentiation of cortical neural stem cells. *Stem cells and development* 19:843-52.
8. Chen J, C Bernreuther, M Dihne and M Schachner. (2005). Cell adhesion molecule l1-transfected embryonic stem cells with enhanced survival support regrowth of corticospinal tract axons in mice after spinal cord injury. *J Neurotrauma* 22:896-906.
9. Appel F, J Holm, JF Conscience and M Schachner. (1993). Several extracellular domains of the neural cell adhesion molecule L1 are involved in neurite outgrowth and cell body adhesion. *J Neurosci* 13:4764-75.
10. Maretzky T, M Schulte, A Ludwig, S Rose-John, C Blobel, D Hartmann, P Altevogt, P Saftig and K Reiss. (2005). L1 is sequentially processed by two differently activated metalloproteases and presenilin/gamma-secretase and regulates neural cell adhesion, cell migration, and neurite outgrowth. *Mol Cell Biol* 25:9040-53.
11. Schultheis M, S Diestel and B Schmitz. (2007). The role of cytoplasmic serine residues of the cell adhesion molecule l1 in neurite outgrowth, endocytosis, and cell migration. *Cell Mol Neurobiol* 27:11-31.
12. Chen S, N Mantei, L Dong and M Schachner. (1999). Prevention of neuronal cell death by neural adhesion molecules L1 and CHL1. *J Neurobiol* 38:428-39.
13. Nishimune H, C Bernreuther, P Carroll, S Chen, M Schachner and CE Henderson. (2005). Neural adhesion molecules L1 and CHL1 are survival factors for motoneurons. *J Neurosci Res* 80:593-9.
14. Anderson RB, KN Turner, AG Nikonenko, J Hemperly, M Schachner and HM Young. (2006). The cell adhesion molecule l1 is required for chain migration of neural crest cells in the developing mouse gut. *Gastroenterology* 130:1221-32.
15. Panicker AK, M Buhusi, A Erickson and PF Maness. (2006). Endocytosis of beta1 integrins is an early event in migration promoted by the cell adhesion molecule L1. *Exp Cell Res* 312:299-307.
16. Schmid RS, BR Midkiff, VP Kedar and PF Maness. (2004). Adhesion molecule L1 stimulates neuronal migration through Vav2-Pak1 signaling. *Neuroreport* 15:2791-4.
17. Bernreuther C, M Dihne, V Johann, J Schiefer, Y Cui, G Hargus, JS Schmid, J Xu, CM Kosinski and M Schachner. (2006). Neural cell adhesion molecule L1-transfected embryonic stem cells promote functional recovery after excitotoxic lesion of the mouse striatum. *J Neurosci* 26:11532-9.
18. Dihne M, C Bernreuther, M Sibbe, W Paulus and M Schachner. (2003). A new role for the cell adhesion molecule L1 in neural precursor cell proliferation, differentiation, and transmitter-specific subtype generation. *J Neurosci* 23:6638-50.
19. Pereira M, RI Sharma, R Penkala, TA Gentzel, JE Schwarzbauer and PV Moghe. (2007). Engineered cell-adhesive nanoparticles nucleate extracellular matrix assembly. *Tissue Eng* 13:567-78.
20. Sharma RI, M Pereira, JE Schwarzbauer and PV Moghe. (2006). Albumin-derived nanocarriers: substrates for enhanced cell adhesive ligand display and cell motility. *Biomaterials* 27:3589-98.
21. Sharma RI, DI Shreiber and PV Moghe. (2008). Nanoscale Variation of Bioadhesive Substrates as a Tool for Engineering of Cell Matrix Assembly. *Tissue Eng* 14:1237-50.

22. Pereira M, RI Sharma, R Penkala, T Gentzel, JE Schwarzbauer and PV Moghe. (2007). Engineered Cell Adhesive Nanoparticles Nucleate Extracellular Matrix Assembly. *Tissue Eng* 13:567-78.
23. Appel F, J Holm, JF Conscience, F von Bohlen und Halbach, A Faissner, P James and M Schachner. (1995). Identification of the border between fibronectin type III homologous repeats 2 and 3 of the neural cell adhesion molecule L1 as a neurite outgrowth promoting and signal transducing domain. *J Neurobiol* 28:297-312.
24. Kamiguchi H and F Yoshihara. (2001). The role of endocytic l1 trafficking in polarized adhesion and migration of nerve growth cones. *J Neurosci* 21:9194-203.
25. Cavalcanti-Adam EA, A Micoulet, J Blummel, J Auernheimer, H Kessler and JP Spatz. (2006). Lateral spacing of integrin ligands influences cell spreading and focal adhesion assembly. *Eur J Cell Biol* 85:219-24.
26. Cavalcanti-Adam EA, T Volberg, A Micoulet, H Kessler, B Geiger and JP Spatz. (2007). Cell spreading and focal adhesion dynamics are regulated by spacing of integrin ligands. *Biophys J* 92:2964-74.
27. Maheshwari G, G Brown, DA Lauffenburger, A Wells and LG Griffith. (2000). Cell adhesion and motility depend on nanoscale RGD clustering. *J Cell Sci* 113 (Pt 10):1677-86.
28. Mannix RJ, S Kumar, F Cassiola, M Montoya-Zavala, E Feinstein, M Prentiss and DE Ingber. (2008). Nanomagnetic actuation of receptor-mediated signal transduction. *Nat Nanotechnol* 3:36-40.
29. Koo LY, DJ Irvine, AM Mayes, DA Lauffenburger and LG Griffith. (2002). Co-regulation of cell adhesion by nanoscale RGD organization and mechanical stimulus. *Journal of Cell Science* 115:1423-1433.
30. Lee KY, E Alsberg, S Hsiong, W Comisar, J Linderman, R Ziff and D Mooney. (2004). Nanoscale adhesion ligand organization regulates osteoblast proliferation and differentiation. *Nano Letters* 4:1501-1506.
31. Dennes TJ, GC Hunt, JE Schwarzbauer and J Schwartz. (2007). High-yield activation of scaffold polymer surfaces to attach cell adhesion molecules. *J Am Chem Soc* 129:93-7.
32. Dennes TJ and J Schwartz. (2008). Controlling cell adhesion on polyurethanes. *Soft Matter* 4:86-89.
33. Tysseling-Mattiace VM, V Sahni, KL Niece, D Birch, C Czeisler, MG Fehlings, SI Stupp and JA Kessler. (2008). Self-assembling nanofibers inhibit glial scar formation and promote axon elongation after spinal cord injury. *J Neurosci* 28:3814-23.
34. Sharma RI, DI Shreiber and PV Moghe. (2008). Nanoscale variation of bioadhesive substrates as a tool for engineering of cell matrix assembly. *Tissue Eng Part A* 14:1237-50.
35. Langer K, S Balthasar, V Vogel, N Dinauer, H von Briesen and D Schubert. (2003). Optimization of the preparation process for human serum albumin (HSA) nanoparticles. *Int J Pharm* 257:169-80.
36. Naczynski DJ, T Andelman, D Pal, S Chen, RE Riman, CM Roth and PV Moghe. (2010). Albumin nanoshell encapsulation of near-infrared-excitable rare-Earth nanoparticles enhances biocompatibility and enables targeted cell imaging. *Small* 6:1631-40.
37. Rossi MP, J Xu, J Schwarzbauer and PV Moghe. (2010). Plasma-micropatterning of albumin nanoparticles: Substrates for enhanced cell-interactive display of ligands. *Biointerphases* 5:105-13.

38. Tai HC and HM Buettner. (1998). Neurite outgrowth and growth cone morphology on micropatterned surfaces. *Biotechnol Prog* 14:364-70.
39. Doherty P, E Williams and FS Walsh. (1995). A soluble chimeric form of the L1 glycoprotein stimulates neurite outgrowth. *Neuron* 14:57-66.
40. Iwamoto T. (2013). Clinical application of drug delivery systems in cancer chemotherapy: review of the efficacy and side effects of approved drugs. *Biol Pharm Bull* 36:715-8.
41. Cui M, DJ Naczynski, M Zevon, CK Griffith, L Sheihet, I Poventud-Fuentes, S Chen, CM Roth and PV Moghe. (2013). Multifunctional Albumin Nanoparticles As Combination Drug Carriers for Intra-Tumoral Chemotherapy. *Adv Healthc Mater*.
42. Rao SS, N Han and JO Winter. (2011). Polylysine-modified PEG-based hydrogels to enhance the neuro-electrode interface. *J Biomater Sci Polym Ed* 22:611-25.
43. Webb K, E Budko, TJ Neuberger, S Chen, M Schachner and PA Tresco. (2001). Substrate-bound human recombinant L1 selectively promotes neuronal attachment and outgrowth in the presence of astrocytes and fibroblasts. *Biomaterials* 22:1017-28.
44. Park KH, H Kim and K Na. (2009). Neuronal Differentiation of PC12 Cells Cultured on Growth Factor-Loaded Nanoparticles Coated on PLGA Microspheres. *Journal of Microbiology and Biotechnology* 19:1490-1495.
45. Nojehdehian H, F Moztarzadeh, H Baharvand, H Nazarian and M Tahriri. (2009). Preparation and surface characterization of poly-L-lysine-coated PLGA microsphere scaffolds containing retinoic acid for nerve tissue engineering: In vitro study. *Colloids and Surfaces B-Biointerfaces* 73:23-29.
46. Nojehdehian H, F Moztarzadeh, H Baharvand, NZ Mehrjerdi, H Nazarian and M Tahriri. (2010). Effect of poly-L-lysine coating on retinoic acid-loaded PLGA microspheres in the differentiation of carcinoma stem cells into neural cells. *The International journal of artificial organs* 33:721-30.
47. Xu J. (2010). Albumin-derived nanoparticles: a flexible biointerface for enhanced adhesion, spatial guidance, and growth factor stimulation of human mesenchymal stem cells. In: *Cell and Development Biology*. Rutgers, The State University of New Jersey, New Brunswick, NJ. pp 81.

Chapter 3

Oriented, multimeric biointerfaces of the L1 cell adhesion molecule: An approach to enhance neuronal and neural stem cell functions on 2-D and 3-D polymer substrates

Note: This chapter is reproduced from the following publication: **Cherry JF, Carlson AC, Benarba FL, Sommerfeld S, Verma D, Loers G, Kohn J, Schachner M, Moghe PV. *Oriented, multimeric biointerfaces of the L1 cell adhesion molecule: An approach to enhance neuronal and neural stem cell functions on 2-D and 3-D polymer substrates. Biointerphases, 2012. 7(1-4):22.***

Abstract

This article focuses on elucidating the key presentation features of neurotrophic ligands at polymer interfaces. Different biointerfacial configurations of the human neural cell adhesion molecule L1 were established on two-dimensional films and three-dimensional fibrous scaffolds of synthetic tyrosine-derived polycarbonate polymers and probed for surface concentrations, microscale organization, and effects on cultured primary neurons and neural stem cells. Underlying polymer substrates were modified with varying combinations of protein-A and poly-D-lysine to modulate the immobilization and presentation of the Fc fusion fragment of the extracellular domain of L1 (L1-Fc). When presented as an oriented and multimeric configuration from protein A-pretreated polymers, L1-Fc significantly increased neurite outgrowth of rodent spinal cord neurons and cerebellar neurons as early as 24 hours compared to the traditional presentation via adsorption onto surfaces treated with poly-D-lysine. Cultures of human neural progenitor cells screened on the L1-Fc/polymer biointerfaces showed significantly enhanced neuronal differentiation and neuritogenesis on all PA oriented substrates. Notably, the highest degree of β -III-tubulin expression for cells in 3-D fibrous scaffolds were observed in

protein-A oriented substrates with PDL pretreatment, suggesting combined effects of cell attachment to polycationic charged substrates with subcellular topography along with L1-mediated adhesion mediating neuronal differentiation. Together, these findings highlight the promise of displays of multimeric, neural adhesion ligands via biointerfacially engineered substrates to "cooperatively" enhance neuronal phenotypes on polymers of relevance to tissue engineering.

3.1. Introduction

Neurodegenerative diseases and traumatic injuries can cause irreversible damage to the central nervous system (CNS), resulting in a significant deficit in motor and sensory function due to a limited endogenous capacity for regeneration and targeted axonal regrowth^[1]. An ideal strategy for CNS repair would promote regrowth/sprouting, neuronal survival, synaptogenesis, and remyelination of host axons while stimulating transplanted exogenous neural cells to survive, migrate, and integrated within host tissue^[2]. Engineered biomaterials involving specific neural cell adhesion ligands have been recently explored for their ability to support neurite outgrowth and neuronal differentiation relevant for CNS repair^[3,4]. However, the effective integration of neuronal bioactivity along with transplantable substrate designs remains a major challenge. Conventional bioactive or biomimetic substrates for neural engineering applications have presented peptides, extracellular matrix proteins, growth factors, and cell adhesion proteins^[5-9].

A key adhesion ligand for promoting neuronal survival and differentiation, as well as regeneration after trauma is the neural cell adhesion molecule L1. L1 is a transmembrane glycoprotein of the immunoglobulin superfamily that also shares several binding domains with fibronectin^[10]. L1 acts through homophilic (L1-L1) interactions, as well as heterophilic interactions^[11-13] and plays a critical role in neural cell adhesion^[14-16], neurite fasciculation,

neuronal protection[17,18], synaptic plasticity, axonal outgrowth and adhesion^[19], subcellular synapse organization and cell migration^[20,21]. It is expressed on the cell surface of postmitotic neurons in the CNS and peripheral nervous system (PNS), as well as Schwann cells in the PNS^[22]. L1 has also been shown to improve functional recovery and improved corticospinal tract regrowth following spinal cord injury in mice^[23].

The role of L1 in neuronal differentiation of neural stem cells has also been investigated. Primary mouse neural stem cells demonstrated enhanced neuronal differentiation and decreased astrocyte differentiation when cultured on substrates pretreated with L1-Fc or fibroblasts engineered to express L1-Fc, compared to poly-D-lysine and laminin-treated surfaces^[24]. Additionally, L1-Fc treated surfaces primarily promoted GABAergic differentiation over other cell types, suggesting that L1 can influence neuronal subtype specification in the absence of growth factors^[24]. In another study, L1-transfected mouse embryonic stem cells exhibited enhanced process extension and migration in comparison to non-transfected stem cells when injected into a spinal cord lesion site, which induced enhanced recovery of function^[25]. Both studies demonstrate that L1 promotes neuronal versus astrocytic differentiation of stem cells.

Despite the widespread interest in the biological activity of L1, mechanisms and approaches for optimally presenting L1 from biomedically relevant materials for cell transplantation remain to be systematically examined. A variety of materials of natural and synthetic origin, have been previously shown to promote adhesion, proliferation, neurite extension, and neuronal differentiation of neural cells *in vitro* and *in vivo*^[26-28]. Synthetic polymer based biomaterial scaffolds have the added advantage of controlled chemistries, resulting in graded mechanical properties and degradation rates, which can all influence protein adsorption, adhesion ligand presentation, and cell behavior^[29,30]. Synthetic polymer based scaffolds are also amenable to specific presentation of bioactive cues that can

promote neurite outgrowth and neuronal differentiation, including growth factors and ECM proteins^[31,32]. Various scaffold configurations have also been proposed including conduits, porous polymer scaffolds, hydrogels, and fibers.^[27,28,30] Electrospun fibrous substrates in particular exhibit high surface area and porosity, controllable geometric features, and the ability to elicit contact guidance cues for neurite orientation and while recapitulating the topography of native extracellular matrix^[33,34].

In this study, we combined both 2-D and 3-D substrate configurations fabricated from biodegradable synthetic polymers, with the goal of modulating controlled surface presentation of the neural adhesion molecule L1. Polymer films (2-D) and fibrous polymer scaffolds (3-D) were fabricated from tyrosine-derived polycarbonates, a combinatorial library of degradable polymers with tunable mechanical properties, surface properties, and degradation rates^[35,36]. Specifically, the base monomer poly(desaminotyrosyl tyrosine ethyl ester carbonate) (poly(DTE carbonate)) can be copolymerized with variable amounts of desaminotyrosyl tyrosine (DT) and/or poly(ethylene glycol) (PEG), resulting in polymers with similar structures but variable degradation rates and protein adsorption properties. We used three different approaches to establish biointerfaces of L1-Fc: 1) the conventional adsorption of L1-Fc onto substrates pretreated with poly-D-lysine, 2) presentation of L1-Fc from substrates pretreated with PDL and protein A and 3) presentation of L1-Fc from substrates pretreated with protein A alone. We hypothesized that the presentation of L1-Fc via substrate-coated protein A would promote the outward display of surface-bound L1-Fc, while presenting L1-Fc in a more optimal, physiologically-relevant manner, compared to the random orientation of L1-Fc/PDL coated substrates. We report that multimeric presentation of L1-Fc via binding to protein A enhanced adhesion and neurite outgrowth in 2-D configurations and that this effect was also replicated in a 3-D configuration, consisting of aligned scaffolds of polymer fibers biofunctionalized with L1-Fc. This is also the first

report of effects of substrate biofunctionalized L1 on human neural progenitor cell behavior.

3.2. Materials and Methods

3.2.1. Biointerfaces on Polymer Thin Films

A 1% (w/v) poly(DTE-co-10% DT-co-1% PEG_{1k} carbonate) polymer solution was prepared by dissolving the polymer in tetrahydrofuran (THF) (Sigma-Aldrich, St. Louis, MO, USA) overnight at room temperature. The polymer solution was then filtered using a 0.45 μm Whatman pTFE filter and spin-coated onto 12 mm coverslips. The thin films were dried for at least 24 hours under vacuum and UV sterilized for 15 minutes, prior to coating with proteins. The thin films were then coated with 100 $\mu\text{g}/\text{ml}$ of poly-D-lysine (PDL) (70-150 kDa; Sigma-Aldrich) for 1 hour at room temperature. After three washes with ultrapure water, the films were coated with 1.25 $\mu\text{g}/\text{ml}$ of protein A (PA) (Invitrogen, Carlsbad, CA, USA) for 1 hour at room temperature. Following three washes with ultrapure water, the films were coated with 2, 10, or 50 $\mu\text{g}/\text{ml}$ of human L1-Fc (R&D Systems, Minneapolis, MN, USA) overnight at 4°C. L1-Fc is the fusion of the Fc region of human IgG₁, which contains two disulfide bonds, to two extracellular domains of human L1. For controls, the thin films were kept hydrated with phosphate buffered saline (PBS, Lonza, Walkersville, MD, USA) overnight. Prior to seeding the cells, the films were washed three times with PBS and used immediately. The resulting conditions were as follows: L1-Fc/PDL, L1-Fc/PA/PDL, and L1-Fc/PA and the corresponding controls.

3.2.2. Verification of L1-Fc Functionality

Enzyme-linked immunosorbent assay (ELISA) was used to determine the presence of L1-Fc on different substrates. Each substrate was prepared as described above. Next, the thin films were washed in PBS one time for 2 minutes and treated with a blocking solution

composed of 1% bovine serum albumin (BSA, Sigma Aldrich, St. Louis, MO, USA), in PBS for 1.5 hours at room temperature. After one wash for 2 minutes in PBS, the samples were incubated with a monoclonal mouse anti-L1 antibody, clone L1.1 (1 μ g/ml) (Invitrogen), specific for the extracellular domain of human L1 for 1.5 hours and washed three times for 5 minutes each with PBS containing 0.05% Tween-20 (PBST). The substrates were then treated with the secondary antibody, alkaline phosphatase conjugated-goat anti-mouse IgG antibody (Sigma-Aldrich) for 1.5 hours at room temperature. Following three, 5 minute washes with PBST, the substrates were reacted with alkaline phosphatase yellow (pNPP) liquid substrate (Sigma-Aldrich) for up to 30 minutes in the dark at room temperature. The reaction was stopped with 3 N NaOH and the substrates were read on an absorbance plate reader at 405 nm. The absorbance readings were used to assess the presence of L1-Fc on each substrate compared to the respective controls.

3.2.3. Quantification of Protein Layer on Polymer Thin Films

Deposition of polypeptide and proteins layers on polymer thin films was measured using a quartz crystal microbalance with dissipation (QCM-D) (Qsense E4, Biolin Scientific, Linthicum Heights, MD, USA). Polymer thin film substrates using gold-coated sensor crystals (QSX301, Biolin Scientific, Linthicum Heights, MD, USA) were prepared as described above using spin coating except dioxane (Fisher Scientific, Pittsburgh, PA, USA) was used as the solvent. Prior to measurement, the polymer coated sensor crystals were equilibrated in PBS for at least 1 hour at 37°C to establish a stable baseline. Subsequently, PDL (100 μ g/ml), PA (20 μ g/ml) and L1-Fc (10 μ g/ml) were perfused through the flow system for 30 minutes at a flow rate of 24.2 μ l/min. The deposition of each layer was followed by a PBS wash for at least 30 minutes. Control experiments were conducted replacing deposition of respective layer with PBS perfusion. The frequency and dissipation were measured during each experiment. For raw data analysis the fifth overtone (25 MHz) was used. Hydrated mass per

surface area of L1-Fc was modeled from the frequency and dissipation of the fifth and seventh overtone according to the Voigt model (Q-tools software)^[37]. From the information obtained from the Voigt model and the bulk L1-Fc concentration applied to the crystals, the percent of L1-Fc deposited onto each thin film was also determined.

3.2.4. AFM Analysis of Biointerfaces on Thin Films

Atomic force microscopy (AFM) was utilized to visualize of L1-Fc spatial distribution and the thickness of each thin film. Each thin film was prepared as described above. Next, films were blocked in a blocking solution of 1% BSA in PBS for 30 minutes at room temperature. Following three washes with PBS, the substrates were treated with the L1.1 antibody (1 μ g/ml) for 30 minutes. The substrates were washed three times with PBS and incubated with Nanogold® goat anti-mouse IgG antibody (1:40 dilution) (Nanoprobes, Yaphank, NY, USA) for 30 minutes. To amplify the gold signal, thin films were treated for 5 minutes with a silver enhancement kit, which would increase the gold particle size from 30-100 nm, depending on treatment time (LI Silver Enhancing Kit, Invitrogen). We chose to use the shortest treatment time possible as large variability in particle size has been shown to increase with time^[38]. The samples were then washed with ultra-pure water and air dried in a desiccator overnight prior to AFM imaging. AFM height images in tapping mode were collected using a Multimode AFM having a Nanoscope-IIIa controller equipped with a J-type piezo scanner (Veeco Metrology Group, Santa Barbara, CA, USA).

3.2.5. Fibrous Polymer Scaffold Fabrication and Characterization

Fibrous scaffolds were fabricated by electrospinning poly(DTE-co-10% DT-co-1% PEG_{1k} carbonate). An 18% (w/v) solution was prepared by dissolving the polymer in glacial acetic acid (Fisher) overnight at room temperature. Fibrous scaffolds were produced by flowing the polymer solution through an 18-gauge needle at a flow rate of 1 ml/hr,

controlled by a programmable syringe pump (KD Scientific, Holliston, MA, USA). A voltage of +24kV was applied to the needle by a 30 kV dual polarity power supply (Gamma High Voltage Research, Inc, Ormond Beach, FL, USA) and the fibers were collected on a rapidly rotating mandrel spaced 18 cm from the needle. The scaffolds were allowed to dry under vacuum for at least 3 days and were UV sterilized for 30 min prior to protein treatment and cell culture.

Surface morphology of the electrospun scaffolds was observed on an AMRAY 1830 I scanning electron microscope (SEM). Samples for SEM imaging were dried under vacuum, and sputter-coated with gold-palladium^[39]. Imaging was performed at 20 kV acceleration potential. Quantification of the fiber diameter distribution was based upon measurement of 100 individual fibers in either 1000x SEM images using NIH-ImageJ software (<http://rsb.info.nih.gov/ij/>).

Fiber alignment was quantified from SEM images using ImageJ, similar to a previously described method^[40]. Briefly, ImageJ was used to measure the angle of alignment of each fiber in a given SEM image and the angle difference between each fiber and the mean fiber angle was calculated. This data is shown as a histogram of angle differences. The alignment of at least 100 fibers was measured.

3.2.6. Primary Neuronal Cell Cultures

Spinal cord neurons (SCNs) were obtained following a protocol that was adopted and modified from what was previously described^[41], using embryonic day 15 rat embryos obtained from pregnant Sprague-Dawley rats (Taconic, Germantown, NY, USA). The spinal cord neurons were cultured in serum free neurobasal medium (Invitrogen) supplemented with 1x B27 supplement (Invitrogen), 2mM glutamine (Invitrogen) and 1% penicillin/streptomycin (Lonza) and maintained for 24 hours.

Cerebellar neurons (CNs) were obtained from P8 Sprague-Dawley rat pups, following a protocol previously described^[42]. The cells were cultured in serum free neurobasal-A medium (Invitrogen), supplemented with 1x B27 supplement, 25mM KCl, 2mM glutamine, and 1% penicillin/streptomycin.

3.2.7. Quantification of Neurite Outgrowth

For neurite outgrowth studies of spinal cord neurons and cerebellar neurons, both cell types were plated at 2×10^4 cells/cm² onto thin films or 3.1×10^4 cells/cm² onto scaffolds pretreated with different L1-Fc presentations and controls. The cells were fixed and immunostained with mouse monoclonal β -III-tubulin (clone TUJ1, Covance, Berkeley, CA, USA) after 24 hours in culture. For each condition, 10 fields of view at 40x magnification were imaged using a Leica TCS.SP2 confocal microscope system (Leica Microscope, Exton, PA). For image analysis, total neurites were measured using NIH-ImageJ imaging software. Only neurites that were equal to or greater than the diameter of a cell body were measured. In the case of SCNs, the average length of the longest neurite was also measured for cells with multiple membrane processes.

3.2.8. Functional Blocking Assays of Cell Adhesion and Neurite Outgrowth

To determine if L1-Fc presentation affected the availability of different binding sites, we investigated how blocking interactions between substrate bound L1-Fc and cellular L1 or $\alpha_v\beta_3$ integrin receptors influenced neurite outgrowth and cell attachment. To block L1-L1 homophilic interactions, each substrate was treated with 50 μ g/ml of anti-L1 antibody, clone L1.1 or mouse IgG1 isotype control (R&D Systems), for 1 hour, prior to seeding SCNs. In order to competitively inhibit the interaction between L1 and $\alpha_v\beta_3$, SCNs were treated with various concentrations of cyclic RGD (cyclo-RGDfV) peptide (Peptides International, Louisville, KY, USA) for 1 hour prior to plating the cells onto the different L1-presenting

substrates. SCNs were cultured for 24 hours, immunostained with β -III-tubulin, and analyzed for cell attachment and neurite outgrowth. For each metric, 10 fields of view were taken for each condition and the number of nuclei for each view was counted or neurites were measured using NIH-ImageJ imaging software.

3.2.9. hESC-Derived Neural Progenitor Cell Culture and Differentiation

ENStem-A neural progenitor cells (NPCs) were purchased from Millipore (Millipore, Temecula, CA, USA). These neural progenitor cells were derived from NIH approved H9 human embryonic stem cells (hESCs). For cell expansion and maintenance, NPCs were cultured in 6 cm culture dishes coated with $\frac{1}{4} \times$ stock Matrigel (BD Biosciences, Franklin Lakes, NJ, USA) in ENStem-A neural expansion medium (Millipore) at 37°C in 5% CO₂. Medium was changed every 2 days and cells were passaged, by mechanical dissociation, once they reached 90-95% confluence (every 4-5 days) at a ratio of 1:2 or 1:3.

NPC differentiation was initiated once the cells reached about 85-90% confluence, by removing ENStem-A medium, washing two times with warm neurobasal medium, and replacing the medium with neural differentiation medium (NDM) composed of neurobasal medium, 1x B27 supplement, 2mM glutamax (Invitrogen), 1% penicillin/streptomycin. After four days in NDM, the cells were passaged with Accutase (Invitrogen) and plated on L1-Fc coated thin films and scaffolds at a density of 6.25×10^4 cells/cm² or 2×10^4 cells/cm², respectively and allowed to differentiate for 7 days, with medium changes every two days.

3.2.10. Immunocytochemistry of Neuronal Phenotypes

After 24 hours (SCNs or CNs) or 7 days (NPCs), culture medium was removed and the cells were fixed in 4% paraformaldehyde for 20 minutes at room temperature and then washed three times with PBS. The cells were then permeabilized with 0.1% Triton-X,

followed by three PBS washes. To prevent non-specific antibody binding, the samples were blocked with 5% normal goat serum (MP Biomedicals, Solon, OH, USA) in PBS (blocking buffer), for 1 hour at room temperature. Primary antibodies were then diluted in the blocking buffer and applied to the samples overnight at 4°C. Following the removal of the primary antibody, the cells were washed three times, for 20 minutes each time, and the secondary antibodies, along with 1 µg/ml of Hoechst 33258 (Sigma-Aldrich) were diluted in blocking buffer and applied for 1 hour at room temperature, followed by three, 20 minutes washes with PBS. Primary antibodies mouse anti-β-III-tubulin and mouse anti-nestin (IgG1) (Millipore) followed by isotype specific Alexa Fluor 488, 594, or 647 goat-anti mouse secondary antibodies (Invitrogen) were used for the studies.

3.2.11. Statistical Analysis

The data is expressed as mean ± the standard error of the mean. Variance of analysis using one-way ANOVA was used followed by *post hoc* means comparison with Tukey's test. Differences between conditions were considered statistically significant with p values < 0.05. All data represents three independent experiments performed in duplicate.

3.3. Results

3.3.1. Protein A Coated Polymer Films Support Increased Surface Adsorption of L1-Fc

The relative amount of the neuritogenesis-promoting domain exposed within L1-Fc adsorbed onto polymer thin films treated with PDL, PA/PDL, or PA was determined by ELISA (Figure 3.1A). We examined three different concentrations (2 µg/ml, 10 µg/ml, and 50 µg/ml) to characterize L1-Fc epitope exposure on the surface using multimeric versus random modes of presentation. ELISA results showed increased and dose-dependent L1-Fc increased exposure of the neuritogenesis-promoting epitope on PA containing substrates compared to PDL controls. These results support a more outward display of L1 on PA-

treated substrates, given the nature and location of antibody binding epitopes within the N-terminal, first and second Ig-like domains of the ectodomain of L1^[43].

The amount of L1-Fc adsorbed on the polymer thin films was quantified using QCM-D. Representative QCM-D plots of frequency over time show subsequent frequency drops indicating deposition of PDL, PA, and L1-Fc, respectively (Figure 3.1B). An average frequency change for the deposition of PDL of $\Delta f = -9 \pm 0.9$ Hz was observed. The frequency change for the deposition of PA was higher for surfaces with prior PDL deposition with $\Delta f = -15 \pm 0.3$ Hz as compared to $\Delta f = 7 \pm 4.1$ Hz for PA on uncoated polymer surfaces. For both PDL and PA, only small changes of dissipation were observed with $\Delta D < 10$. Deposition of L1-Fc subsequent to deposition of PA and PDL led to much larger changes of -70 ± 17.3 Hz and a dissipation change of $\Delta D = 8 \pm 3.4$. The hydrated mass per surface area of L1-Fc was calculated using the Voigt model for all conditions (Figure 3.1C). The Voigt mass of L1-Fc was highest with $m = 2.8 \pm 0.84$ $\mu\text{g}/\text{cm}^2$ subsequent to coating the polymer surface with both PDL and PA. A slightly lower mass of L1-Fc was deposited on the polymer surface treated only with PA with $m = 1.9 \pm 0.56$ $\mu\text{g}/\text{cm}^2$. In comparison, the deposited mass of L1-Fc onto the exclusively PDL treated polymer surfaces was even lower with $m = 0.8 \pm 0.15$ $\mu\text{g}/\text{cm}^2$. The percent of L1-Fc deposited onto the surface from the added bulk ligand concentration is shown in (Figure 3.1D). The results of the ELISA and QCM-D studies confirm that PA-based presentation of L1-Fc results in increased levels of L1-Fc adsorption onto the polymer thin films.

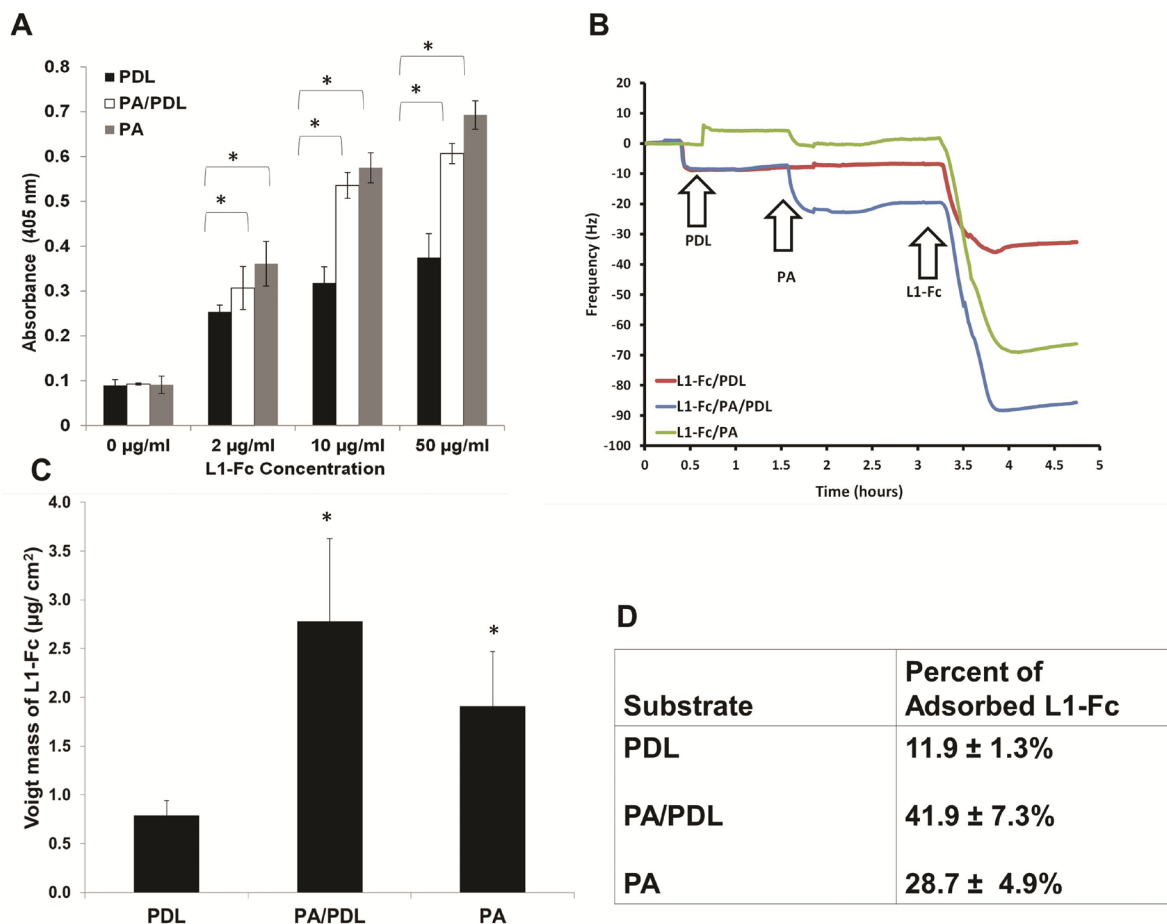


Figure 3.1. Presentation of L1-Fc by protein A results in enhanced L1 adsorption and improved directed presentation of L1-Fc. (A) ELISA was used to determine the relative amounts of L1-Fc on the polymer thin films treated with and without PA. L1-Fc (2, 10, 50 µg/ml) was adsorbed on PDL with and without PA (PDL, PA/PDL) or PA alone (PA). (B) Representative QCM-D plots of frequency versus time: L1-Fc deposition on PDL (red); PA/PDL (blue), and PA (green). (C) Voigt mass of L1-Fc deposition modeled from QCM-D data subsequent to PDL, PA/PDL, or PA deposition. (D) The percent of L1-Fc adsorbed onto each surface during the QCM-D, from a bulk concentration of 10 µg/ml of L1-Fc. PDL: poly-D-lysine. PA: protein A. (* denotes $p < 0.05$).

3.3.2. Spatial Distribution of L1-Fc when Presented on PDL and Protein A

We hypothesized that L1-Fc presentation was multimeric and oriented on PA coated polymer thin films (Figure 3.2B) compared to a more randomly, oriented presentation on PDL coated polymer films (Figure 3.2A). Atomic force microscopy, using dry tapping mode, was used to quantify the spatial distribution, substrate thickness, and relative sizes of L1 complexes using gold-conjugated antibodies and silver counterstaining. L1-Fc adsorbed

onto PDL resulted in complexes diffusely distributed on the thin films with a surface thickness of 23.5 ± 1.9 nm. L1-Fc presented from PDL and PA or PA alone also resulted in diffusely distributed L1-Fc protein complexes with surface thicknesses 23.5 ± 1.8 nm and 23.2 ± 1.5 nm respectively (Figure 3.2C). While there was no difference in the thickness of each substrate, which was a result of adsorbed L1-Fc complexed with the primary and gold-conjugated-silver enhanced secondary antibodies, it was clear that PA-presented L1-Fc resulted in increased L1-Fc adsorbed to the surface, as is indicated by the increase in the density of the complexes in the two-dimensional images and three-dimensional images of substrate topography (Figure 3.2C). We also measured the width of the protein complexes using the cross-sectional profiles of the complexes shown in the third column of Figure 3.2C. Thin films of L1-Fc/PDL exhibited well-defined peaks indicative of less aggregation, whereas L1-Fc presented from PA/PDL or PA alone resulted in peaks that were wider and less defined, suggesting the close apposition of multiple complexes, and greater density that is consistent with increased surface concentrations of L1-Fc quantified via ELISA in Figure 3.1A.

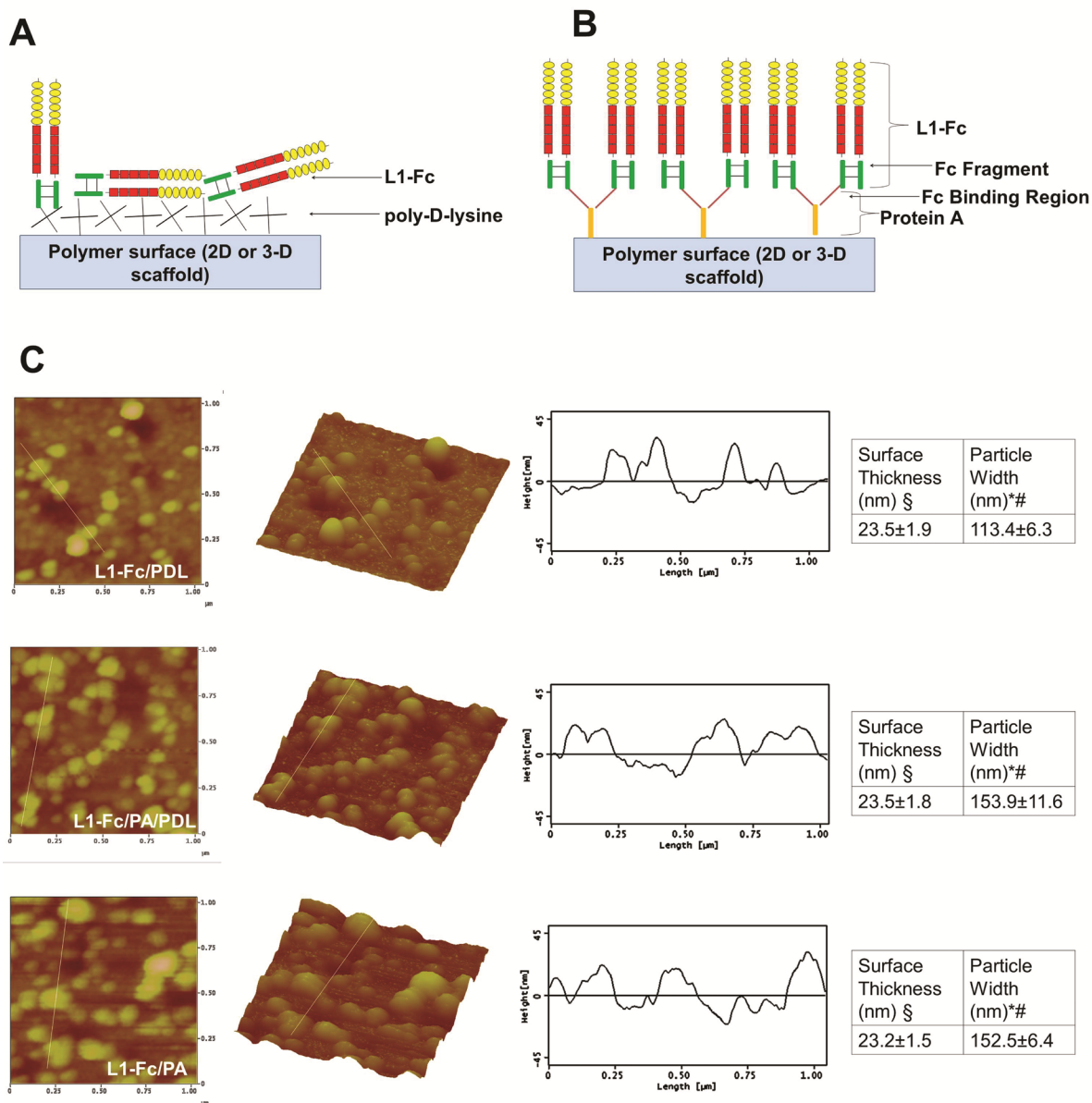


Figure 3.2. Differentially treated polymer films alter surface presentation of L1-Fc. (A) Schematic representation of how L1-Fc might randomly orient when coated onto a layer of PDL. (B) PA presentation will result in four L1-Fc molecules per PA molecule^[68] enabling the multimeric, oriented presentation of L1-Fc. (C) AFM images ($1 \times 1 \mu\text{m}^2$, two and three dimensional) and cross-sectional profiles of the protein complexes, which correspond to the lines drawn on the images of thin polymer films coated with L1-/Fc/PDL, L1-Fc/PA/PDL, or L1-Fc/PA. Thin films in which L1-Fc is presented from PA revealed increased in L1-Fc adsorption as shown by the increase in protein complexes in the 2-D and 3-D images. PA presented L1-Fc resulted in cross-sectional profiles with wider peaks compared to L1-Fc adsorbed on PDL. A summary of the thickness of the thin films and the width of the protein complexes is shown in the tables to the far right. PDL: poly-D-lysine. PA: protein A. (* denotes $p < 0.05$ compared to both PDL and PA/PDL controls, § denotes $p < 0.05$ compared to PA control, # denotes $p < 0.05$ compared to the L1-Fc/PDL condition).

3.3.3. Multimeric L1 Presentation Enhances Neurite Outgrowth of Cultured Neurons on 2-D Films

Spinal cord neurons (SCNs) were cultured on variable L1-Fc configurations for 24 hours (Figure 3.3A-3.3C). At increasing concentrations of L1-Fc, L1-Fc elicited longer neurite extensions of SCNs when presented on PA containing films compared to thin films only coated with PDL (Figure 3.3A). The average SCN neurite lengths on the L1-deficient controls PDL, PA/PDL, and PA averaged around $53 \pm 2.4 \mu\text{m}$ (Figure 3.3B) and were comparable to $2 \mu\text{g/ml}$ of L1-Fc presented from PDL and PA/PDL. In contrast, the earliest significant increase in neurite length ($75.9 \pm 8.4 \mu\text{m}$) was elicited by $2 \mu\text{g/ml}$ of L1-Fc presented from PA alone. Increased L1-Fc concentrations progressively elicited enhanced neurite extension. Both L1-Fc/PA/PDL and L1-Fc/PA promoted increased neurite lengths on $10 \mu\text{g/ml}$ ($145.1 \pm 12.1 \mu\text{m}$ and $154.8 \pm 12.7 \mu\text{m}$, respectively) and $50 \mu\text{g/ml}$ ($186.4 \pm 5.5 \mu\text{m}$ and $182.8 \pm 13.4 \mu\text{m}$, respectively) of L1-Fc in comparison to the PDL/L1-Fc substrates ($73.4 \pm 4.5 \mu\text{m}$ and $93.1 \pm 10.3 \mu\text{m}$). These results show that 1) PA presentation greatly improves L1-Fc mediated neurite outgrowth of spinal cord neurons and 2) PDL does not additionally contribute to enhanced cell attachment or extensions when L1-Fc is presented from PA.

Cell-L1 binding has been reported to be cell type specific^[44]. Therefore, we also examined how a different source of neurons, namely cultured cerebellar neurons (CNs), responded to variable L1-Fc presentation after 24 hours. Similar to the observation with SCNs, polymer films where L1-Fc was presented via PA/PDL or PA alone promoted enhanced neurite outgrowth ($112 \pm 5.8 \mu\text{m}$ and $115.3 \pm 7.8 \mu\text{m}$, respectively) when compared to L1-Fc coated onto PDL ($82.4 \pm 6.6 \mu\text{m}$) (Figure 3.3E). In addition, CNs grown on L1-Fc/PA extended thinner, finer neurites compared to thicker extension observed on

L1-Fc/PA/PDL surfaces (Figure 3.3D) suggesting that PDL may have a modest cooperative influence over neurite adhesion for cerebellar neurons.

3.3.4. Multimeric L1 Presentation Enhances Neurite Outgrowth of Cultured Neurons in 3-D, Fibrous Substrates

Next, neurite extension was examined on fibrous scaffolds fabricated from poly(DTE carbonate) polymer, combined with fiber-based multimeric L1-Fc presentation. Scaffolds with aligned fiber orientation were designed to promote directional neuronal cell growth,[45,46] fabricated by electrospinning and visualized using SEM. The morphology of the aligned scaffolds is shown in Figure 3.4A, where the average fiber diameter was found to be $1.25 \pm 0.5 \mu\text{m}$. The alignment quantification of the fibers demonstrates that the scaffolds have a high degree of fiber alignment, with the predominant fiber counts falling at an angle difference of 0 degrees, the fiber axis parallel to the reference line (Figure 3.4B). All scaffolds treated with L1-Fc showed extensive neurite outgrowth along the direction of the aligned fibers (Figure 3.4C). However, L1-Fc/PA/PDL and L1-Fc/PA promoted significantly longer neurite outgrowth ($99.5 \pm 5.2 \mu\text{m}$ and $103 \pm 6.7 \mu\text{m}$, respectively) compared to PDL/L1-Fc ($71.8 \pm 5.1 \mu\text{m}$) and the controls (Figure 3.4D). As observed with SCNs, all presentations of L1-Fc resulted in directional growth of CNs, but enhanced neuritogenesis was observed on L1-Fc/PA/PDL ($97.04 \pm 5.6 \mu\text{m}$) or L1-Fc/PA ($104.88 \pm 9.1 \mu\text{m}$) presenting scaffolds as well (Figure 3.4E-3.4F).

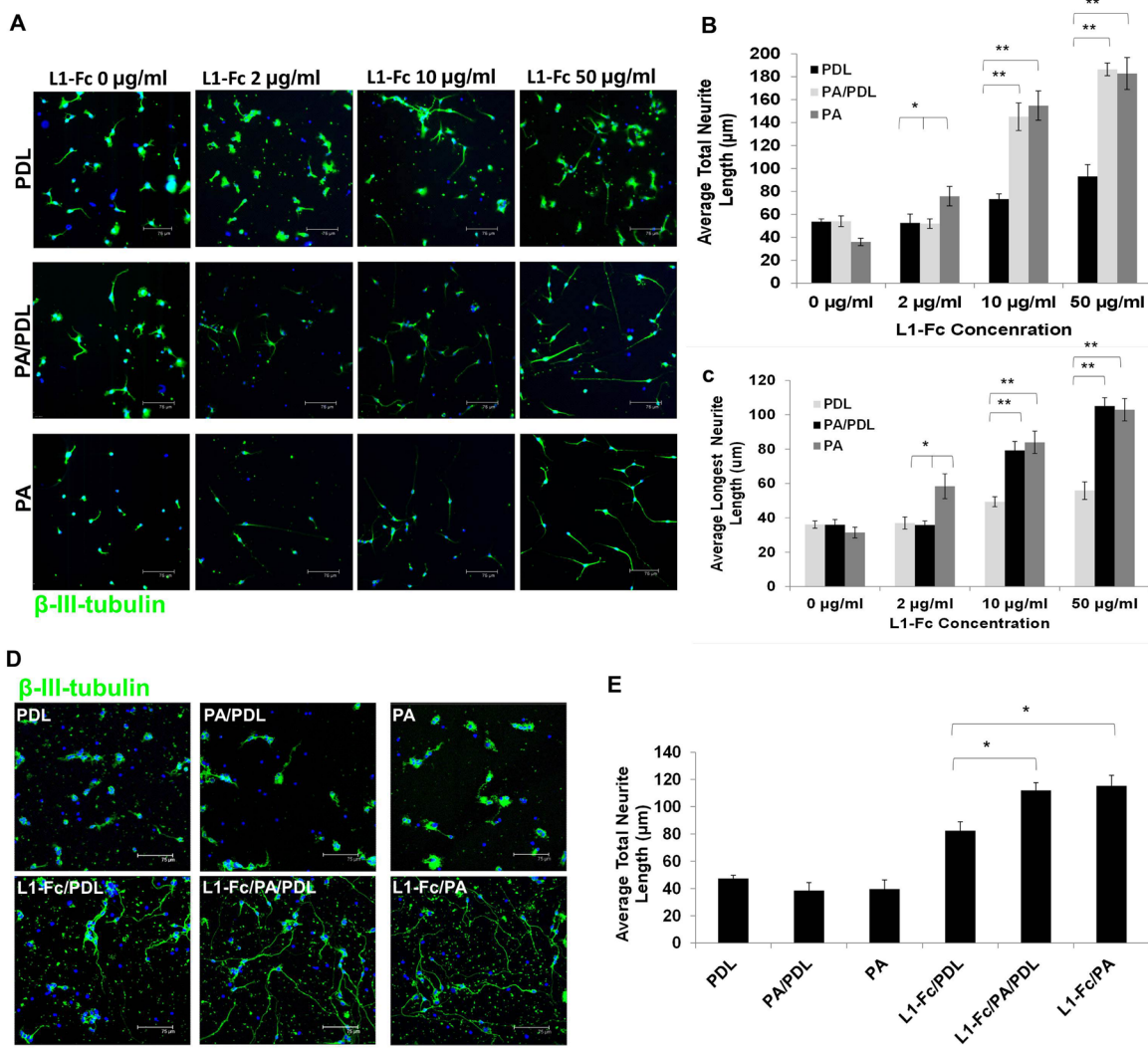


Figure 3.3. Protein A presentation of L1-Fc enhances neurite outgrowth in spinal cord and cerebellar neurons. (A) Spinal cord neurons (SCNs) were plated on L1-Fc adsorbed onto PDL (L1-Fc/PDL), a combination of PDL and PA (L1-Fc/PA/PDL), and PA alone (L1-Fc/PA), as well as control surfaces that did not contain L1-Fc. SCNs cultured for 24 hours on L1-Fc/PA/PDL or L1-Fc/PA extended longer neurites compared to those on L1-Fc/PDL treated films. At 2 µg/ml, L1-Fc/PA was the only condition in which neurites were longer compared to the controls, suggesting that PA promoted more L1-Fc adsorption to this surface, making small amounts of L1-Fc effective. (B) Quantification of the average total neurite outgrowth indicated that on 10 or 50 µg/ml of L1-Fc, there was no significant difference in outgrowth between the two conditions in which L1-Fc was presented from protein A (with or without PDL). (C) Quantification of the average length of the longest neurite per cell. (D) Morphology of cerebellar neurons that were seeded onto the same substrates listed above, where 10 µg/mL of L1-Fc was used. (E) Substrates in which L1-Fc was presented using PA resulted in enhanced neurite outgrowth of cerebellar neurons compared to neurons cultured on L1-Fc presented from PDL. Scale bar = 75 µm. PDL: poly-D-lysine. PA: protein A. (* denotes $p < 0.05$, ** denotes $p < 0.01$).

3.3.5. Role of L1-L1 Homophilic Cell-Substrate Adhesion Underlying Neurite

Outgrowth on Multimeric L1 Films

To establish that the multimeric L1-Fc presenting films engendered L1 cell receptor-mediated adhesion, each surface was treated with a monoclonal antibody against L1 prior to plating spinal cord neurons. A significant reduction in neurite outgrowth of SCNs cultured on L1-Fc/PA/PDL and L1-Fc/PA treated surfaces in the presence of the anti-L1 antibody was observed, with a more pronounced inhibition seen in the L1-Fc/PA condition. Given that L1 multimeric exposure is differentially more amenable to inhibition on L1-Fc/PA substrates indicates a more potent role for L1-L1 adhesion underlying neurite outgrowth of SCNs cultured on L1-Fc/PA compared to L1-Fc/PDL (Figure 3.5A). In the case of SCNs cultured on L1-Fc/PDL, neurite outgrowth was also reduced in the presence of the anti-L1 antibody, however not as markedly as on the other substrates (Figure 3.5B), suggesting that the binding epitopes on L1 are not as accessible for SCN binding when L1-Fc is adsorbed onto PDL treated films. Thin films treated with the isotype control resulted in SCNs with a similar morphology to SCNs cultured on untreated thin films. Additionally, we examined specific binding of the Fc region of L1-Fc to protein A by blocking the Fc region of L1-Fc with an anti-Fc antibody. Neurite outgrowth was greatly reduced in spinal cord neurons cultured on L1-Fc/PA/PDL and L1-Fc/PA surfaces, but not on L1-Fc/PDL treated surfaces, suggesting that L1-Fc is oriented in a specific manner when coupled with protein A (data not shown).

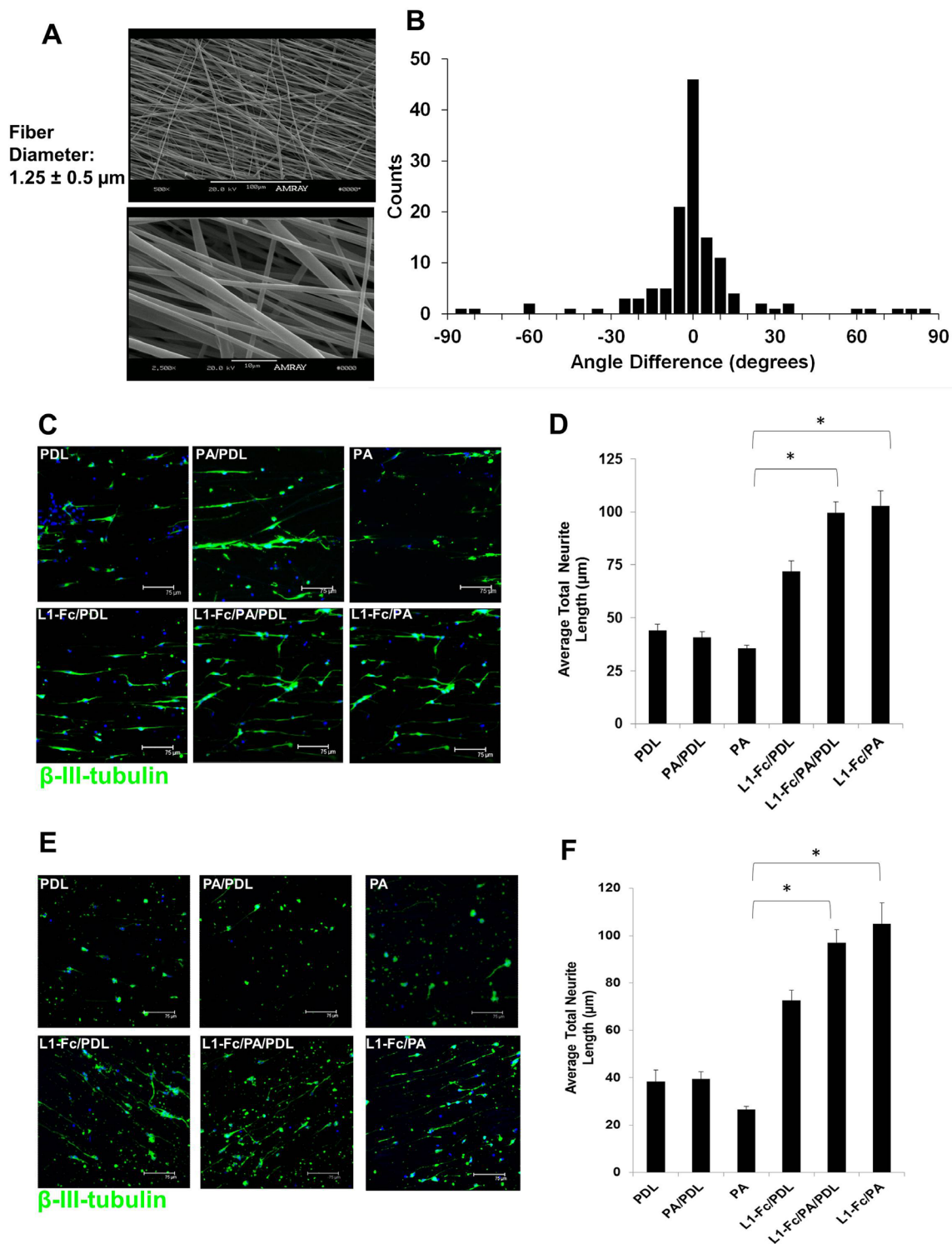


Figure 3.4. Protein A-presented L1-Fc increases neurite outgrowth in aligned, polymeric scaffolds. (A) Morphology and fiber diameter of aligned scaffolds that were fabricated by electrospinning. (B) Histogram depicting the degree of fiber alignment of the scaffolds. (C) Spinal cord neurons (SCNs) were plated onto scaffolds treated with L1-Fc presented from PDL, PA/PDL, or PA alone, as well as control surfaces that did not contain L1-Fc. PA presented L1-Fc results in longer

neurite lengths when cultured on aligned scaffolds. Neurons cultured on 10 $\mu\text{g/ml}$ L1-Fc passively adsorbed onto the fibers extended longer neurites than on the PDL control. The three-dimensional scaffold results are similar to those observed on the polymer thin films. (D) Quantification of the average total neurite lengths of SCNs cultured on the different L1-Fc presentations showed L1-Fc/PDL resulted in SCNs with shorter neurites compared to L1-Fc/PA/PDL and L1-Fc/PA, suggesting that the manner in which L1-Fc is presented on nanofibrous scaffolds influences its efficacy. (E, F) Cerebellar neurons (CNs) were plated onto scaffolds pretreated with different L1-Fc presentations and controls as mentioned above. PA presented L1-Fc resulted in CNs that were more spread and grew longer along the fibers compared to CNs cultured on L1-Fc adsorbed onto PDL. The three-dimensional scaffold results correlate to the results observed on the polymer thin films. Scale bar = 75 μm . PDL: poly-D-lysine, PA: protein A. (* denotes $p < 0.05$).

3.3.6. Multimeric L1 Films Support RGD Peptide-Sensitive Integrin Mediated Cell

Adhesion and Neurite Outgrowth

The L1 molecule contains one RGD sequence located within the sixth-Ig like domain, which has been reported to bind to integrins $\alpha_5\beta_1$ and $\alpha_v\beta_3$ ^[47]. The interaction of $\alpha_v\beta_3$ and L1 has been reported to stimulate neurite outgrowth of the rat pheochromocytoma cell line, PC12, as well as chick dorsal root ganglion cells^[48,49]. We examined the possible interactions of $\alpha_v\beta_3$ cell adhesion receptors and L1-presentation and the resultant effects on cell responses. To this end, cyclic RGD peptides (cyclo-RGDfV) reported to bind $\alpha_v\beta_3$ with high affinity^[50] and inhibit binding of L1 and $\alpha_v\beta_3$ ^[48], were added to SCNs at different concentrations, prior to cell plating onto the different substrates, and cell attachment and neurite outgrowth were examined. Attachment of SCNs cultured on L1-Fc/PA (Figure 3.5C) was considerably reduced to $14.9 \pm 3.2\%$ in the presence of 1 $\mu\text{g/ml}$ of cyclic RGD and further reduced to $8.2 \pm 2.9\%$ when treated with 10 $\mu\text{g/ml}$ of cyclic RGD. Cell attachment was mildly affected, following cyclic RGD peptide treatment of SCNs cultured on L1-Fc/PDL with no significant decrease, compared to untreated cells. These results suggest that cell attachment on L1-Fc/PDL-based substrates is only partially dependent on L1-integrin binding. In contrast, on L1-Fc/PA substrates, $\alpha_v\beta_3$ -L1 binding plays a major role in cell attachment. When PDL and PA were combined to present L1-Fc, only treatment with 20 $\mu\text{g/ml}$ of cyclic RGD peptide resulted in a significant reduction of cell attachment.

Reduced neurite lengths were observed in SCNs pretreated with cyclic RGD peptides and the results were quantified (Figure 3.5D). Neurite outgrowth was reduced by 51% from $88.7 \pm 7.5 \mu\text{m}$ to $45 \pm 4.2 \mu\text{m}$ in SCNs cultured on L1-Fc/PA coated substrates. A further reduction in neurite length was observed after treatment with 10 $\mu\text{g/ml}$ and 20 $\mu\text{g/ml}$ of cyclic RGD peptide with no significant difference between the three concentrations of cyclic RGD peptide. In contrast, neurite outgrowth was not affected by cyclic RGD treatment in SCNs cultured on L1-Fc/PDL. In the case of SCNs cultured on L1-Fc/PA/PDL coated thin films, outgrowth was reduced by 28.5% from $77.2 \pm 3.7 \mu\text{m}$ to $55 \pm 11.1 \mu\text{m}$ when treated with 1 $\mu\text{g/ml}$ of cyclic RGD peptide.

3.3.7. L1 Films Promote Neuronal Differentiation of Human Neural Progenitor Cells but Oriented Presentation is Not Necessary in 2-D.

Next, we examined the ability of L1-Fc to support neuronal differentiation and outgrowth of human embryonic derived-NPCs. We used laminin coated PDL substrates (LN/PDL) as the positive control. NPCs were cultured in NDM for 4 days, plated onto substrates treated with PDL, LN/PDL, L1-Fc/PDL, PA/PDL, and L1-Fc/PA/PDL and cultured an additional 7 days in NDM. In contrast to the primary neuronal cultures, L1-Fc/PA coated substrates were not included for the human NPC studies as NPCs failed to attach to this surface, suggesting the importance of cooperative presentation of PDL and multimeric presentation of L1 for these cells. After 7 days in culture, NPCs were fixed and immunostained for the neural stem cell marker nestin and the early neuronal marker β -III-tubulin, clone TUJ1 (Figure 3.6A). A reduction in nestin expression and an increase in β -III-tubulin, along with neurite extensions, confirmed early differentiation into neurons. In

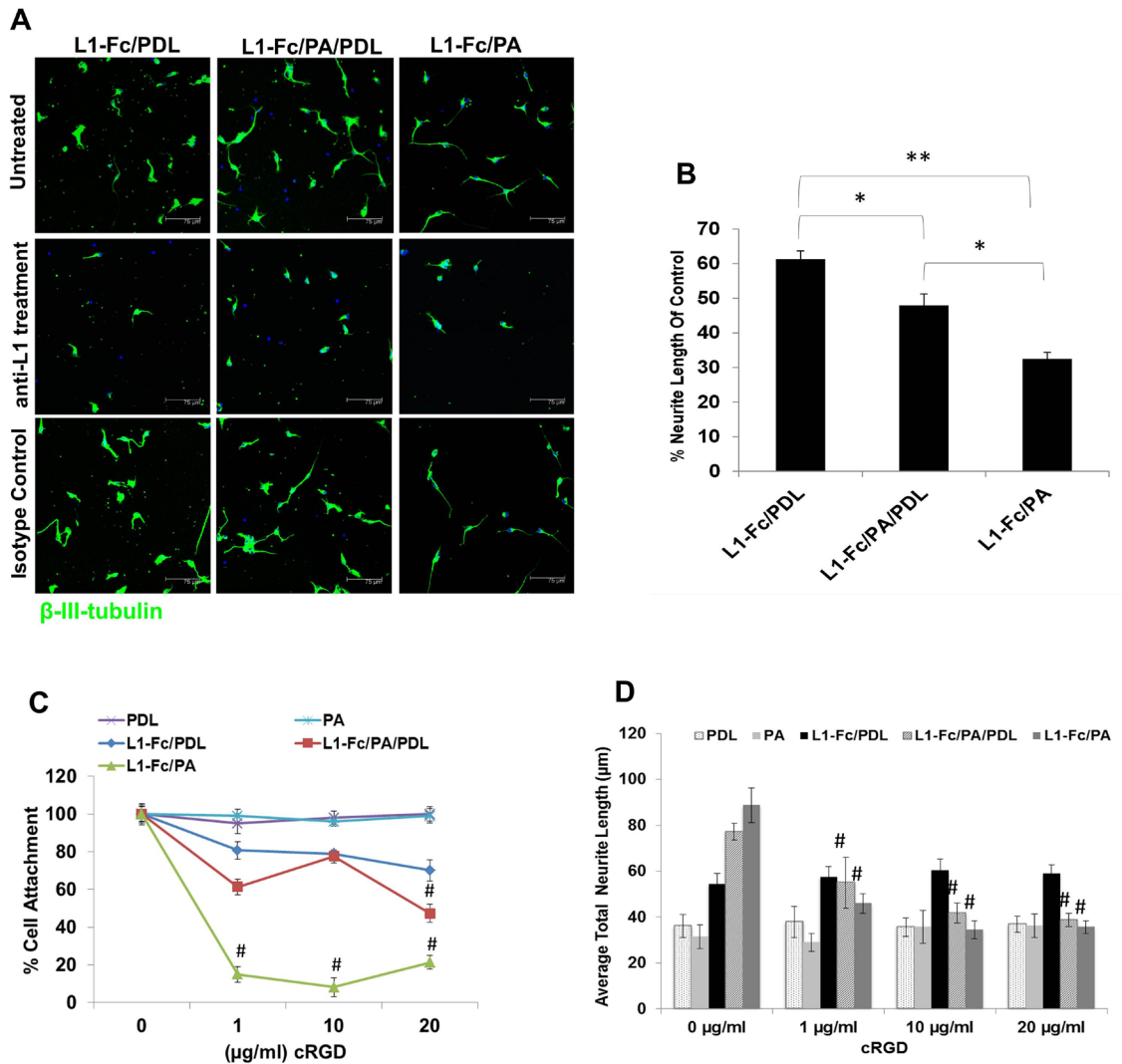


Figure 3.5. Anti-L1 Antibody and cyclic RGD treatment reduces cell attachment and neurite outgrowth. (A) Reduced neurite outgrowth of SCNs was observed for each L1-Fc presentation (L1-Fc/PDL, L1-Fc/PA/PDL, and L1-Fc/PA) when the surface was pretreated with a monoclonal anti-L1 antibody. (B) SCNs cultured on L1-Fc/PA treated thin films exhibited a drastic decrease in neurite outgrowth compared to SCNs cultured on L1-Fc/PDL and L1-Fc/PA/PDL treated thin films when the anti-L1 antibody directed against the second Ig-like domain was added, suggesting that the epitope to which the L1 antibody binds is more exposed due to an outward display of L1-Fc presented from PA. (C) Dose-dependent reduction in cell attachment was observed in SCNs pretreated with cyclic RGD peptide prior to plating onto the different L1-Fc containing substrates. SCNs cultured on L1-Fc/PA treated thin films exhibited the greatest reduction in cell attachment indicating that L1-Fc presented from PA strongly interacts with $\alpha_v\beta_3$ integrins, which was interrupted by the presence of cyclic RGD peptide. Cell attachment on control substrates was not affected. (D) Similar to cell attachment, neurite outgrowth of SCNs was greatly diminished, in a dose-dependent manner, in the presence of cyclic RGD peptide. The greatest inhibition of neurite outgrowth, compared to untreated SCNs, was observed in SCNs cultured on L1-Fc/PA thin films in the presence of cyclic RGD peptide, where as little as 1 μ g/ml of cyclic RGD peptide inhibited cell attachment by 80%. Addition of 10 μ g/ml of cyclic RGD peptide also resulted in a decrease in average neurite length of SCNs cultured on L1-Fc/PA/PDL coated thin films, although the effect was less prominent. The average neurite length

of SCNs cultured on L1-Fc/PDL was not affected by any concentration of cyclic RGD, similar to the controls. Scale bar = 75 μm . SCNs: spinal cord neurons, PDL: poly-D-lysine, PA: protein A. (* denotes $p < 0.05$, ** denotes $p < 0.01$).

order to quantify the degree of neuronal differentiation, the percent of nestin positive+ cells and β -III-tubulin+ cells was determined by taking the ratio of nestin+ or β -III-tubulin+ cells to the total number of cells, as indicated by Hoechst stained nuclei. Both presentations of L1-Fc resulted in an increase in β -III-tubulin+ cells compared to the PDL and PA/PDL (Figure 3.6B), suggesting that L1-Fc promoted neuronal differentiation of NPCs. However, there was no significant difference in the degree of neuronal differentiation elicited by the two different L1-Fc presentations in 2-D.

Additionally, neurite outgrowth was quantified for NPCs cultured on each substrate (Figure 3.6C). L1-Fc/PDL and L1-Fc/PA/PDL coated thin films significantly promoted increased neurite outgrowth compared to PDL or PA/PDL controls. The average neurite lengths on L1-Fc/PDL and L1-Fc/PA/PDL were $71.1 \pm 12.7 \mu\text{m}$ and $79.1 \pm 16.5 \mu\text{m}$, respectively, which was comparable to those elicited by LN/PDL coated controls ($71.1 \pm 11.8 \mu\text{m}$). There was no significant difference in lengths of neurites observed on LN/PDL, L1-Fc/PDL, and L1-Fc/PA/PDL. Thus, while L1-Fc promoted neurite outgrowth comparable to that of laminin, the nature of L1-Fc presentation did not appear to sensitively influence the extent of neurite length of differentiating NPCs on 2-D films.

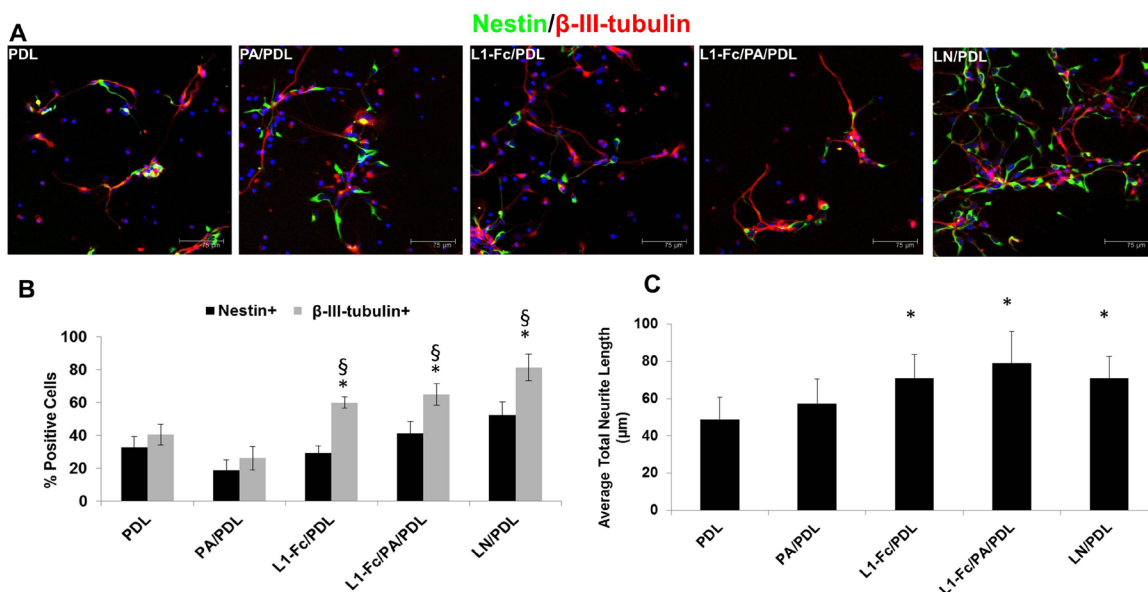


Figure 3.6. L1-Fc Supports neuronal differentiation and neuritogenesis of neural progenitor cells. (A) NPCs were cultured on PDL, PA/PDL, L1-Fc/PDL, L1-Fc/PA/PDL, and LN/PDL for 7 days in neuronal differentiation media and then immunostained for the nestin (green) to identify neural stem/progenitor cells, β -III-tubulin (red) to identify neurons, and Hoechst 33258 (blue) to label the nuclei. After 7 days, NPCs differentiated toward the neuronal lineage, to some degree, when cultured on all substrates, as indicated the β -III-tubulin+ cells. (B) Quantification of the percent of NPCs (nestin+) and neuronal cells (β -III-tubulin+) of NPCs after 7 days of differentiation. Both L1-Fc substrates promoted increased neuronal differentiation over controls and had a greater neuronal to neural progenitor cell population. (C) Average neurite lengths were quantified for NPCs after 7 days in culture. L1-Fc/PDL and L1-Fc/PA/PDL coated thin films promote a significant increase in neurite length compared to the PDL and PA/PDL controls. LN/PDL served as a positive control. Scale bar = 75 μ m. NPCs: neural progenitor cells, PDL: poly-D-lysine, PA: protein A, LN: laminin. (* denotes $p < 0.05$ compared to PDL and PDL/PA controls, \S denotes $p < 0.05$ comparing nestin+ cells to β -III-tubulin+ cells within each condition).

3.3.8. Oriented, Multimeric L1 Presentation triggers Enhanced Neuronal

Differentiation of Human Neural Progenitor Cells in 3-D Fibrous Scaffolds.

The human NPCs were cultured on aligned, fibrous scaffold pretreated with different L1-Fc presentations, laminin, and controls to investigate how the combination of topographical cues from the scaffold and L1-Fc affect neuronal differentiation and neurite outgrowth of NPCs. Scaffolds treated with L1-Fc, with or without PA, promoted directed neuritogenesis of NPCs, comparable to LN, as is indicated by the elongated processes that follow the direction of the aligned scaffolds (Figure 3.7A). To determine the degree to

which L1-Fc influenced neuronal differentiation of NPCs, the percent of nestin+ and β -III-tubulin+ cells were quantified by taking the ratio of nestin+ and β -III-tubulin+ cells to the total number of cells, as labeled by Hoechst (Figure 3.7B). A smaller nestin+ population compared to β -III-tubulin population was observed on both L1-Fc presentations, similar to the LN/PDL treated scaffold, which served as a positive control. Additionally, both L1-Fc treated scaffolds yielded in an increase in neuronal differentiation compared to PDL and PA/PDL controls (Figure 3.7B). Both presentations of L1-Fc from the fibrous scaffolds promoted increased neurite lengths compared to the controls. Notably, NPCs cultured on protein A-presented L1-Fc (L1-Fc/PA/PDL) exhibited an increase in β -III-tubulin+ cells ($65.9\% \pm 5.4\%$) compared to those cultured on L1Fc/PDL ($48.1\% \pm 4.6\%$). Further, the average total neurite length of β -III-tubulin+ positive cells was quantified (Figure 3.7C). The oriented display of L1-Fc, presented from PA/PDL, promoted increased neurite lengths over L1-Fc adsorbed onto PDL treated scaffolds. These results suggest that protein-A presented L1-Fc has a greater influence on neuronal differentiation of NPCs when presented from aligned fibrous scaffolds compared to two-dimensional thin films.

3.4. Discussion

Biointerfacial displays of neurotrophic factors has the potential to significantly influence neural cell behaviors relevant to CNS repair, including adhesion, differentiation, and neurite extension.[51,52] In this study, we investigated multiple presentation schemes for the neural cell adhesion molecule L1 to elucidate the effects of presentation on primary neurons and human embryonic stem cell-derived neural progenitor cells (NPCs) on 2-D and 3-D polymer substrates. We found that protein A (PA)-mediated oriented and multimeric display of L1-Fc significantly enhanced neurite extension of primary spinal cord and cerebellar neurons relative to L1-Fc presented from poly-D-lysine (PDL). We also report

that the combination of multimeric L1-Fc presentation and fibrous geometries of 3-D scaffolds cooperatively enhanced neuronal differentiation of human NPCs.

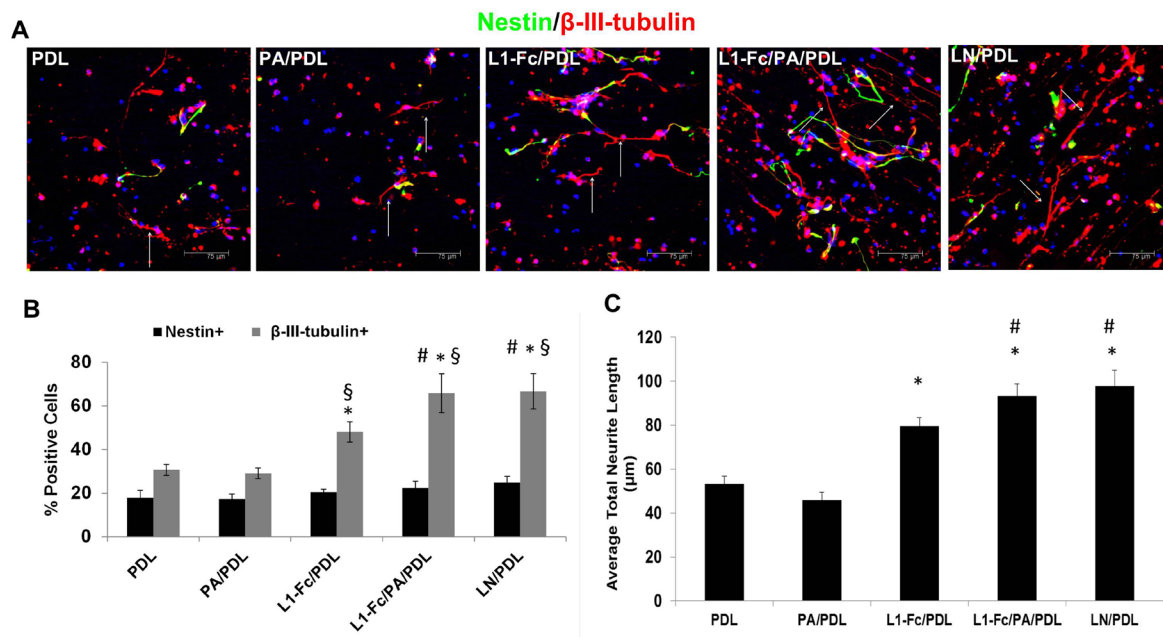


Figure 3.7. L1-Fc supports neuronal differentiation and neuritogenesis of neural progenitor cells within aligned scaffolds. (A) NPCs were cultured on aligned, fibrous scaffolds pretreated with L1-Fc presented from PDL or PA/PDL. After 7 days of differentiation, the NPCs were immunostained for the nestin (green) to identify neural progenitor cells, β -III-tubulin (red) to identify neurons, and Hoechst 33258 (blue) to label the nuclei. NPCs cultured on scaffolds treated with L1-Fc, with or without PA, extended neurites along the scaffold fibers. NPCs differentiated toward the neuronal lineage, to some degree, when cultured on all substrates, as in indicated the β -III-tubulin+ cells. (B) Quantification of the percent of NPCs (nestin+) and neuronal cells (β -III-tubulin+). Both L1-Fc substrates promoted increased neuronal differentiation over controls and had a greater neuronal to neural progenitor cell population. L1-Fc/PA/PDL scaffolds resulted in more β -III-tubulin+ cells compared to L1-Fc/PDL coated scaffolds. (C) Quantification of the average total neurite length. NPCs cultured on L1-Fc/PA/PDL treated scaffolds extended longer neurites compared to those cultured on L1-Fc/PDL. Scale bar = 75 μ m. NPCs: neural progenitor cells, PDL: poly-D-lysine, PA: protein a, LN: laminin. (* denotes $p < 0.05$ compared to PDL and PA/PDL controls, § denotes $p < 0.05$ comparing nestin+ cells to β -III-tubulin+ cells within each condition, # denotes $p < 0.05$ compared to the L1-Fc/PDL condition).

The spatial mode of presentation of biochemical cues such as growth factors and adhesion ligands plays a critical role in determining their bioactivity and function. For example, immobilized interferon gamma can potentiate neuronal differentiation of rat

neural progenitor cells compared to soluble interferon gamma^[53]. Similarly, while L1 has been largely used as a soluble ligand^[54,55], L1 can also be anchored onto substrates as L1-Fc and presented via PA^[56,57], or used in a trimeric form, which was reported to result in increased PC12 cell neurite outgrowth relative to monomeric L1^[58]. Using a combination of PDL treatment to enable improved cell-polymer adhesion and L1-Fc/PA presentation, we report on the concentrations and biointerfacial configurations that promote and enhance L1 bioactivity. We also obtained two broad insights regarding L1-functionalized tyrosine-derived polycarbonate biomaterials: (a) PA/polymer interfaces can elicit multimeric and oriented presentation of L1 from such biomaterials (b) The L1-biointerfaces can markedly modulate adhesion and neuronal activity of both primary neurons and human neural progenitor cells. While the biomaterials used in this study are biodegradable, we do not expect the degradation of the polymer to be significant enough to have an effect on cell behavior within the time frame of the studies conducted. Magno et al. found no change in the behavior of pre-osteoblasts (metabolic rate) cultured on polymers from the same tyrosine-derived polycarbonate library, which had faster degradation rate compared to the polymer used in this study.^[59] Furthermore, tyrosine-derived polycarbonate biomaterials, with varying degradation rates, did not elicit any changes in cell behavior (proliferation and differentiation) after 14 days in culture^[60].

L1-functionalized substrates can selectively promote neuronal cell attachment compared to astrocytes and fibroblasts^[61] and thus be potentially advantageous over more generic cell adhesive treatments such as poly-lysine (PDL or PLL). The multimeric nature of PA-based L1-Fc presentation could be important for both promoting cell adhesion for a given concentration of L1 as well as enhancing neurite extension activity as the second Ig-like domain of L1 regulates neurite outgrowth of neural retinal cells and directly mediates L1-L1 homophilic interactions^[62,63]. The marked inhibition of neurite outgrowth following

antibody-based blocking studies of the L1-Fc/PA treated surfaces suggests that the second Ig-like domain of L1 is more exposed on PA-treated substrates compared to those based on PDL. Another domain within L1 is the RGD domain located within the sixth Ig-like domain. Our studies with cyclic RGD peptide pretreatment showed reduction in SCN attachment and neurite outgrowth when plated onto L1-Fc/PA/PDL and L1-Fc/PA treated thin films, suggesting that this domain was also exposed and available for $\alpha_v\beta_3$ integrin binding. Thus, we propose that the PA-based treatment of the polymers not only facilitated oriented display of L1-Fc, but also engendered a display of L1-Fc molecules in close proximity to one another, which may mirror the close apposition of highly organized and clustered L1 molecules on the cell surface.[43,64] Using AFM imaging of substrate counterstained with L1 antibodies, we established that L1-Fc/PA substrates showed adsorbed L1-Fc. The cross-sectional profiles acquired from the AFM images of L1-Fc/PA/PDL and L1-Fc/PA substrates depicted wider, less defined peaks, which suggest that these protein complexes were more proximally associated compared to L1-Fc adsorbed on PDL, where the peaks were narrow and more defined. The results of the AFM images, in combination with the functional results, where neurons extended longer neurites on L1-Fc/PA treated substrates, indicate that the arrangement of PA-presented L1-Fc influences the efficacy of L1-Fc. The presentation of multimeric, closely associated L1-Fc, in combination with fibrous scaffolds could prove beneficial to the design of neurotrophic materials for neural tissue engineering.

Both spinal cord and cerebellar neurons displayed increased neurite lengths when cultured on PA-presented L1-Fc. One interesting difference between the behaviors of rodent neurons and human neural progenitor cells was evident through the polymer-treatment with PA and PDL. While the neuronal cultures showed robust adhesion and neurite extension even in the absence of PDL, a combination of PDL and PA was necessary for the NPC cultures suggesting that multimeric L1-based receptor-ligand binding is critical

but not sufficient for the NPC cultures, requiring cooperative cell-substrate adhesion facilitated by polycationic PDL treatment.

The possible role of L1 presentation on neurogenesis in three-dimensional substrates is of great interest to scalable constructs for cell transplantation. We observed that fibrous, aligned polymer scaffolds treated with L1-Fc resulted in an increase in neuronal differentiation and neurite lengths compared to the scaffolds that were not treated with L1-Fc. However, in contrast to the two-dimensional thin films, NPCs cultured on L1-Fc/PA/PDL treated scaffolds had a larger neuronal population and enhanced neurite lengths relative to NPCs cultured on L1-Fc/PDL treated scaffolds. These results suggest that the NPC response to the different L1-Fc presentations on 2-D thin films and the 3-D fibrous scaffolds could be due to the combined effects of fiber topography and the outward display of L1-Fc. This suggests cooperative enhancement of L1 signaling on subcellular scales of substrate geometry, a phenomenon that deserves further mechanistic analysis. Scaffold topography has been shown to influence and enhance cellular responses^[65-67], as the 3-D architecture better emulates *in vivo* conditions compared to 2-D thin films.

3.5. Summary and Conclusions

We investigated biointerfaces incorporating L1-Fc on to polymer films and aligned, fibrous polymer scaffolds that would elicit multimeric, oriented presentation of L1-Fc. While L1-Fc has been shown to be effective in the treatment of nervous system injury models, we have demonstrated that the function of L1-Fc can be enhanced *in vitro* with the optimal substrate presentation using protein A. We showed that on two-dimensional films and aligned, fibrous scaffolds treated with protein A-presented L1-Fc promotes enhanced neurite lengths of primary neuronal cells, as well as increased neuronal differentiation and neuritogenesis of human embryonic stem cell-derived neural progenitor cells. We

combined this presentation of L1-Fc with poly(DTE carbonate), which can be fine-tuned for the desired stiffness, degradation rate, and protein adsorption, all of which are important factors to consider when designing implantable devices for nerve injury repair. The bioactive, three-dimensional substrates investigated in this study could prove as useful implantable devices for neural tissue engineering applications.

3.6. Acknowledgments

The authors gratefully acknowledge the support of our work from the New Jersey Commission on Science and Technology Stem Cell CORE Grant (PIs: Moghe PV; Grumet M), New Jersey Commission on Spinal Cord Research Exploratory Grant (PI: Moghe PV), and NSF IGERT 0801620 (IGERT on Stem Cell Science and Engineering) (PI: Moghe PV).

3.7. References

1. Xu X, AE Warrington, AJ Bieber and M Rodriguez. (2011). Enhancing CNS repair in neurological disease: challenges arising from neurodegeneration and rewiring of the network. *CNS drugs* 25:555-73.
2. Thuret S, LD Moon and FH Gage. (2006). Therapeutic interventions after spinal cord injury. *Nature reviews. Neuroscience* 7:628-43.
3. Yue XS, Y Murakami, T Tamai, M Nagaoka, CS Cho, Y Ito and T Akaike. (2010). A fusion protein N-cadherin-Fc as an artificial extracellular matrix surface for maintenance of stem cell features. *Biomaterials* 31:5287-96.
4. Niere M, B Braun, R Gass, S Sturany and H Volkmer. (2006). Combination of engineered neural cell adhesion molecules and GDF-5 for improved neurite extension in nerve guide concepts. *Biomaterials* 27:3432-40.
5. Cooke MJ, SR Phillips, DS Shah, D Athey, JH Lakey and SA Przyborski. (2008). Enhanced cell attachment using a novel cell culture surface presenting functional domains from extracellular matrix proteins. *Cytotechnology* 56:71-9.
6. Shin H, S Jo and AG Mikos. (2003). Biomimetic materials for tissue engineering. *Biomaterials* 24:4353-64.
7. Yu TT and MS Shoichet. (2005). Guided cell adhesion and outgrowth in peptide-modified channels for neural tissue engineering. *Biomaterials* 26:1507-14.
8. Silva GA, C Czeisler, KL Niece, E Beniash, DA Harrington, JA Kessler and SI Stupp. (2004). Selective differentiation of neural progenitor cells by high-epitope density nanofibers. *Science* 303:1352-5.
9. Cooke MJ, T Zahir, SR Phillips, DS Shah, D Athey, JH Lakey, MS Shoichet and SA Przyborski. (2010). Neural differentiation regulated by biomimetic surfaces presenting motifs of extracellular matrix proteins. *Journal of biomedical materials research. Part A* 93:824-32.

10. Moos M, R Tacke, H Scherer, D Teplow, K Fruh and M Schachner. (1988). Neural adhesion molecule L1 as a member of the immunoglobulin superfamily with binding domains similar to fibronectin. *Nature* 334:701-3.
11. Castellani V. (2002). The function of neuropilin/L1 complex. *Adv Exp Med Biol* 515:91-102.
12. Felding-Habermann B, S Silletti, F Mei, CH Siu, PM Yip, PC Brooks, DA Cheresh, TE O'Toole, MH Ginsberg and AM Montgomery. (1997). A single immunoglobulin-like domain of the human neural cell adhesion molecule L1 supports adhesion by multiple vascular and platelet integrins. *J Cell Biol* 139:1567-81.
13. Silletti S, F Mei, D Sheppard and AM Montgomery. (2000). Plasmin-sensitive dibasic sequences in the third fibronectin-like domain of L1-cell adhesion molecule (CAM) facilitate homomultimerization and concomitant integrin recruitment. *J Cell Biol* 149:1485-502.
14. Appel F, J Holm, JF Conscience and M Schachner. (1993). Several extracellular domains of the neural cell adhesion molecule L1 are involved in neurite outgrowth and cell body adhesion. *J Neurosci* 13:4764-75.
15. Maretzky T, M Schulte, A Ludwig, S Rose-John, C Blobel, D Hartmann, P Altevogt, P Saftig and K Reiss. (2005). L1 is sequentially processed by two differently activated metalloproteases and presenilin/gamma-secretase and regulates neural cell adhesion, cell migration, and neurite outgrowth. *Molecular and cellular biology* 25:9040-53.
16. Schultheis M, S Diestel and B Schmitz. (2007). The role of cytoplasmic serine residues of the cell adhesion molecule L1 in neurite outgrowth, endocytosis, and cell migration. *Cellular and molecular neurobiology* 27:11-31.
17. Loers G, S Chen, M Grumet and M Schachner. (2005). Signal transduction pathways implicated in neural recognition molecule L1 triggered neuroprotection and neuritogenesis. *J Neurochem* 92:1463-76.
18. Roonprapunt C, W Huang, R Grill, D Friedlander, M Grumet, S Chen, M Schachner and W Young. (2003). Soluble cell adhesion molecule L1-Fc promotes locomotor recovery in rats after spinal cord injury. *J Neurotrauma* 20:871-82.
19. Loers G and M Schachner. (2007). Recognition molecules and neural repair. *J Neurochem* 101:865-82.
20. Huang ZJ. (2006). Subcellular organization of GABAergic synapses: role of ankyrins and L1 cell adhesion molecules. *Nature neuroscience* 9:163-6.
21. Mehrke G, H Jockusch, A Faissner and M Schachner. (1984). Synapse formation and synaptic activity in mammalian nerve-muscle co-culture are not inhibited by antibodies to neural cell adhesion molecule L1. *Neuroscience letters* 44:235-9.
22. Maness PF and M Schachner. (2007). Neural recognition molecules of the immunoglobulin superfamily: signaling transducers of axon guidance and neuronal migration. *Nat Neurosci* 10:19-26.
23. Chen J, J Wu, I Apostolova, M Skup, A Irintchev, S Kugler and M Schachner. (2007). Adeno-associated virus-mediated L1 expression promotes functional recovery after spinal cord injury. *Brain : a journal of neurology* 130:954-69.
24. Dihne M, C Bernreuther, M Sibbe, W Paulus and M Schachner. (2003). A new role for the cell adhesion molecule L1 in neural precursor cell proliferation, differentiation, and transmitter-specific subtype generation. *J Neurosci* 23:6638-50.
25. Chen J, C Bernreuther, M Dihne and M Schachner. (2005). Cell adhesion molecule l1-transfected embryonic stem cells with enhanced survival support regrowth of corticospinal tract axons in mice after spinal cord injury. *J Neurotrauma* 22:896-906.

26. Cooke MJ, K Vulic and MS Shoichet. (2010). Design of biomaterials to enhance stem cell survival when transplanted into the damaged central nervous system. *Soft Matter* 6:4988-4998.
27. Madigan NN, S McMahon, T O'Brien, MJ Yaszemski and AJ Windebank. (2009). Current tissue engineering and novel therapeutic approaches to axonal regeneration following spinal cord injury using polymer scaffolds. *Respiratory physiology & neurobiology* 169:183-99.
28. Nomura H, CH Tator and MS Shoichet. (2006). Bioengineered strategies for spinal cord repair. *Journal of neurotrauma* 23:496-507.
29. Delcroix GJ, PC Schiller, JP Benoit and CN Montero-Menei. (2010). Adult cell therapy for brain neuronal damages and the role of tissue engineering. *Biomaterials* 31:2105-20.
30. Subramanian A, UM Krishnan and S Sethuraman. (2009). Development of biomaterial scaffold for nerve tissue engineering: Biomaterial mediated neural regeneration. *Journal of biomedical science* 16:108.
31. Horne MK, DR Nisbet, JS Forsythe and CL Parish. (2010). Three-dimensional nanofibrous scaffolds incorporating immobilized BDNF promote proliferation and differentiation of cortical neural stem cells. *Stem cells and development* 19:843-52.
32. Koh HS, T Yong, CK Chan and S Ramakrishna. (2008). Enhancement of neurite outgrowth using nano-structured scaffolds coupled with laminin. *Biomaterials* 29:3574-82.
33. Timnak A, FY Gharebaghi, RP Shariati, SH Bahrami, S Javadian, H Emami Sh and MA Shokrgozar. (2011). Fabrication of nano-structured electrospun collagen scaffold intended for nerve tissue engineering. *Journal of materials science. Materials in medicine* 22:1555-67.
34. Griffin J, R Delgado-Rivera, S Meiners and KE Uhrich. (2011). Salicylic acid-derived poly(anhydride-ester) electrospun fibers designed for regenerating the peripheral nervous system. *Journal of biomedical materials research. Part A* 97:230-42.
35. Ertel SI and J Kohn. (1994). Evaluation of a series of tyrosine-derived polycarbonates as degradable biomaterials. *Journal of biomedical materials research* 28:919-30.
36. Meechaisue C, R Dubin, P Supaphol, VP Hoven and J Kohn. (2006). Electrospun mat of tyrosine-derived polycarbonate fibers for potential use as tissue scaffolding material. *Journal of biomaterials science. Polymer edition* 17:1039-56.
37. Voinova MV RM, Jonson M, Kasemo B. (1999). Viscoelastic acoustic response of layered polymer films at fluid-solid interfaces: Continuum mechanics approach. *Physica Scripta* 59:391-396.
38. Neagu C, KO van der Werf, CA Putman, YM Kraan, BG de Grooth, NF van Hulst and J Greve. (1994). Analysis of immunolabeled cells by atomic force microscopy, optical microscopy, and flow cytometry. *Journal of structural biology* 112:32-40.
39. Rossi MP, J Xu, J Schwarzbauer and PV Moghe. (2010). Plasma-micropatterning of albumin nanoparticles: Substrates for enhanced cell-interactive display of ligands. *Biointerphases* 5:105-13.
40. Wang HB, ME Mullins, JM Cregg, A Hurtado, M Oudega, MT Trombley and RJ Gilbert. (2009). Creation of highly aligned electrospun poly-L-lactic acid fibers for nerve regeneration applications. *Journal of neural engineering* 6:016001.
41. Jiang XY, SL Fu, BM Nie, Y Li, L Lin, L Yin, YX Wang, PH Lu and XM Xu. (2006). Methods for isolating highly-enriched embryonic spinal cord neurons: a comparison between enzymatic and mechanical dissociations. *Journal of neuroscience methods* 158:13-8.

42. Mercado ML, A Nur-e-Kamal, HY Liu, SR Gross, R Movahed and S Meiners. (2004). Neurite outgrowth by the alternatively spliced region of human tenascin-C is mediated by neuronal alpha7beta1 integrin. *The Journal of neuroscience : the official journal of the Society for Neuroscience* 24:238-47.
43. Dahlin-Huppe K, EO Berglund, B Ranscht and WB Stallcup. (1997). Mutational analysis of the L1 neuronal cell adhesion molecule identifies membrane-proximal amino acids of the cytoplasmic domain that are required for cytoskeletal anchorage. *Molecular and cellular neurosciences* 9:144-56.
44. Kadmon G and P Altevogt. (1997). The cell adhesion molecule L1: species- and cell-type-dependent multiple binding mechanisms. *Differentiation; research in biological diversity* 61:143-50.
45. Xie J, MR MacEwan, X Li, SE Sakiyama-Elbert and Y Xia. (2009). Neurite outgrowth on nanofiber scaffolds with different orders, structures, and surface properties. *ACS nano* 3:1151-9.
46. Xie J, SM Willerth, X Li, MR Macewan, A Rader, SE Sakiyama-Elbert and Y Xia. (2009). The differentiation of embryonic stem cells seeded on electrospun nanofibers into neural lineages. *Biomaterials* 30:354-62.
47. Montgomery AM, JC Becker, CH Siu, VP Lemmon, DA Cheresch, JD Pancook, X Zhao and RA Reisfeld. (1996). Human neural cell adhesion molecule L1 and rat homologue NILE are ligands for integrin alpha v beta 3. *The Journal of cell biology* 132:475-85.
48. Yip PM and CH Siu. (2001). PC12 cells utilize the homophilic binding site of L1 for cell-cell adhesion but L1-alpha v beta 3 interaction for neurite outgrowth. *Journal of neurochemistry* 76:1552-64.
49. Yip PM, X Zhao, AM Montgomery and CH Siu. (1998). The Arg-Gly-Asp motif in the cell adhesion molecule L1 promotes neurite outgrowth via interaction with the alpha v beta 3 integrin. *Molecular biology of the cell* 9:277-90.
50. Pfaff M, K Tangemann, B Muller, M Gurrath, G Muller, H Kessler, R Timpl and J Engel. (1994). Selective recognition of cyclic RGD peptides of NMR defined conformation by alpha IIb beta 3, alpha V beta 3, and alpha 5 beta 1 integrins. *The Journal of biological chemistry* 269:20233-8.
51. Stabenfeldt SE, G Munglani, AJ Garcia and MC LaPlaca. (2010). Biomimetic microenvironment modulates neural stem cell survival, migration, and differentiation. *Tissue engineering. Part A* 16:3747-58.
52. Potter W, RE Kalil and WJ Kao. (2008). Biomimetic material systems for neural progenitor cell-based therapy. *Frontiers in bioscience : a journal and virtual library* 13:806-21.
53. Leipzig ND, C Xu, T Zahir and MS Shoichet. (2010). Functional immobilization of interferon-gamma induces neuronal differentiation of neural stem cells. *Journal of biomedical materials research. Part A* 93:625-33.
54. Doherty P, E Williams and FS Walsh. (1995). A soluble chimeric form of the L1 glycoprotein stimulates neurite outgrowth. *Neuron* 14:57-66.
55. Lavdas AA, R Efrose, V Douris, M Gaitanou, F Papastefanaki, L Swevers, D Thomaidou, K Iatrou and R Matsas. (2010). Soluble forms of the cell adhesion molecule L1 produced by insect and baculovirus-transduced mammalian cells enhance Schwann cell motility. *Journal of neurochemistry* 115:1137-49.
56. Oliva AA, Jr., CD James, CE Kingman, HG Craighead and GA Banker. (2003). Patterning axonal guidance molecules using a novel strategy for microcontact printing. *Neurochemical research* 28:1639-48.

57. Shi P, K Shen and LC Kam. (2007). Local presentation of L1 and N-cadherin in multicomponent, microscale patterns differentially direct neuron function in vitro. *Developmental neurobiology* 67:1765-76.
58. Hall H, D Bozic, C Fauser and J Engel. (2000). Trimerization of cell adhesion molecule L1 mimics clustered L1 expression on the cell surface: influence on L1-ligand interactions and on promotion of neurite outgrowth. *J Neurochem* 75:336-46.
59. Magno MHR, J Kim, A Srinivasan, S McBride, D Bolikal, A Darr, JO Hollinger and J Kohn. (2010). Synthesis, degradation and biocompatibility of tyrosine-derived polycarbonate scaffolds. *Journal of Materials Chemistry* 20:8885-8893.
60. Abramson SD. (2002). Selected bulk and surface properties and biocompatibility of a new class of tyrosine-derived polycarbonates. Dissertation, Rutgers University and University of Medicine and Dentistry of New Jersey and Robert Wood Johnson Medical School, New Brunswick, USA, New Brunswick, USA.
61. Webb K, E Budko, TJ Neuberger, S Chen, M Schachner and PA Tresco. (2001). Substrate-bound human recombinant L1 selectively promotes neuronal attachment and outgrowth in the presence of astrocytes and fibroblasts. *Biomaterials* 22:1017-28.
62. Zhao X and CH Siu. (1995). Colocalization of the homophilic binding site and the neuritogenic activity of the cell adhesion molecule L1 to its second Ig-like domain. *The Journal of biological chemistry* 270:29413-21.
63. Zhao X, PM Yip and CH Siu. (1998). Identification of a homophilic binding site in immunoglobulin-like domain 2 of the cell adhesion molecule L1. *Journal of neurochemistry* 71:960-71.
64. Hall H, S Carbonetto and M Schachner. (1997). L1/HNK-1 carbohydrate- and beta 1 integrin-dependent neural cell adhesion to laminin-1. *Journal of neurochemistry* 68:544-53.
65. Levenberg S, NF Huang, E Lavik, AB Rogers, J Itskovitz-Eldor and R Langer. (2003). Differentiation of human embryonic stem cells on three-dimensional polymer scaffolds. *Proceedings of the National Academy of Sciences of the United States of America* 100:12741-6.
66. Smith LA, X Liu, J Hu and PX Ma. (2010). The enhancement of human embryonic stem cell osteogenic differentiation with nano-fibrous scaffolding. *Biomaterials* 31:5526-35.
67. Shahbazi E, S Kiani, H Gourabi and H Baharvand. (2011). Electrospun nanofibrillar surfaces promote neuronal differentiation and function from human embryonic stem cells. *Tissue engineering. Part A* 17:3021-31.
68. Semler EJ, A Dasgupta and PV Moghe. (2005). Cytomimetic engineering of hepatocyte morphogenesis and function by substrate-based presentation of acellular E-cadherin. *Tissue engineering* 11:734-50.

Chapter 4

N-cadherin and L1 Biomimetic Substrates Modulate Neuronal Differentiation and Neurite Extension of Human Embryonic Stem Cell Derived-Neural Stem Cells

Note: This chapter is in preparation for publication elsewhere as part of an article entitled: *"N-cadherin and L1 Biomimetic Substrates Modulate Neuronal Differentiation and Neurite Extension of Human Embryonic Stem Cell Derived-Neural Stem Cells."* Jocie F. Cherry, Neal K. Bennett, Melitta Schachner, Prabhav V. Moghe

Abstract

The field of neural tissue engineering seeks to recapitulate the complex microenvironment that arises as molecular events drive neurodevelopment in hopes of promoting regeneration of neural tissue following traumatic injury or disease. Given the diverse set of biological molecules required for nervous system development and regeneration following traumatic injury or degeneration of neural cells, we hypothesized that a combined biomimetic strategy could realize both enhanced differentiation into the appropriate lineage as well as the maintenance of responses such as neurite outgrowth and survival. Specifically, we sought to determine the effects of recombinant chimera proteins N-cadherin-Fc and L1-Fc in promoting neuronal differentiation of neural stem cells (NSCs) derived from H9 human embryonic stem cells (H9), given their established roles in neuronal differentiation and their somewhat distinct regulation of dendritic and axonal development and axonal outgrowth. Using protein-A pre-adsorbed substrates, N-cadherin-Fc was presented alone and in combination with L1-Fc from two-dimensional substrates and fibrous, electrospun scaffolds fabricated from tyrosine-derived polycarbonate polymers. H9 human embryonic derived-neural stem cells (H9-NSCs) were cultured on the biofunctionalized substrates and the effects on neuronal differentiation, neuritogenesis and

neurite extension, and survival were quantified. We found that substrates presenting a relatively low concentration (0.6875 – 1.375 $\mu\text{g/ml}$) of N-cadherin-Fc, alone, promoted an increase in MAP2+ positive cells and improved cell survival in the presence of oxidative stress compared to responses elicited by a high concentration (2.75 – 5.5 $\mu\text{g/ml}$) of N-cadherin-Fc. Additionally, the combination of low N-cadherin-Fc and a relatively higher concentration of L1-Fc resulted in enhanced neurite outgrowth, MAP2+, and neurofilament-M+ cells compared those either on low or high concentrations of N-cadherin-Fc alone, or following combinations of L1-Fc with a higher concentration of N-cadherin-Fc. H9-NSCs displayed better neuronal differentiation, as well as survival within low N-cad-Fc presenting 3-D fibrous scaffolds. These trends highlight the differential nature of the cooperative effect between N-cadherin and L1 in inducing neuronal differentiation. To understand why lower neuronal yields were observed with substrates presenting a higher density of N-cadherin-Fc, we blocked cell surface N-cadherin with an antibody against extracellular N-cadherin and treated cultures with a pharmacologic antagonist to fibroblast growth factor receptor, PD173074, to inhibit N-cadherin or L1 mediated activation. We found by blocking cell surface N-cadherin, newly formed neurons extended longer neurites when cultured on high N-cadherin- alone or in combination with L1-Fc and neuronal differentiation improved following PD173074 treatment, suggesting high concentrations of surface presented N-cadherin hinders neurite outgrowth due to increased cell-surface N-cadherin interactions and triggers FGFR pathways that impede neuronal differentiation of H9-NSCs. These studies highlight two key new findings: (1) The substrate-display of selected combinations of N-cadherin and L1 recapitulates a biomimetic, “neurotrophic” microenvironment that enhances neuronal differentiation and neurite outgrowth of human neural stem cells; (2) The substrate-based biofunctionalization with N-cadherin and L1 can be further combined with 3-D microfabricated scaffolds, which can similarly promote neuronal differentiation

and neurite extension within “transplantable” scaffolds with high surface area per volume. Thus, the insights from this study have both fundamental and translational impacts for neural stem cell-based regenerative medicine.

4.1. Introduction

Traumatic central nervous system (CNS) injury and neurodegenerative diseases result in irreplaceable cell loss and concomitant deficit in function. Cell transplantation therapy represents a promising approach for treatment for traumatic injury to the CNS as it holds the potential to replace damaged or diseased cells and reestablish functional neuronal circuits^[1,2]. Progress in stem cell biology has generated much interest in regeneration-based treatment of CNS injuries and diseases, using stem cells with engineered levels of lineage plasticity. Various stem cell sources have been explored as candidates for treatment of CNS injuries such as mesenchymal stem cells and olfactory ensheathing cells^[3], as well as neural stem cells ^[4-13]. Neural stem cells (NSCs) are multipotent in nature and have the ability to differentiate into neurons, astrocytes, or oligodendrocytes and their effectiveness in models of CNS injuries and ailments has been explored, demonstrating their potential for use in cell replacement therapy^[14-16]. Human embryonic stem cells are an excellent source for NSCs due to their ability to self-renew and differentiate into various types of neural cells^[17-19]. While cell transplantation holds promise for treatment of the injured CNS, limitations such as poor engraftment efficiency and altered cell state, such as differentiation into an undesired lineage, leaves room for improvement of this approach^[20-22]. Neural tissue engineering aims to create tissue equivalents by mimicking natural microenvironments *in vitro*, through the combination of cells, bioactive molecules, and a biomaterial scaffold to support survival of transplanted cells, control the local microenvironment of transplanted cells with the ultimate goal to replace damaged or diseased tissue. Cells receive cues and signals mediated by cell-cell and cell-substrate

contacts that are governed by the local extracellular matrix (ECM), and the manipulation of each can sensitively modulate and direct cell behaviors such as aggregation, proliferation, differentiation, and survival^[23-25]. Determining the right combination and appropriate presentation of self-renewal and differentiation promoting molecules is a key component of the design of the next generation of substrates to be used for functional replacement of degenerative disease states. Substrates presenting a combination of peptides derived from extracellular matrix proteins, laminin and fibronectin, promoted increased neuronal differentiation compared to either sequence alone or combinations including collagen I and collagen IV^[26]. Haque et al determined that the combined presentation of E-cadherin and N-cadherin supported self-renewal of mouse embryonic stem cells and induced pluripotent stem cells under proliferative conditions, and promoted neural differentiation under differentiating culture conditions^[27]. In addition, the manner by which bioactive molecules are presented greatly influences function, as was demonstrated when tethered BDNF stimulated improved differentiation over the soluble form^[28], and immobilized EGF fostered differentiation and neuritogenesis, while soluble EGF promoted proliferation^[29].

Nervous system development and function are dependent on a concert of sequenced, regulatory processes that include neural induction, cell proliferation, differentiation, cell migration, and synapse formation^[30]. A multitude of growth promoting and guidance molecules are present that facilitate proper nervous system development and regeneration such as neurotrophic factors, ECM proteins, and cell adhesion molecules^[31]. Two neural cell adhesion molecules that play a major role in normal central nervous system development are N-cadherin and L1. N-cadherin is homophilic binding glycoprotein that mediates cell adhesion, cell migration, synaptogenesis, and synaptic plasticity^[32,33]. N-cadherin was shown to promote neurite outgrowth through fibroblast growth factor receptor (FGFR) activation and signaling and is involved in dendritic arborization^[32]. N-

cadherin, expressed early during development, is expressed on the surface of neural stem cells and involved in migration differentiation. Recombinant N-cadherin, when presented as an extracellular matrix cue, is able to maintain neural stem cell cultures and promote differentiation^[27,34]. L1, a homophilic binding, transmembrane protein expressed on the cell surface of post mitotic neurons, plays a role in axonal extension and guidance, neuronal survival, and L1 overexpressing stem cells promote cortical tract regeneration following spinal cord injury^[35-39]. L1 participates in heterophilic binding with integrins, as well as fibroblast growth factor receptor^[30,38,40-42]. Both N-cadherin and L1 are involved in axonal extension and are promising candidates for designing bioactive scaffolds that promote axonal outgrowth of newly derived/differentiated neurons. Together these two proteins have the potential to result in increased maturation of neurons derived from human embryonic stem cells, as synergistic effects, on neurite outgrowth, between N-cadherin and L1 rat hippocampal and cortical neurons^[43,44]. Both Shi et al and Castellanos et al showed preferential dendritic growth on N-cadherin coated surfaces, while axons preferentially extended along areas functionalized with L1^[43,44]. Previously, we demonstrated that cellular-presented N-cadherin induced neural differentiation of hESCs^[45], demonstrating the ability of N-cadherin to promote neuronal differentiation of hESCs. Additionally, we demonstrated that electrospun scaffolds functionalized with protein-A presented L1-Fc positively influences neuronal differentiation of H9 hESC-derived neural stem cells (H9-NSCs)^[46]. While the results suggested the potential for L1-Fc substrates to promote and support neuronal differentiation and neurite outgrowth of H9-NSCs, several gaps remained to be addressed. Firstly, the L1-adhesivity for cells is low, and thus robust cell adhesion and differentiation on purely L1-functionalized substrates is difficult to sustain. Secondly, the L1-display does not adequately recapitulate the early lineage restriction of undifferentiated NSCs, which was one of the goals of the current study. In contrast to the later expression of

L1 during nervous system development^[47], N-cadherin expression is upregulated during neural tube formation and closure and regulates maintenance and neuronal differentiation of neural stem cells^[48-50].

Current research efforts aim to develop optimal scaffolds for transplantation of neuronal precursor or stem cells that will provide structural support to both transplanted cells and those spared after injury, generate cues to direct the behavior of transplanted cells, and direct growth of newly formed axons^[20,25]. Several types of scaffold configurations have been studied, such as hydrogels, porous polymeric scaffolds, conduits and electrospun fibers^[14,20,22,25,51]. Electrospun, fibrous scaffolds hold great potential for neural tissue engineering due to the ease in controlling geometric features, they possess high surface area, and ability to recapitulate the topography of native extracellular matrix. To promote the bioactivity of fibrous scaffolds, biologically relevant molecules such as peptides, growth factors, and recombinant proteins can be incorporated onto or within scaffolds resulting in a bioactive platform that directs and modulate cell behavior^[21,25,52]. A combinatorial approach with biofunctionalized scaffolds and neural stem cells has been shown to improve not only survival of transplanted cells, but also functional recovery in vivo^[53].

This study aimed to systematically discern the role of the substrate display of varying combinations of recombinant N-cadherin-Fc (N-cad-Fc) and L1-Fc that would promote neuronal differentiation and maturation of H9 human embryonic stem cell-derived neural stem cells (H9-NSCs). We first tested the ability of N-cad-Fc, at varying concentrations, to promote adhesion, neuritogenesis and outgrowth, neuronal differentiation, and oxidative stress survival. We then examined whether and how these behaviors were further augmented when L1-Fc was combined with N-cad-Fc at varying concentrations, and presented from 2-D films and 3-D scaffolds of synthetic polymers. The substrates were fabricated from tyrosine-derived polycarbonates, a combinatorial library of

degradable polymers in which surface and mechanical properties, as well as degradation rates can be finely tuned^[54,55]. For example, variable amounts of desaminotyrosyl tyrosine (DT) and/or poly(ethylene glycol (PEG), can be copolymerized with the base monomer, Poly(desaminotyrosyl tyrosine ethyl ester carbonate) [poly(DTE carbonate)], leading to polymers that are relatively similar in structure, but with different rates of degradation and protein adsorption properties. In this study, we kept the polymer composition constant. We report that surfaces presenting low concentrations of N-cad-Fc combined with L1-Fc enhance neuronal differentiation and neurite outgrowth of H9-NSCs versus when L1-Fc is co-presented with higher concentrations of N-cad-Fc. We also found that the use of low concentrations of N-cad-Fc alone, resulted in increased neuronal differentiation and survival compared to high N-cad-Fc functionalized substrates, demonstrating the influence of surface protein density in modulating cellular response. The research outcomes show new insights regarding 1) dose-dependent responsiveness of H9-NSCs to N-cad-Fc and 2) the effects of the co-presentation of N-cad-Fc and L1-Fc, at different ratios, on behaviors of hESC-derived neural stem cells.

4.2. Materials and Methods

4.2.1. Fabrication of Polymer Thin Films and Electrospun Scaffolds

Polymer thin films were generated by spin coating a solution of 1% (w/v) poly(DTE-co-10% DT-co-1% PEG_{1k}) in tetrahydrofuran (Sigma-Aldrich, St. Louis, MO, USA). Prior to spin coating, the polymer solution was filtered with a 0.45 μm Whatman pTFE filter and spin coated onto 12 mm coverslips. After 24 hours under vacuum, the films were UV sterilized for 15 minutes prior to treatment with proteins.

For scaffold fabrication, glacial acetic acid (Fisher) was used to dissolve poly(DTE-co-10% DT-co-1% PEG_{1k}) polymer, overnight at room temperature, for an 18% solution

(w/v). The polymer solution was flowed through an 18-gauge needle, with a syringe pump (KD Scientific, Holliston, MA, USA), at a flow rate of 1 ml/hr. The morphology of the scaffolds was visualized using an AMRAY 1830 I scanning electron microscope (SEM) (See chapter 3). The samples were for SEM imaging by drying under the samples under vacuum and sputter coating with gold palladium and images were taken at 20 kV acceleration potential. Fiber diameter was quantified by measuring 100 individual fibers in 1000x SEM images using NIH-ImageJ software (<http://rsb.info.nih.gov/ij/>).

4.2.2. Preparation of N-cadherin-and L1-Fc Culture Substrates

To prepare the culture substrates, 2-D films and 3-D scaffolds were coated with 1.25 $\mu\text{g}/\text{ml}$ of protein A (PA) (Life Technologies, Carlsbad, CA, USA) for 1 hour at room temperature. Following three washes with Dulbecco's phosphate buffered saline (DPBS), the substrates were coated with 0.6875, 1.375, 2.75, or 5.5 $\mu\text{g}/\text{ml}$ of human N-cadherin-Fc (N-cad-Fc) (R&D Systems, Minneapolis, MN, USA), alone, or in combination with 10 $\mu\text{g}/\text{ml}$ of human L1-Fc (R&D Systems) for 1 hour at room temperature. For L1-Fc only substrates, 10 $\mu\text{g}/\text{ml}$ was used as well. The schematic of substrate preparation and the resulting substrates are shown in Figure 4.1A. Control substrates were kept hydrated with 2 mM calcium chloride, the buffer used to make N-cadherin- and L1-Fc protein solutions. For poly-D-lysine (PDL) and poly-D-lysine/laminin (PDL/LN), 2-D films and 3-D scaffolds were coated with 10 $\mu\text{g}/\text{ml}$ of PDL for 1 hour at room temperature. Surfaces were washed three times with DPBS and coated with 10 $\mu\text{g}/\text{ml}$ of mouse laminin (Sigma).

4.2.3. Detection of Substrate Bound N-cadherin-Fc and L1-Fc

Enzyme-linked immunosorbent assay (ELISA) was used to detect N-cadherin-Fc and L1-Fc as previously described^[46]. In brief, 2-D films were prepared as described above, washed one time with phosphate buffered saline (PBS), and blocked with 1% bovine serum

albumin (BSA, Sigma Aldrich, St. Louis, MO, USA) for 1.5 hours. A polyclonal sheep antibody against the extracellular domain of N-cadherin was used to detect N-cad-Fc (R&D Systems), while a monoclonal mouse anti-L1 antibody was used to detect L1-Fc. Both antibodies were used at 1 µg/ml. Following incubation with the primary antibody, secondary antibodies alkaline phosphatase conjugated-goat anti-sheep IgG was applied to N-cad-Fc substrates and alkaline phosphatase goat anti-mouse IgG was applied to L1-Fc substrates. Following three washes, the 2-D films were reacted with alkaline phosphatase yellow (pNPP) liquid substrate (Sigma-Aldrich), the reaction was stopped after 30 min with 3 N NaOH, and the samples were analyzed using an absorbance plate reader at 405 nm.

4.2.4. H9-NSC Neural Stem Cell Culture

H9-NSCs, derived from NIH approved H9 hESCs were purchased from Millipore (ENStem-A neural progenitor cells, Millipore, Temecula, CA, USA). During cell expansion and maintenance, H9-NSCs were cultured in 75cm² flasks, coated with 0.25x Matrigel (BD Biosciences, Franklin Lake, NJ, USA) in neural proliferation medium (NPM), composed of 1:1 mixture of DMEM/F12:Neurobasal medium (Life Technologies), supplemented with 0.5x B27 supplement without vitamin A and 0.5x N2 (Life Technologies), in addition to 20 ng/ml bFGF (Peprotech, New Jersey, USA) and 1% penicillin/streptomycin (Lonza), at 37°C in 5% CO₂. The medium was changed every 2-3 days and H9-NSCs were passaged, using Accutase (Stem Cell Technologies, Vancouver, Canada) once they reached 90-95% confluence.

To start the differentiation process, once H9-NSCs reached 85-90% confluence, NPM was removed and replaced with neural differentiation medium (NDM), following two washes with warm neurobasal medium. NDM contained of neurobasal medium, 1x B27 supplement without vitamin A, 1% penicillin/streptomycin, and 10 ng/ml of BDNF (Peprotech). Following 4 days in NDM, H9-NSCs were dissociated using Accutase and plated onto N-cad-/L1-Fc coated 2-D films and fibrous scaffolds at a density of 7.5x10⁴

cells/cm² or 1.75x10⁵ cells/cm², respectively and allowed to differentiate for 7 days. The medium was changed every two days, during the differentiation period.

4.2.5. Immunocytochemistry of H9-NSCs

After the desired culture period, H9-NSCs were fixed in 4% paraformaldehyde for 20 minutes at room temperature and washed 3 times with DPBS. Cells were permeabilized with 0.1% Triton-X for 5 min, followed by 3 DPBS washes. Non-specific antibody binding was prevented by blocking the samples with 5% normal goat serum (NGS) (MP Biomedicals, Solon, OH, USA) or 5% donkey serum (DS) (Millipore), depending on the source of the secondary antibody. Primary antibodies were diluted in either 5% NGS or 5% DS and applied to the samples overnight at 4C°. The samples were then washed 3 times with DPBS, for 20 minutes each time, and the secondary antibodies along with 1 µg/ml of Hoechst 33258 (Sigma-Aldrich), diluted in either NGS or DS, was applied for 1 hour at room temperature, followed by 3, 20 minute washes. The following antibodies were used: polyclonal sheep anti-N-cadherin, 1:100 (extracellular domain), mouse anti-βIII-tubulin IgG2_a, 1:1000 (Covance), mouse anti-MAP2 IgG1, 1:500 (BD Biosciences), mouse anti-neurofilament-M IgG2_a, 1:500 (Life Technologies), mouse anti-β-catenin IgG3, 1:50 (R&D Systems). All secondary antibodies, purchased from Life Technologies, were isotype specific Alexa Fluor 488, 594, or 647 goat-anti mouse antibodies, or Alexa Fluor 488 donkey anti-sheep.

4.2.6. Quantification of Neurite Outgrowth and Neuronal Differentiation

To quantify neurite outgrowth, after the desired culture times, H9-NSCs were immunostained as described above and analyzed for neurite outgrowth. Images were taken using confocal microscopy (Leica TCS.SP2, Leica Microscope, Exton, PA, USA). To get a sense of how the substrates influenced neuritogenesis, the percent of cells that extended

neurites was quantified. The number of cells possessing a neuronal phenotype and neurites were manually counted and the ratio of cells that met these criteria to the total number of cells, as indicated by Hoechst nuclei. Total neurite length and the length of the longest neurite was determined using ImageJ imaging software. Only neurites equal to or greater than the diameter of a cell body were measured. Neuronal differentiation was quantified by counting the number of neurofilament-M+ and/or MAP2+ cells and normalizing to the total number of cells present, for each condition.

4.2.7. Antibody Blocking of Cellular N-cadherin

To understand the role of N-cadherin/N-cadherin interactions played in neuronal differentiation and neurite outgrowth, an antibody against the extracellular domain of N-cadherin was used to interrupt cell-substrate N-cadherin interactions. Following dissociated H9-NSCs as described above, H9-NSCs were treated with 50 or 100 $\mu\text{g/ml}$ anti-N-cadherin or sheep IgG isotype control (R&D Systems) for 1 hour prior to seeding the cells onto 2-D films. After 5 days in culture, H9-NSCs were immunostained with β III-tubulin, MAP2, and neurofilament-M. The extent of neuronal differentiation and neurite outgrowth of the longest neurite was determined as described above.

4.2.8. Fibroblast Growth Factor Receptor Inhibition Assay

Interactions of both N-cadherin and L1 with fibroblast growth factor receptor (FGFR) have been reported to play a role in the neurite outgrowth of primary neurons^[56]. Additionally, FGFR signaling influences proliferation and differentiation activity of NSCs^[57]. Therefore, the inhibition of FGFR signaling was used as a tool to determine if activation of FGFR mediated any of the responses observed in H9-NSCs on N-cad-Fc and N-cad-/L1-Fc substrates. H9-NSCs were plated onto N-cad-Fc and N-cad-/L1-Fc 2-D films. After 24 hours,

H9-NSCs were treated with the FGFR inhibitor, PD173074 (Tocris, Minneapolis, MN, USA), and cultured for an additional 6 days. The medium was changed every two days, with or without PD173074.

4.2.9. Oxidative Stress Survival Assay

The stress-protective capacity of N-cad-Fc and N-cad-/L1-Fc 2-D films and 3-D scaffolds was tested by inducing oxidative stress with hydrogen peroxide (H_2O_2) treatment. H9-NSCs were cultured and plated onto 2-D films and scaffolds at the same seeding as mentioned above in NDM. After a 7 day culture period, the medium was switched from NDM to neurobasal medium supplemented with anti-oxidant free, 1x B27 without vitamin A and 1% pen/strep for 24 hours prior to H_2O_2 treatment. BDNF was not added to the medium for survival studies, as BDNF can act as a neuroprotective agent^[58] and we wanted to discern to what degree the biofunctionalized substrates were neuroprotective. After a 24 hour acclimation period in anti-oxidant free medium, 20 μM of H_2O_2 was added to culture medium and the cells were exposed for 6 hours. Alamar Blue (Life Technologies), a cell viability probing reagent, was applied to each sample and cells were incubated at 37°C for an additional 24 hours. The samples were analyzed using a fluorescent plate reader, where samples were read at 570 nm and 600 nm. Cell viability was determined using calculations provided in the manufacturer's instructions. The test conditions were normalized to fluorescent readings of H9-NSCs cultured on PDL/LN substrates in NDM containing BDNF. Cells treated with 1% saponin, in anti-oxidant free NDM, were used as a condition to in which the yield of cell death was high.

4.2.10. Statistical Analysis

The data shown represents the means \pm standard error of the mean. For the FGFR inhibition study, student's t-test, for unpaired samples, was used to determine statistical differences between treated and control samples. Variance of analysis using one-way ANOVA, along with *post hoc* means comparison with Tukey's test was used to determine statistical differences amongst conditions for the remaining studies. Statistical significance was indicated with p values < 0.05 .

4.3. Results

4.3.1. N-cad-Fc and L1-Fc Functionalized 2-D Films

To verify the presence of both N-cad-Fc and L1-Fc and 2-D polymers films, an ELISA was employed. The relative amount of N-cad-Fc on the surface increased in a dose dependent manner (Figure 4.1B) where N-cad-Fc was applied alone or in combination with L1-Fc. N-cad-/L1-Fc substrates resulted in less N-cad-Fc on the surface in comparison N-cad-Fc only substrates. An L1-Fc ELISA was performed on substrates that were treated with both recombinant proteins and compared to substrates that were only treated with L1-Fc. The results indicate the amount of L1-Fc present on the surface was relatively similar in magnitude on 2-D films alone or in combination with all concentrations of N-cad-Fc (Figure 4.1C).

4.3.2. N-cad-/L1-Fc Substrates Promote H9-NSC Attachment

In order for a substrate to be a candidate for promoting differentiation and growth of H9-NSCs, the substrate must be permissive for cell attachment. The adhesion of the H9-NSCs was determined after 24 hours by counting the number of Hoechst 33258 stained nuclei in each field of view (10 per condition) (Figure 4.1D). Poly-D-lysine (PDL) and laminin (LN) treated substrates were effective in promoting attachment of neurons and NSCs. Integrins bind to laminin, while the positive charge of PDL interacts with the negative

charge of the cells membrane. To this end, the percent cell attachment to each surface was determined using PDL/LN as the substrate that resulted in maximum H9-NSC attachment. There was a slight decrease in cell attachment as the N-cad-Fc concentration was increased (77%, 74%, and 74.1%). H9-NSC attachment was only slightly lower for conditions where L1-Fc was presented along with N-cadherin-Fc (70.5%, 73.7%, and 68.1%) compared to the corresponding N-cad-Fc concentrations. L1-Fc alone and protein A (PA) treated substrates resulted in the very low cell attachment (12.4% and 12%, respectively) and were considered non-permissive for cell attachment.

4.3.3. Surface N-cad-Fc Induces Differential Localization of Cellular N-cadherin

Immunofluorescence was used to determine cellular localization within H9-NSCs after 24 hours in culture. H9-NSCs were immunostained with an antibody against the extracellular domain of N-cad, which could also label surface adsorbed N-cad-Fc. Due to surface binding of the extracellular N-cad antibody to substrate-functionalized N-cad-Fc, areas where cells appear black and the surrounding regions look green, represent surface N-cad-Fc (Figure 4.1E). H9-NSCs were also labeled with β -catenin as well as an antibody against an intracellular epitope of N-cadherin. Using confocal microscopy, 0.5 μ m optical sections (top to bottom) were taken to visualize N-cadherin localization throughout the cells. N-cadherin in H9-NSCs cultured on low N-cad-Fc 2-D films appeared to be localized around or at the cell membrane (Figure 4.1E, middle), similar to that observed in H9-NSCs, grown on PDL/laminin, in contact with one another (Figure 4.1E, top). Images that were taken closer to the basement membrane of H9-NSCs on low N-cad-Fc substrates revealed areas where N-cadherin was not localized at the cell membrane, but as clusters more central to the cell. In the case of H9-NSCs grown on high N-cad-Fc 2-D films, cellular N-cadherin was localized, away from the membrane, in a cluster more central within the cell (Figure 4.1E, bottom). β -catenin assumed a similar localization pattern as extracellular N-

cadherin (4.S1), suggesting that the engagement of substrate presented N-cad-Fc with cellular N-cadherin promoted sequestration of β -catenin.

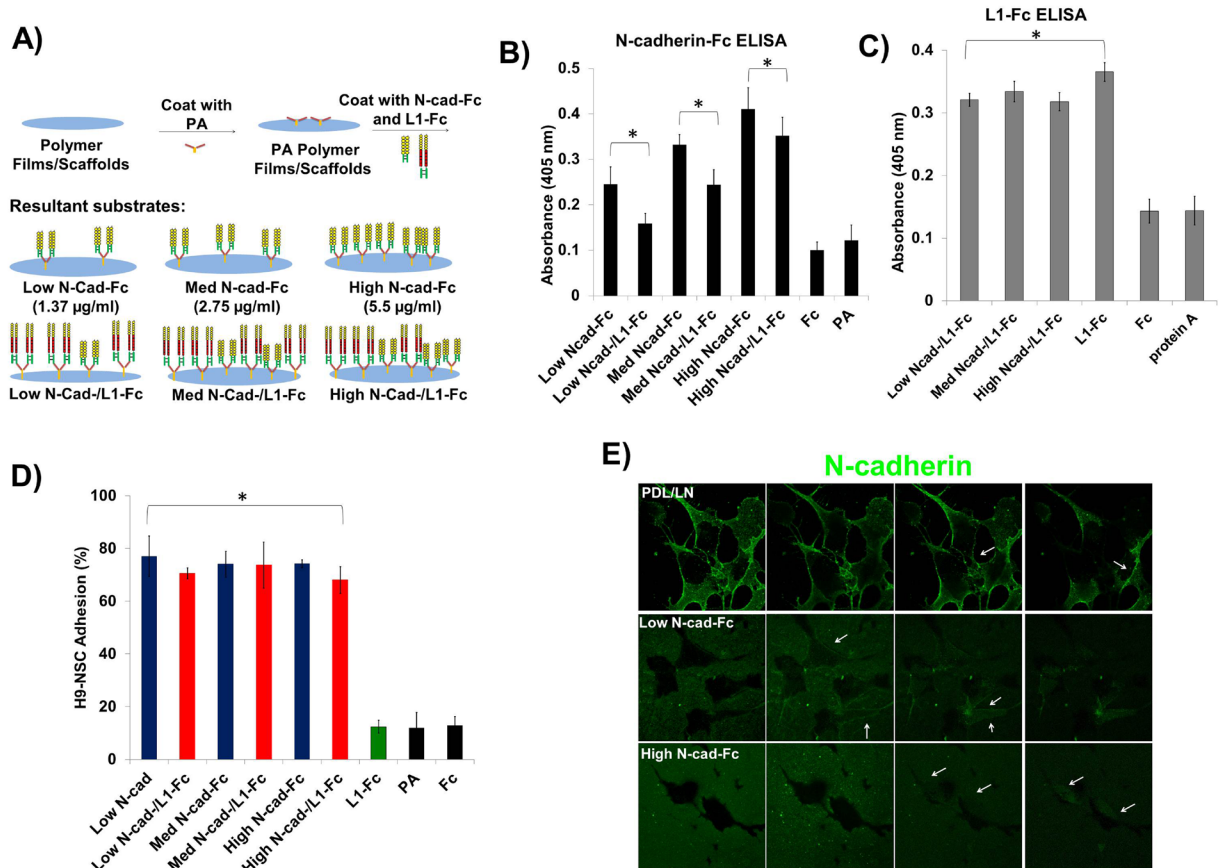


Figure 4.1: H9-NSC attachment and N-cadherin localization in response to N-cad-Fc 2-D films.

A) Schematic showing the treatment of polymer films with N-cad- and L1-Fc. B) 1.375, 2.75, 5.5 μ g/ml (Low, Med, High, respectively) of N-cad-Fc was applied alone or in combination with 10 μ g/ml of L1-Fc and an ELISA was used to detect relative amounts of N-cad-Fc on the surface. An increase of N-cad-Fc was detected in a dose dependent manner whether applied to 2-D films alone or in combination with L1-Fc, but less N-cad-Fc was detected when applied with L1-Fc. (§ denotes $p < 0.05$) C) L1-Fc ELISA where the relative amounts of L1-Fc was detected when combined with varying concentrations of N-cad-Fc or deposited on the polymer film alone. The absorbance reading for L1-Fc was the same when combined with all concentrations of N-cad-Fc or applied to the 2-D films alone. D) H9-NSCs attached to N-cad-Fc or N-cad-L1-Fc 2-D films with the same efficiency after 24 hours, with very low attachment to L1-Fc and PA substrates. Each condition was normalized to H9-NSC attachment to PDL/LN 2-D films. E) After 24 hours in culture, H9-NSCs, immunocytochemistry was used to determine cellular N-cadherin localization (white arrows) in response to low and high N-cad-Fc 2-D films and optical sections were taken using confocal microscopy. The antibody used against extracellular domain of N-cadherin also detected surface adsorbed N-cad-Fc, causing black areas where cells attached for low and high N-cad-Fc substrates. H9-NSCs grown on PDL/LN exhibited typical N-cadherin localization, resulting in bright green bands at cell-cell borders (white arrows) at each section. N-cadherin localization in H9-NSCs cultured on low-N-cad-Fc 2-D films was similar to that observed on PDL/LN, with bright bands of green at the cell membrane in the first two

sections, as well as areas more central within the cell. H9-NSCs cultured on high N-cad-Fc exhibited localization of N-cadherin away from the membrane a large cluster more central within the cell. (* denotes $p < 0.05$ compared to PA and Fc controls [C,D] or between N-cad-Fc and N-cad-/L1-Fc conditions [B].)

4.3.4. N-cad-Fc Combined with L1-Fc Influences Neuritogenesis and Neurite Outgrowth

During neural development, neural stem cell, cell-cell contacts are strongly mediated by homophilic engagement of N-cadherin and the degree of engagement influences neural stem cell differentiation [50]. To test the role of N-cadherin presentation of NSC neuronal differentiation, H9-NSCs were cultured on 2-D films low, med, or high (1.375, 2.75, or 5.5 $\mu\text{g/ml}$) of N-cad-Fc alone or in combination with 10 $\mu\text{g/ml}$ of L1-Fc. After 7 days in culture, the cells were immunostained with β -III-tubulin, and the following was quantified: the percent of cells that extended neurites, the average total neurite length, and the longest neurite lengths. Due to low attachment of H9-NSCs to L1-Fc and PA treated 2-D films, those two conditions were omitted from these studies. The morphology of H9-NSCs grown on N-cad-Fc and N-cad-/L1-Fc substrates was observed through immunolocalization studies of a key early neuronal marker, β -III-tubulin (Figure 4.2A). All conditions possessed cells that were β -III-tubulin+ and the typical neuronal morphology. In addition, there were also β -III-tubulin+ cells that did not possess a neuronal morphology, but were larger in size, compared to the neuronal looking cells, and did not extend neurites. The percent of cells that possessed a neuronal morphology and extended neurites was quantified for each condition (Figure 4.2B). As N-cad-Fc concentration increased, the percent of H9-NSCs extending neurites decreased, with 40.8%, 29.6%, and 24.7% of H9-NSCs extending neurites on low, med, and high concentrations of N-cad-Fc on 2-D films, respectively (Figure 4.2B). When N-cad-Fc and L1-Fc were combined, low N-cad-/L1-Fc presenting substrates

enhanced neuritogenesis (56.2%) compared to the equivalent low concentration of N-cad-Fc alone. Additionally, med N-cad-/L1-Fc 2-D films promoted an increase in cells extending neurites (43.3%) compared to med N-cad-Fc alone. However, in the case where N-cadherin- and L1-Fc were presented at equal molar ratios (high N-cad-/L1-Fc), the percentage of cells that extended was greatly reduced, almost down to the levels elicited by high N-cad-Fc alone, demonstrating there might be threshold of N-cadherin that might impede neuronal differentiation of neural stem cells. Neurite lengths (total and longest) were also quantified, after 7 days. The total neurite length indirectly correlated to N-cad-Fc concentrations as low N-cad-Fc substrates promoted longer total neurite lengths, at 251.5 μm compared to lengths observed on med-N-cad-Fc (191.7 μm) and high N-cad-Fc (165.2 μm) 2-D films (Figure 4.2C). H9-NSCs grown on N-cad-/L1-Fc 2-D films displayed enhanced total neurite outgrowth compared to substrates presenting N-cad-Fc alone. The greatest lengths were observed on low N-cad-/L1-Fc (383.9 μm), followed by med N-cad-/L1-Fc (282.6 μm), and high N-cad-/L1-Fc (254.72 μm). Quantification of the longest neurite lengths revealed there was only a slight decrease in H9-NSCs cultured on high N-cad-Fc (97.6 μm) compared to low and med N-cad-Fc presenting substrates (125.3 μm , 122.6 μm , respectively) (Figure 4.2D). In contrast, there was a significant decrease in the lengths of the longest neurite as the N-cad-Fc concentration increased when combined with L1-Fc (Figure 4.2D) suggesting that as N-cad-Fc concentration increases, the influence of L1-Fc in promoting neurite extension decreases.

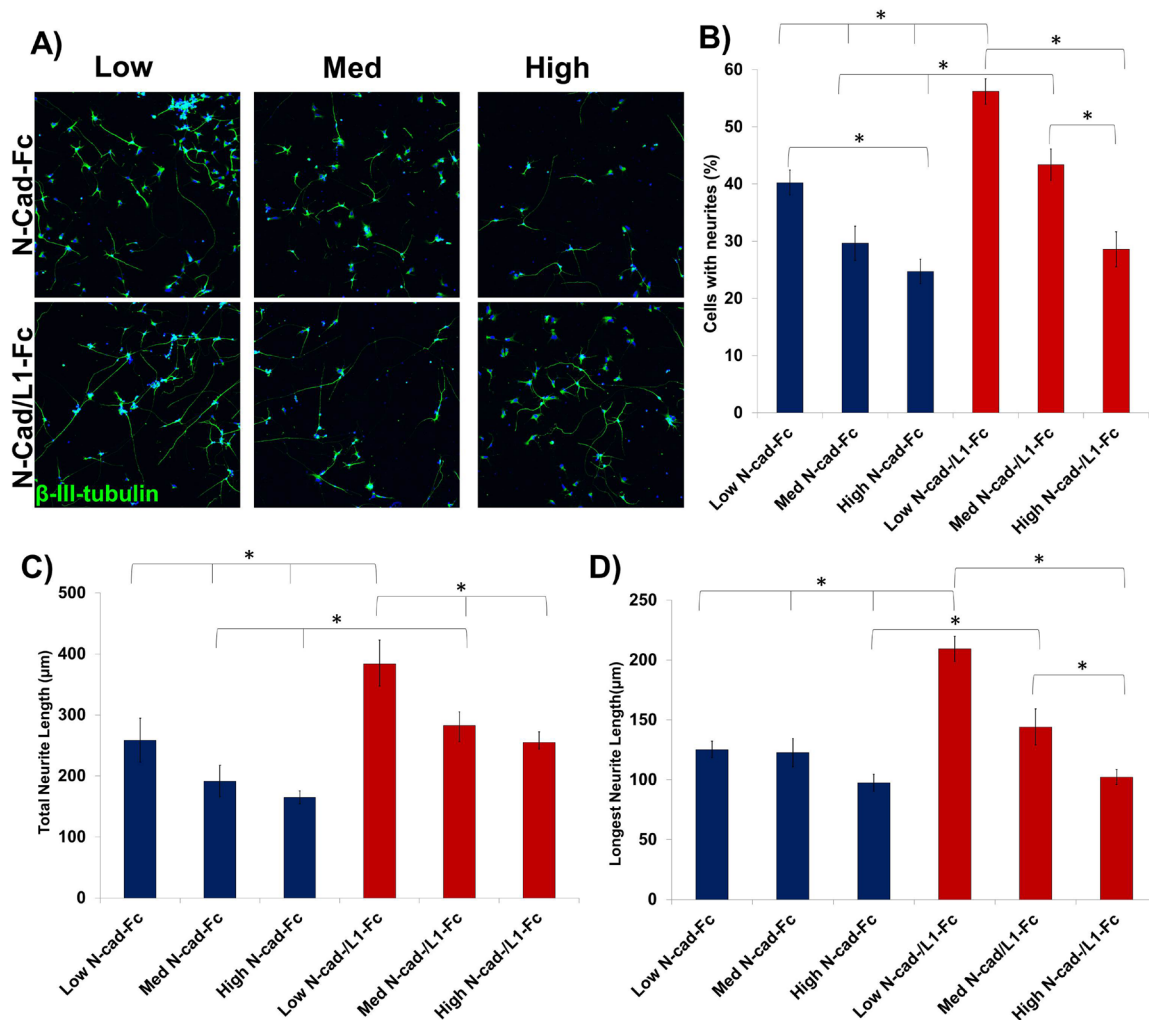


Figure 4.2. N-cad-and L1-Fc, combined, influence neuritogenesis and neurite outgrowth of H9-NSCs on 2-D substrates. A) Morphology of H9-NSCs, after immunolabeling with β -III-tubulin (green) and Hoechst (blue) cultured on varying concentrations of N-cad-Fc low, med, and high (1.375, 2.75, and 5.5 μ g/ml, respectively) alone and in combination with L1-Fc (10 μ g/ml), which resulted in 0.25; 0.5; and a 1:1 ratio of N-cadherin-Fc:L1-Fc, respectively. B) Quantification of the percent of H9-NSCs that extended neurites after 7 days. The lowest concentration of N-cad-Fc (1.375 μ g/ml), co-presented with L1-Fc, induced greater neuritogenesis compared to other combinations of N-cad- and L1-Fc and N-cad-Fc alone. C) Quantification of the average total neurite lengths of NSCs after 7 days. D) Quantification of the longest neurite length of H9-NSCs after 7 days in culture. (* denotes $p < 0.05$).

4.3.5. Surface Presented N-cad-Fc Combined with L1-Fc Enhances Neuronal Differentiation

To obtain a more comprehensive readout of NSC differentiation patterns, in addition to probing for the early neuronal marker β -III-tubulin, H9-NSCs were immunolabeled with antibodies against MAP2 and neurofilament-M, which are both markers used to detect

maturing neurons^[59]. H9-NSCs, positive for both MAP2 and neurofilament-M, were observed across all N-cad-Fc or N-cad-/L1-Fc presenting 2-D films (Figure 4.3A). However, quantification of MAP2 cells, possessing a neuronal morphology showed that low N-cad-Fc (1.375 $\mu\text{g/ml}$) contained a higher percentage of MAP2+ cells (37%) compared to medium N-cad-Fc (2.75 $\mu\text{g/ml}$) (25.3%) and high N-cad-Fc (5.5 $\mu\text{g/ml}$) (18%) (Figure 4.3B). Low N-cad-Fc substrates also promoted a slightly higher percentage of neurofilament-M+ cells (31%) compared to cells grown on substrates presenting medium concentration of N-cad-Fc (21%) and high concentration of N-cad-Fc (22.5%) (Figure 4.3C). Similar to our previous observations with β -III-tubulin immunofluorescence, there were some MAP2+/neurofilament-M negative cells that also did not show a neuronal morphology. As a result, those cells were excluded for quantifying MAP2+ cells. Notably, the presentation of low concentration of N-cad-Fc, combined with 10 $\mu\text{g/ml}$ of L1-Fc, resulted in the highest percentage of MAP2+ cells (49%) (Figure 4.3B), as well as the highest percentage of neurofilament-M+ cells (58.1%) (Figure 4.3C). The percentage of MAP2+ and neurofilament-M+ cells decreased with increasing concentrations of N-cad-Fc when combined with L1-Fc (Figure 4.3B-4.3C). The NSCs were also immunostained with an antibody against NeuN, which is a mature, post-mitotic neuronal marker. NeuN+ cells were not observed on any of the N-cad-Fc or N-cad-/L1-Fc 2-D films (data not shown), suggesting that neither N-cad-Fc alone or N-cad-/L1-Fc substrates promoted post-mitotic maturation of the newly formed neurons within the first 7 days in culture. The lengths of the longest, neurofilament-M neurites per cell was quantified and low N-cad-Fc combined with L1-Fc promoted the longest neurite lengths (Figure 4.3D), similar to that observed of the longest neurite length that was β -III-tubulin positive. These results indicate that the density of surface presented N-cad-Fc greatly modulates signaling linked to neuronal differentiation

and neurite outgrowth and that there may be a certain threshold in which the synergy of N-cadherin and L1 is attenuated in altering H9-NSC behaviors.

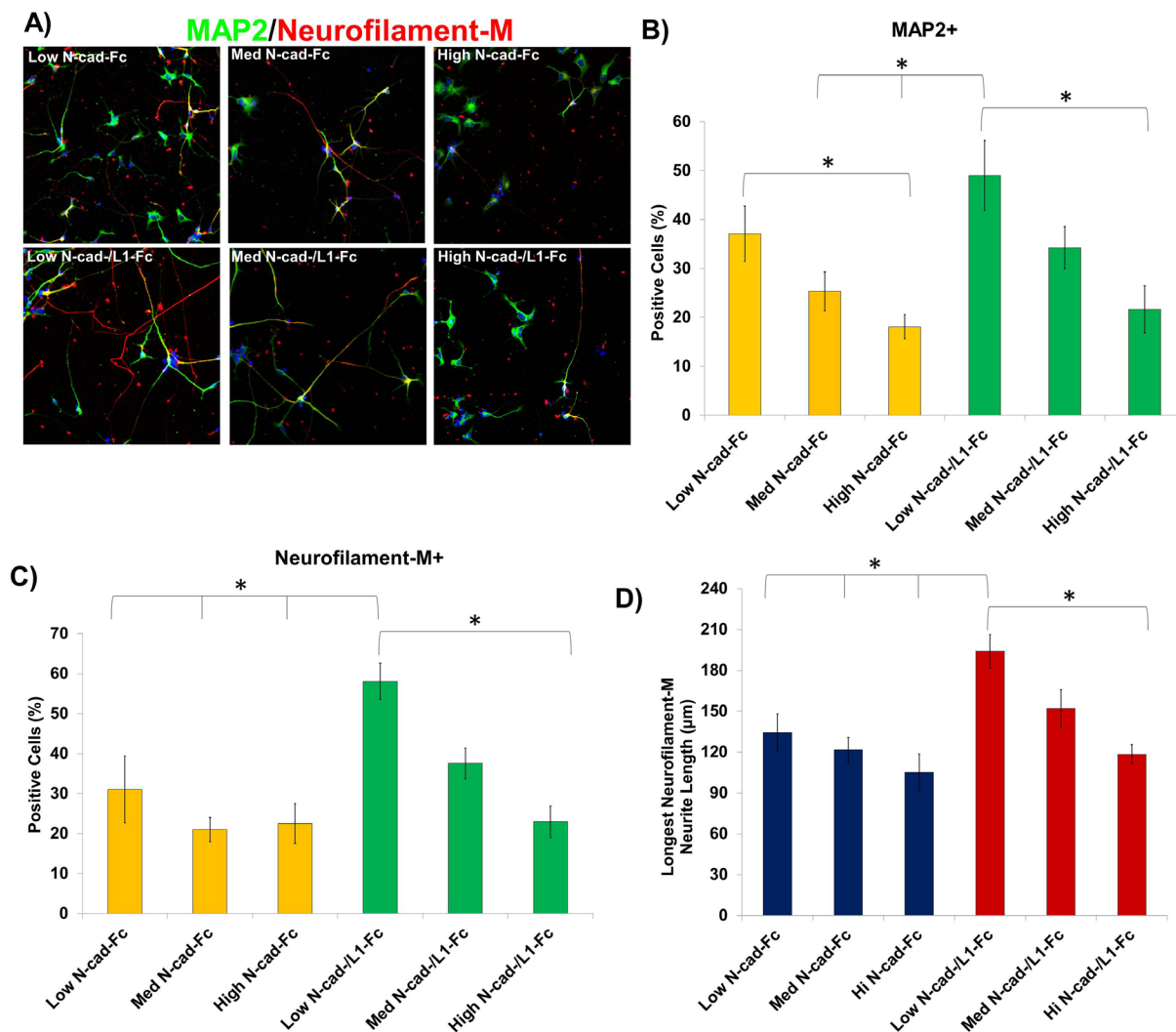


Figure 4.3. Neuronal differentiation of neural stem cells in response to N-cadherin-Fc and L1-Fc presenting 2-D substrates. A) H9-NSCs were immunostained with neuronal markers MAP2 (green) and neurofilament-M (red), and nuclei were stained with Hoechst (blue) after 7 days in culture. All conditions supported neuronal differentiation and H9-NSCs positive for both neuronal markers. B) Quantification of the percent of MAP2 positive cells showed that low levels of N-cad-Fc alone or combined with L1-Fc resulted in a greater percentage of MAP2+ cells, with a neuronal morphology, followed med N-cad-Fc combined with L1-Fc. C) All the substrates in which N-cad- and L1-Fc were combined yielded a higher percentage of neurofilament-M+ cells compared to substrates where N-cad-Fc was presented alone, with low N-cad-/L1-Fc 2-D films resulting in the highest percentage of neurofilament-M+ cells. D) Low N-cad-/L1-Fc combined promoted longer neurofilament-M+ neurites, while medium (2.75 µg/ml) and high (5.5 µg/ml) concentrations of N-cad-Fc, co-presented with L1-Fc, resulted in a modest increase in neurite length compared to the presentation of N-cad-Fc alone. (* denotes $p < 0.05$)

4.3.6. Interruption of Cell-Substrate N-cadherin Engagement Leads to Improved Neurite Outgrowth, But No Change in Neuronal Differentiation

A limited degree of neurite outgrowth was observed in H9-NSCs grown on high N-cad-Fc (5.5 $\mu\text{g}/\text{ml}$) substrates, even in the presence of L1-Fc. We hypothesized that this response was likely governed by an increase in cell-substrate adhesion, mediated by homophilic N-cad-N-cad engagement. A previous study demonstrated that oligodendrocytes displayed increased migration along astrocytes following the inhibition of N-cadherin function^[60], while another study found that N-cadherin inhibits Schwann cell migration along astrocytes^[61]. Additionally, Kawauchi showed that high N-cadherin expression interrupted neuronal migration *in vivo*^[62]. To determine if cell-substrate N-cadherin interaction played a role in the neuronal differentiation in our studies, cellular N-cadherin was blocked with an antibody against the extracellular domain of N-cadherin prior to seeding H9-NSCs onto high N-cad-Fc (5.5 $\mu\text{g}/\text{ml}$) alone or co-presented with L1-Fc. An increase in neurite lengths was observed following treatment with anti-N-cadherin (Figure 4.4A). When H9-NSCs were treated with 50 $\mu\text{g}/\text{ml}$ or 100 $\mu\text{g}/\text{ml}$ of anti-N-cadherin and cultured on high N-cad-Fc or high N-cad-/L1-Fc coated substrates, neurite lengths were significantly greater than those observed on high N-cad-Fc alone and combined with L1-Fc. Notably, neurite lengths of H9-NSCs treated with 100 $\mu\text{g}/\text{ml}$ of anti-N-cadherin on high N-cad-Fc alone or combined with L1-Fc conditions were comparable to that of H9-NSCs that had been grown on low N-cad-/L1-Fc substrates. The results of this study suggest that there is a threshold level of substrate presented N-cadherin that causes longer neurite extensions. In the case of anti-N-cadherin-treated NSCs, which were cultured on PDL and laminin coated substrates, there were no differences in NSC organization and outgrowth compared to H9-NSCs that were not treated with the antibody (data not shown), indicating that the antibody itself was not responsible for promoting increased neurite lengths of NSCs

following antibody treatment. Additionally, there were no differences observed in isotype control treated H9-NSCs (4.S2), indicating the response was specific to N-cad/N-cad interactions. Additionally, we investigated the degree to which the N-cad/N-cad interactions between the substrate and cells influenced the expression of neuronal markers MAP2 and neurofilament-M. Treatment of H9-NSCs with anti-N-cadherin did not appear to alter neuronal differentiation, as the percentage of MAP⁺ cells was relatively similar in H9-NSCs treated with 50 (20%) or 100 $\mu\text{g}/\text{ml}$ of anti-N-cadherin compared to untreated H9-NSCs (20.7%) cultured on high N-cad-Fc 2-D films (Figure 4.4B). The same trend was also observed in the percentage of neurofilament-M⁺ (Figure 4.4B) cells and in H9-NSCs cultured on N-cad-/L1-Fc presenting 2-D films (Figure 4B).

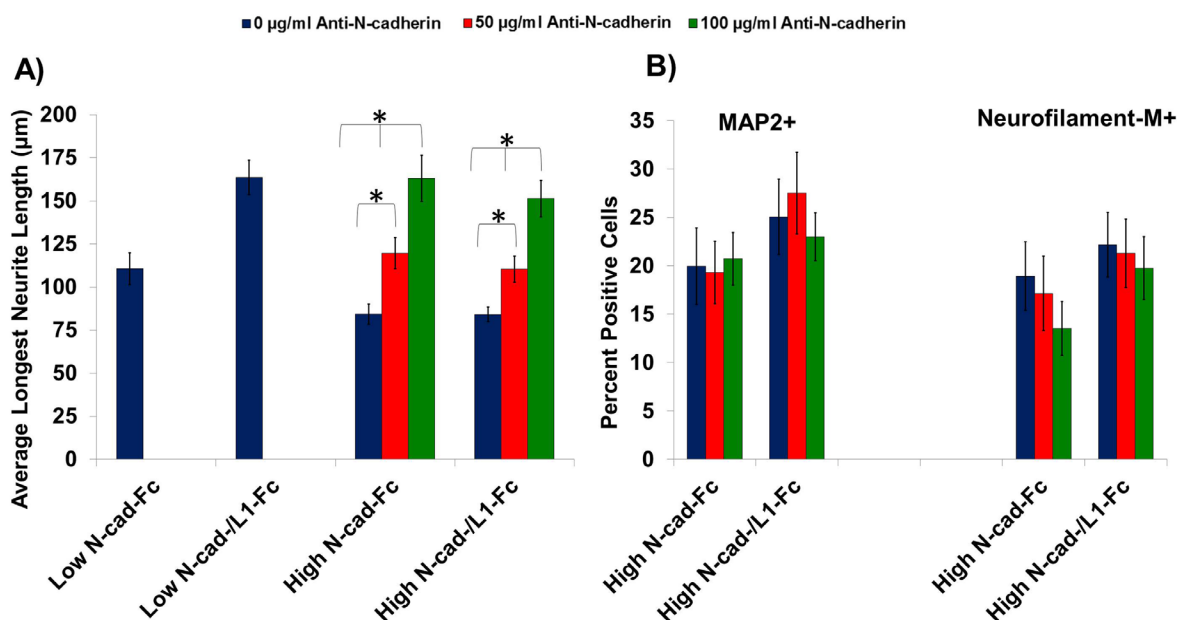


Figure 4.4. Interruption of N-cadherin Interactions Improves Neurite Outgrowth on 2-D substrates. A) H9-NSCs were treated with either 50 or 100 $\mu\text{g}/\text{ml}$ of anti N-cadherin and cultured on thin films treated with high N-cadherin-Fc (5.5 $\mu\text{g}/\text{ml}$) alone or in combination with 10 $\mu\text{g}/\text{ml}$ of L1-Fc and compared to cells cultured on low N-cadherin-Fc (1.375 $\mu\text{g}/\text{ml}$) alone or combined with L1-Fc (10 $\mu\text{g}/\text{ml}$), for 5 days. Quantification of the longest neurite length showed improved neurite

growth following treatment with 100 µg/ml of anti N-cadherin for NSCs cultured on high N-cadherin-Fc alone or combined with L1-Fc, which was comparable to neurite lengths observed on low N-cad-/L1-Fc surfaces. There was no difference observed between N-cadherin alone and the combination of N-cadherin- and L1-Fc. (* denotes $p < 0.05$).

4.3.7. Inhibition of Fibroblast Growth Factor Receptor Modulates Neuronal Differentiation

The fibroblast growth factor receptor (FGFR) is known to regulate neural stem cell proliferation and differentiation. Further, N-cadherin/FGFR interactions have been implicated in N-cadherin mediated neurite outgrowth of primary neuronal cells cultured along cells overexpressing N-cadherin or on substrates where N-cadherin was adsorbed. Studies have also demonstrated that L1-mediated neurite outgrowth of primary neurons involves L1/FGFR interactions^[30,42]. To inhibit FGFR activity, PD173074, a molecule known to prevent auto-phosphorylation of FGFR, was applied to cultures at 750 nM 24 hours after plating onto functionalized 2-D films and applied to culture medium every two days for a period of 6 days. H9-NSCs neuronal differentiation was assessed by quantifying the percent of MAP2+ and neurofilament-M+ cells that possessed neuronal morphology. Following treatment with the FGFR inhibitor, H9-NSCs grown on high N-cad-Fc 2-D films exhibited an increase in MAP2+ cells to 48.5%, from the 29.1% observed in H9-NSCs that were not treated with the inhibitor (Figure 4.5A). Similarly, the percentage of MAP2+ H9-NSCs also increased to 48.2% from 30.8% when cultured high N-cad-/L1-Fc 2-D films (Figure 4.5A). FGFR inhibition also resulted in an increase in neurofilament-M+ cells in H9-NSCs grown on high-N-cad-Fc to 38.4% and high N-cad-/L1-Fc to 44.7%, over untreated cells (26.5% and 30% respectively) (Figure 4.5B). In the case of low N-cad-Fc presenting substrates, there was a more modest increase in MAP2+ cells (from 39.2% to 48.3%) (Figure 4.5A) and neurofilament-M+ cells (34.4% to 40.6%) (Figure 5B). In contrast, FGFR inhibition in H9-NSCs that were exposed to low N-cad-/L1-Fc 2-D films resulted in minute increases in

MAP2+ and neurofilament-M+ cells (Figure 4.5A-4.5B). H9-NSCs cultured on PDL 2-D films did not display a change in neuronal differentiation following treatment with the FGFR inhibitor (data not shown), suggesting that the changes observed were specific to substrate N-cad-Fc and FGFR interactions.

Treatment of H9-NSCs cultured on high N-cad-Fc may have reduced the activity of N-cad-Fc/FGFR signaling to levels comparable with the activity of low N-cad-Fc/FGFR interactions. An increase in neuronal differentiation of H9-NSCs grown on high-N-cad-Fc 2-D alone or with L1-Fc, following FGFR inhibition, suggests that high N-cad-Fc presenting substrates activate or alter FGFR signaling that, in turn, reduces neuronal differentiation of H9-NSCs. Additionally, the lack of improvement or decline in neuronal differentiation, following FGFR inhibition, in H9-NSCs from low N-cad-/L1-Fc 2-D films, indicates that FGFR is not solely responsible for the synergy between N-cad-Fc and L1-Fc and other receptors and signaling pathways are involved in neuronal differentiation are activated.

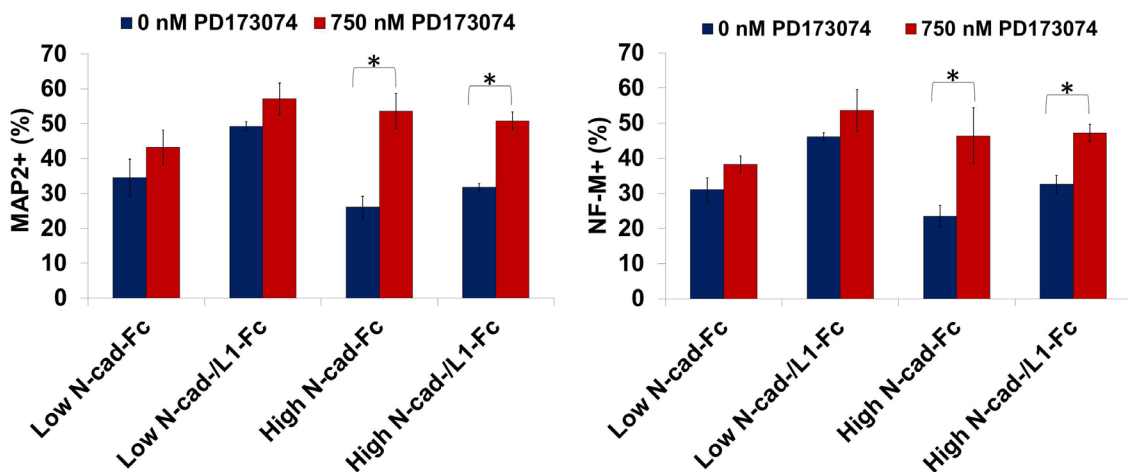


Figure 4.5. Inhibition of FGFR improves neuronal differentiation of H9-NSCs cultured on high N-cad-Fc 2-D films. H9-NSCs were cultured on N-cad-Fc or N-cad-/L1-Fc substrates were treated with the FGFR inhibitor, PD173074 and neuronal differentiation was compared to H9-NSCs not exposed to the inhibitor. A) Following FGFR inhibition, the percentage of MAP2+ cells increased in H9-NSCs cultured on high N-cad-Fc and high N-cad-/L1-Fc functionalized 2-D films. There was a marginal increase in MAP2+ in H9-NSCs grown on low N-cad-Fc substrates and effectively no change

in observed on low N-cad-/L1-Fc substrates. B) The percentage of neurofilament-M+ cells also increased in H9-NSCs exposed to high N-cad-Fc and high N-cad-/L1-Fc 2-D films. (* denotes $p < 0.05$).

4.3.8. Combined Display of N-cadherin and L1-Fc has Synergistic Outcomes in NSCs cultured in Fibrous 3-D Scaffolds

As neural tissue engineering aims to combine bioactive molecules and biomaterials, we sought to determine how the cell responses elicited by 2-D, N-cad-/L1-Fc functionalized surfaces can be translated to 3-D, fibrous scaffolds. We tested all of the conditions that were tested in 2-D, and given the inherent surface area and curvature of the fibrous scaffolds, we also included an even lower concentration of N-cad-Fc (very low, 0.6875 $\mu\text{g/ml}$) (Figure 4.6A) as well as L1-Fc (Figure 4.6B). Very low N-cad-Fc and low N-cad-Fc, in combination with L1-Fc, promoted longer neurite lengths (240.5 μm and 210.8 μm , respectively) compared to the corresponding very low N-cad-Fc (150.9 μm) and low N-cad-Fc (137.9 μm) only treated scaffolds (Figure 4.6C). L1-Fc functionalized scaffolds promoted neurite extensions that were comparable in length (150.3 μm) to H9-NSCs grown on very low N-cad-Fc and low N-cad-Fc functionalized scaffolds, as well as that of med-N-cad-/L1-Fc (160.5 μm) and high N-cad-/L1-Fc (157.7 μm), but slightly longer than that observed on med N-cad-Fc (113.2 μm) and high N-cad-Fc (117.4 μm) treated scaffolds. Another cellular response of note was the difference in organization displayed by H9-NSCs in response to the different substrates. At lower concentrations of N-cad-Fc (very low and low), H9-NSCs appeared to cluster slightly more in comparison to med and high N-cad-Fc treated scaffolds (Figure 4.6A). The addition of L1-Fc somewhat disrupted clustering of H9-NSCs on lower N-cad-Fc presenting scaffolds. As the concentration of N-cad-Fc increased, H9-NSCs appear more spaced out with fewer cell-cell contacts. H9-NSC attachment was also observed on PA only treated scaffolds, indicating non-specific interactions between cells and the scaffold, such as surface chemistry or topography, which facilitates adhesion to the scaffolds. It is

also possible that PA modulates hydrophilicity^[63] of the substrates, thereby facilitating non-specific adhesion, although this was not the case on 2-D films; further indicating the role scaffold topography plays in cell adhesion. The results of these studies suggest that 1) the display of N-cad-Fc and L1-Fc from the scaffolds further support the importance and benefit of three dimensional topography, as cells were able to attach and exhibit a favorable response at an even lower N-cad-Fc, as well as L1-Fc in contrast to 2-D films and 2) The synergistic effect of N-cad-Fc and L1 translates over to electrospun scaffolds, thereby highlighting the potential of the use of this biofunctionalized scaffold for neural tissue engineering applications. The influence of N-cad-Fc or N-cad-/L1-Fc functionalized scaffolds on neuronal differentiation was determined by quantifying the number of MAP2+ cells (Figure 4.6D) and neurofilament-M+ cells (Figure 4.6E). Very low N-cad-Fc resulted in 32.2% MAP2+ cells, while 43.9% of H9-NSCs grown on low N-cad-Fc were positive for MAP2. We observed a peak in MAP2+ cells on low N-cad-Fc substrates, as both med and high N-cad-Fc substrates resulted in a lower MAP2+ population at 21.9% and 17.3%, respectively. A similar trend in MAP2+ was observed on N-cad-/L1-Fc treated scaffolds, where very low and low N-cad-/L1-Fc substrates resulted more MAP2+ cells (32.7% and 35.9%, respectively), followed by med N-cad-/L1-Fc (22.2%) and high N-cad-/L1-Fc (21.4%). L1-Fc resulted 20.6% MAP2+ H9-NSCs, followed by PA where only 6.8% of H9-NSCs were MAP2+. In the case neurofilament+ H9-NSCs, both very low N-cad-Fc (24.6%) and low N-cad-Fc (23.6%) substrates possessed more neurofilament-M+ cells compared to med N-cad-Fc (14.1%) and high N-cad-Fc (13.5%) functionalized scaffolds (Figure 4.6E). Combining L1-Fc with very low and low N-cad-Fc promoted an increase in the percent of neurofilament-M+ cells compared to med N-cad and high N-cad combined with L1-Fc (Figure 4.6E). H9-NSCs grown on L1-Fc scaffolds had a neurofilament-M+ population

comparable to med and high N-cad-Fc alone or combined with L1-Fc and PA treated scaffolds resulted in the neurofilament-M positive population (4.1%).

4.3.9. Low N-cad-Fc Presenting 2-D films and Scaffolds Promote H9-NSC Survival

The release of reactive oxygen species following injury to CNS is a major trigger for neuronal cytotoxicity-related death^[64]. Substrates designed for cell transplantation therapies that promote survival under harsh conditions following injury would be ideal candidates for priming cells prior to transplantation and providing the appropriate neuroprotective and neurotrophic cues post-transplantation. N-cadherin and L1 have been reported to promote cell survival^[65,66]. Therefore, we sought to determine the degree to which 2-D films and 3-D scaffolds functionalized with N-cad-Fc and/or L1-Fc promoted survival of H9-NSCs. H9-NSCs, cultured on 2-D films or scaffolds functionalized with N-cad-Fc or both N-cad-/L1-Fc, were introduced to oxidative stress conditions through exposure to 20 μM H_2O_2 , for 6 hours in anti-oxidant free medium. Following the 6 hour incubation period, Alamar Blue, a reagent used to assess cell viability, was applied and cells were assayed 24 hours later using a fluorescent plate reader. Cell survival was determined by comparing fluorescent readings of H9-NSCs cultured on PDL/LN substrates, in medium supplemented with BDNF, as BDNF has been shown to provide neuroprotection. H9-NSCs cultured on 2-D films functionalized with low N-cad-Fc alone (120.4%) and combined with L1-Fc (103.7%) resulted in increased cell survival in comparison to med N-cad-Fc presenting substrates (77.9%) or med N-cad-/L1-Fc substrates (74%) and high N-cad-Fc presenting substrates alone (78.3%) or in combination with L1-Fc (69.1%) (Figure 4.7A). We also examined the ability of 3-D scaffolds functionalized with N-cad-Fc to or N-cad-/L1-Fc to promote survival of H9-NSCs (Figure 4.7B). We found that scaffolds functionalized with very low concentrations of N-cad-Fc and low N-cad-Fc resulted in the highest degree of survival (139% and 100.6%, respectively) in comparison to H9-NSCs cultured on high N-

cad-Fc functionalized scaffolds (75.2%). While the addition of L1-Fc caused a reduction in survival, very low N-cad-/L1-Fc did promote better survival compared to L1-Fc combined with low (86.7%) and high N-cad-Fc (78.7%) as well as L1-Fc alone (81.8%). It is important to note that all tested conditions resulted in significantly better cell survival compared PA treated scaffolds, which yielded 32.4% in H9-NSC survival, demonstrating that N-cad-Fc and/or L1-Fc functionalized 2-D films and 3-D scaffolds promote survival of H9-NSCs under oxidative stress conditions.

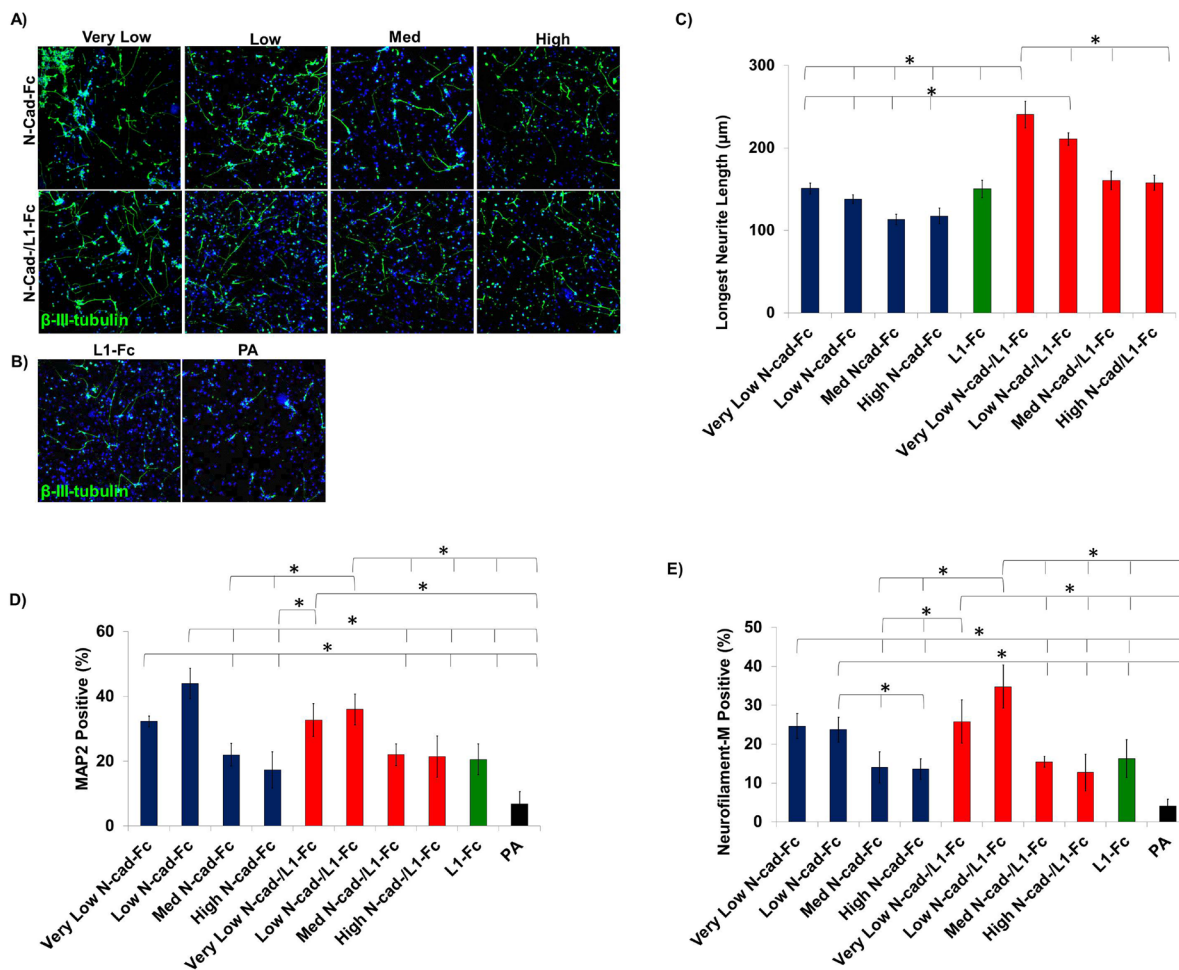


Figure 4.6. N-cad-/L1-Fc presenting scaffolds affect neuritogenesis and neuronal differentiation. A) NSC morphology, after 7 days of growth on electrospun scaffolds biofunctionalized with very low, low, medium, or high N-cad-Fc alone (0.6875, 1.375, 2.75, or 5.5 μ g/ml, respectively) or in combination with L1-Fc (10 μ g/ml). The cells were labeled with β -III-tubulin (green) and nuclei were labeled with Hoechst 33258 (blue). B) The morphology of NSCs cultured on L1-Fc (10 μ g/ml) and PA. C) Scaffolds functionalized with very low and low N-cad-Fc, combined with L1-Fc, promoted the best growth of the longest neurite compared to other conditions, including L1-Fc alone. Quantification of cells positive for D) MAP2 and E) neurofilament-M was used to determine the degree of neuronal differentiation of H9-NSCs on the various N-cad-Fc functionalized scaffolds. As N-cad-Fc concentration increased, MAP2+ and neurofilament-M+ cells decreased indicating a threshold of N-cad-Fc alone or in combination with L1-Fc necessary to promote neuronal differentiation within three dimensional scaffolds. (* denotes $p < 0.05$).

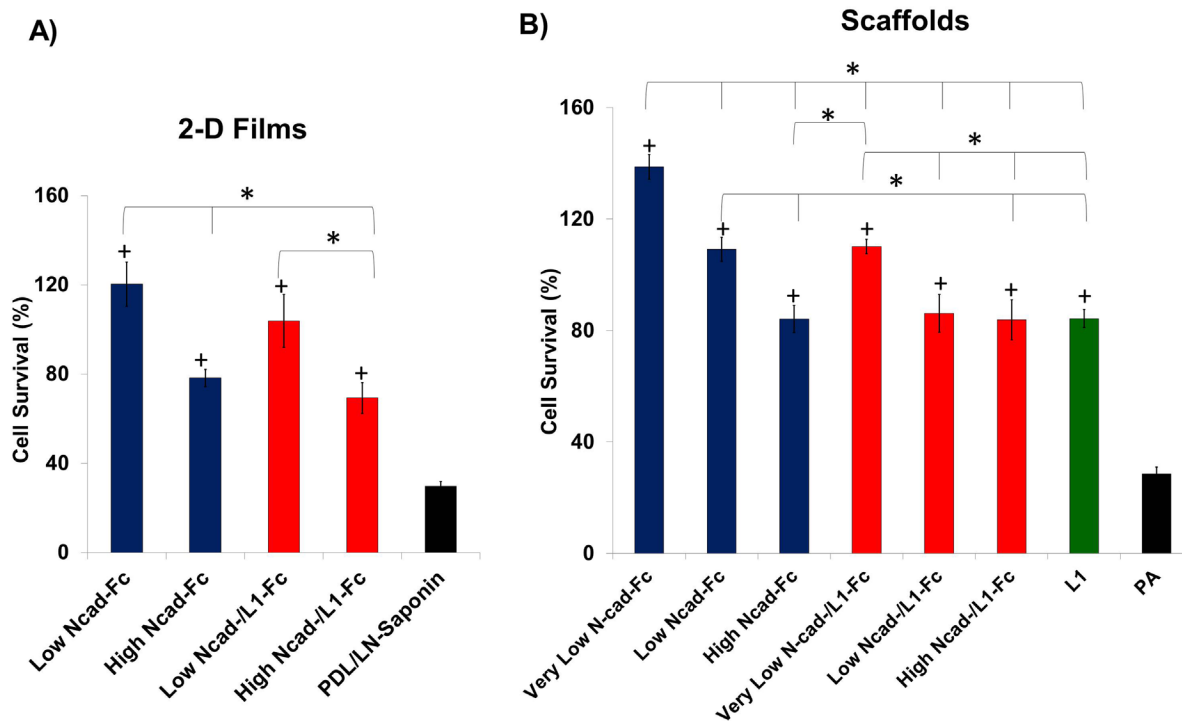


Figure 4.7. Low levels of N-cad-Fc promotes increased H9-NSC survival in the presence of hydrogen peroxide. NSCs were treated with 20 μ M of hydrogen peroxide for 6 hours and then assayed for survival using Alamar blue. A) 2-D films presenting a relatively low concentration of N-cad-Fc (low, 1.375 μ g/ml) promoted the greatest NSC survival over the control H9-NSCs cultured on PDL/LN in BDNF supplemented medium. H9-NSCs cultured on low N-cad-Fc (1.375 μ g/ml) combined with L1-Fc (10 μ g/ml) showed better survival compared to cells cultured on high N-cad-Fc (5.5 μ g/ml) alone or in combination with L1-Fc. However, 2-D films presenting high N-cad-Fc did provide some protection compared to H9-NSCs in the saponin treated control, where cell survival was low as expected. B) Fibrous scaffolds presenting very low N-cad-Fc (0.6875 μ g/ml) promoted better survival of H9-NSCs, followed by very low N-cad-Fc with L1-Fc, suggesting that in the presence of N-cad-Fc, the additional benefit of cell-cell contact enhances survival under oxidative stress conditions. While there were no appreciable differences in survival of H9-NSCs cultured on scaffolds functionalized with high N-cad-Fc with and without L1-Fc, low N-cad-/L1-Fc, and L1-Fc alone, these substrates did prove to be neuroprotective in comparison to PA treated scaffolds. PDL: poly-D-lysine, LN: laminin, PA: protein A. (* denotes $p < 0.05$, + denotes $p < 0.05$ compared to PDL/LN-saponin or PA conditions)

4.4. Discussion

Directing cell behavior *in vitro* for the purpose of cell transplantation following central nervous injury or onset of neurodegenerative diseases requires a balance of relevant, bioactive cues and structural supporting scaffolds to create a transplantable construct for treatment. Several research studies have examined in what manner neurotrophic factors, extracellular matrix proteins, and neural cell adhesion molecules can

be used alone or in combination for directing cell behaviors such as adhesion, proliferation, and differentiation into a specific neural cell type^[26,27,67,68]. In this study, we aimed to investigate how N-cad-Fc, at varying concentrations, influenced adhesion, neuronal differentiation, neurite outgrowth, and survival of H9-NSCs, when presented from 2-D films and 3-D, electrospun scaffolds. We also aimed to discern whether combinations of N-cad-Fc and L1-Fc could generate synergistic effects in these same NSC behaviors. We found that N-cad-Fc supports H9-NSC attachment across a range of concentrations on 2-D polymer films as well as on fibrous scaffolds, while L1-Fc only supported appreciable attachment onto fibrous scaffolds. We determined a range in which N-cad-Fc and L1-Fc can act synergistically in promoting neuronal differentiation and neuritogenesis on both 2-D films and 3-D scaffolds. Specifically, relatively low concentrations of N-cad-Fc afford this cooperative activity with L1-Fc in generating a larger population of cells positive for neuronal markers MAP2 and neurofilament-M and bearing longer neurite extensions, in contrast to relatively higher concentrations of N-cad-Fc. We found as N-cad-Fc concentration increased, the synergistic effect between the two cell adhesion molecules was lost, as was demonstrated by fewer MAP2+ and neurofilament-M+ H9-NSCs, as well as the lack of enhanced neurite outgrowth. To better understand the differential responses, a closer look had to be taken into how H9-NSCs responded to substrates where low N-cad-Fc and high cad-Fc were presented alone. We examined H9-NSC adhesion, differentiation, neurite outgrowth, and survival when cultured on N-cad-Fc presenting substrates.

The role of N-cadherin very early in neural development is well established. In order for neural stem cells to migrate to their target niche and differentiate, N-cadherin mediated cell-cell contacts must first be disrupted^[50]. After 24 hours, H9-NSCs cultured on N-cad-Fc substrates appeared more scattered in comparison to H9-NSCs cultured PDL/laminin substrates, indicating that cell-cell contacts were disrupted. We did not

observe any differences in H9-NSC attachment across the different concentrations of N-cad-Fc, showing that even the lowest concentration tested in 2-D (1.375 $\mu\text{g}/\text{ml}$) was sufficient to promote adhesion. However, there were differences in other cellular responses across the varying concentrations of N-cad-Fc, suggesting a change in signaling due to altering the density of substrate bound N-cad-Fc. Notably, E-cadherin presenting substrates were previously shown to modulate cellular function. For example, primary hepatocytes cultured in the presence of E-cadherin-Fc functionalized microbeads exhibited an increase proliferation and a decrease in differentiation due to the microbeads disrupting E-cadherin engagement, which in turn led to degradation of E-cadherin and an increase in proliferation^[69]. Another study by Semler et al presented substrate bound E-cadherin-Fc either alone or protein A presented to hepatocytes and observed an increase in differentiation of hepatocytes as the concentration of E-cadherin-Fc increased. Low cell densities resulted in the highest degree of functional activity, suggesting hepatocytes responded to substrate E-cadherin despite the lack of cell-cell contacts and juxtacrine signaling^[70]. These two studies demonstrate the effect of protein presentation on cadherin signaling and the resultant epithelial cell function and differences in cadherin activity.

In our studies, we observed contrasting responses of H9-NSCs in response to N-cadherin concentration. On low N-cadherin presenting substrates, we observed more neuronal differentiation compared to high N-cad-Fc presenting substrates, as indicated by MAP2+ cells, with neuronal morphology. The contrasting response of H9-NSCs on low versus high N-cadherin substrates indicates the tunable effects and control of N-cadherin mediated signaling, simply by varying surface density of N-cadherin. Based on the results of the immunocytochemistry of extracellular N-cadherin, it is apparent that the density of surface presented N-cadherin alters the localization of cellular N-cadherin and possibly acting as a switch for directing cellular response and function. We observed bands of N-

cadherin localized at the periphery of cells cultured on low N-cad, but not in cells cultured on high N-cad-Fc, where the localization was more clustered and central, at a single spot. Therefore, we believe that low N-cad-Fc substrates more closely mimic native N-cadherin mediated cell-cell contacts and resulting signaling, while still interrupting cell-cell contacts *in vitro*.

Further support of the idea of low N-cad-Fc substrates being more physiologically relevant and as a mimetic of N-cadherin mediated cell-cell contacts lies in the oxidative stress studies. We observed improved H9-NSC survival, following oxidative stress exposure, in H9-NSCs cultured on low N-cad-Fc presenting substrates, on 2-D films. In the case of 3-D scaffolds, we observed survival was maximal on substrates where N-cad-Fc concentration was lower and cells were able to form cell-cell contacts. Although H9-NSC survival was highest on low N-cad-Fc presenting substrates, high N-cad-Fc presenting substrates also proved to be neuroprotective as demonstrated by a higher percentage of survival compared to saponin treated H9-NSCs or H9-NSCs cultured on PA treated scaffolds. Previously, cancerous, epithelial cells, and neuronal cells have been shown to undergo apoptosis following disruption of cadherin adhesion^[71-73]. Tran et al found that N-cadherin engagement promoted survival in cancer cells through activation of the P13-kinase/Akt anti-apoptotic signaling pathway, resulting in phosphorylation of the pro-apoptotic protein, Bad and suppression of apoptosis^[74]. Pretreatment of rats with amine-modified, single wall nanotubes promoted neuronal protection under ischemic conditions, created by induced stroke, and it was determined that increased N-cadherin expression and activation of Akt survival pathway were, in part, responsible for the neuroprotective effect of the nanotubes^[75]. N-cadherin mediated survival as a result of cell-surface N-cadherin engagement was also demonstrated in primary neurons cultured on N-cadherin substrates in contrast to neurons cultured on poly-D-lysine, signifying the ability of substrate

presented N-cadherin and cellular N-cadherin engagement to be sufficient in promoting anti-apoptotic signaling, through down regulation of BIM within the Erk 1/2 MAP kinase pathway, mediated by N-cadherin engagement^[65]. These studies indicate the various survival signaling pathways that can be activated following N-cadherin engagement through cell-cell contacts or cell-substrate interactions. In our system, the greatest degree of cell survival was observed on substrates presenting low N-cad-Fc, which promoted localization of N-cadherin similar to that observed when two cells come into contact with one another or when cells were actually able to cluster together. Figure 4.8A depicts a proposed model for H9-NSC survival within our system.

N-cadherin homotypic engagement has been shown to maintain neural stem cells in a maintenance state, *in vivo*, and as N-cadherin expression decreases and cell-cell contacts are disturbed, neural stem cells migrate, and differentiation occurs^[50]. Here, by presenting substrate bound N-cad-Fc, cell-cell contacts were interrupted on 2-D films at low, medium, and high N-cad-Fc concentrations, as indicated by the scattered morphology of H9-NSCs on each concentration of N-Cad-Fc, in 2-D. However, neuronal efficiency was greater on low N-cad-Fc presenting substrates compared to high N-cad-Fc presenting substrates after 7 days and 14 days (4.S3). One possibility for enhanced neuronal differentiation across on low N-cad-Fc substrates might involve β -catenin. We observed some β -catenin localized at the membrane in H9-NSCs cultured on low N-cad-Fc substrates, suggesting a recruitment of β -catenin to the cell-substrate interface in response to surface N-cadherin/cellular N-cadherin engagement on low N-cad-Fc substrates. In the case of high N-cad, β -catenin was not found to be localized at the membrane and appeared more diffuse. Several reports have implicated the role of β -catenin signaling in differentiation of stem cells^[76] and the sequestration of β -catenin at the cell membrane due to cadherin engagement has been reported to promote differentiation due to the decrease of β -catenin available for

translocation to the nucleus^[77,78]. β -catenin sequestration to cadherin junctions results in decreased β -catenin signaling^[79] and decreased β -catenin signaling has been linked to neuronal differentiation of cortical neural precursors *in vivo*^[80,81] and *in vitro*^[49], while inhibition of Wnt/ β -catenin signaling has been shown to promote neuronal differentiation of mouse embryonic stem cells^[82]. While studies have shown that N-cadherin engagement is a positive regulator of β -catenin signaling and maintenance of neural stem cells, we believe that β -catenin signaling might play role in neuronal differentiation within our system based on the observation of increased neuronal differentiation of H9-NSCs cultured on low N-cad-Fc substrates, where β -catenin was localized at the cell membrane (Figure 4.8A), similar to N-cadherin. While we do observe a diffuse, cytoplasmic pool β -catenin within H9-NSCs, the cells were not proliferative as indicated by a decrease in the percentage of Ki67+ cells (4.S4), suggesting that β -catenin may not be actively translocating to the nucleus and promoting proliferation.

Across the different N-cad-Fc substrata, we observed differences in cell morphology, with more cells with a non-neuronal phenotype on high N-cad-Fc substrates. These cells did not take on the typical neuronal morphology, yet they were positive for MAP2. Despite being positive for this neuronal marker, these non-neuronal cells could likely be glial in nature as glial precursors have been shown to express MAP2^[83]. While high N-cad-Fc substrates did not promote a high degree of neuronal differentiation, the cells were not proliferative; as these cells had the lowest percentage Ki67+ cells (4.S4). One possible difference in the degree of neuronal differentiation as well as the morphology of H9-NSCs on different N-cad-Fc surfaces could lie in FGFR signaling. Several reports have indicated interactions between FGFR and N-cadherin that mediate several cell behaviors such as survival, neurite outgrowth, and motility^[84-86]. In our studies, following inhibition of FGFR activation, we observed an increase in neuronal differentiation of H9-NSCs cultured on high

N-cad-Fc presenting 2-D films indicating a change in FGFR signaling that influenced neuronal differentiation of H9-NSCs. One possible explanation could be frequent or continuous interactions of N-cadherin and FGFR on high N-cad-Fc substrates, which potentially leads to continuous FGFR signaling, subsequent activation of MAPK/ERK1/2 and PLC γ signaling. Suyama et al found that N-cadherin stabilized and sustained FGFR1 signaling, which lead to tumor metastasis^[85]. In neural stem cells, MAPK/ERK1/2 signaling reportedly reduces induced or spontaneous neuronal differentiation and prompts self-renewal of NSCs, whereas PLC γ signaling is necessary for both neuronal and oligodendrocyte differentiation potential, as inhibition of PLC γ signaling resulted in astroglial differentiation^[57]. We suspect the latter is the case as H9-NSCs cultured on high N-cadherin substrates have a low percentage of Ki67+ cells, suggesting the cells are no longer proliferative. Additionally, N-cadherin dependent activation of FGFR signaling results in activation of the PLC γ cascade, leading to a transient influx of Ca²⁺, and ultimately neurite outgrowth^[30]. Perhaps the change in substrate density of N-cad-Fc turns influences differentiation of H9-NSCs into the neuronal or oligodendroglial direction (Figure 4.8B) by modulating the activation of FGFR. This change in FGFR signaling warrants further investigation and may be the molecular switch responsible for differences in H9-NSC behaviors such as differentiation observed across varying N-cad-Fc concentrations.

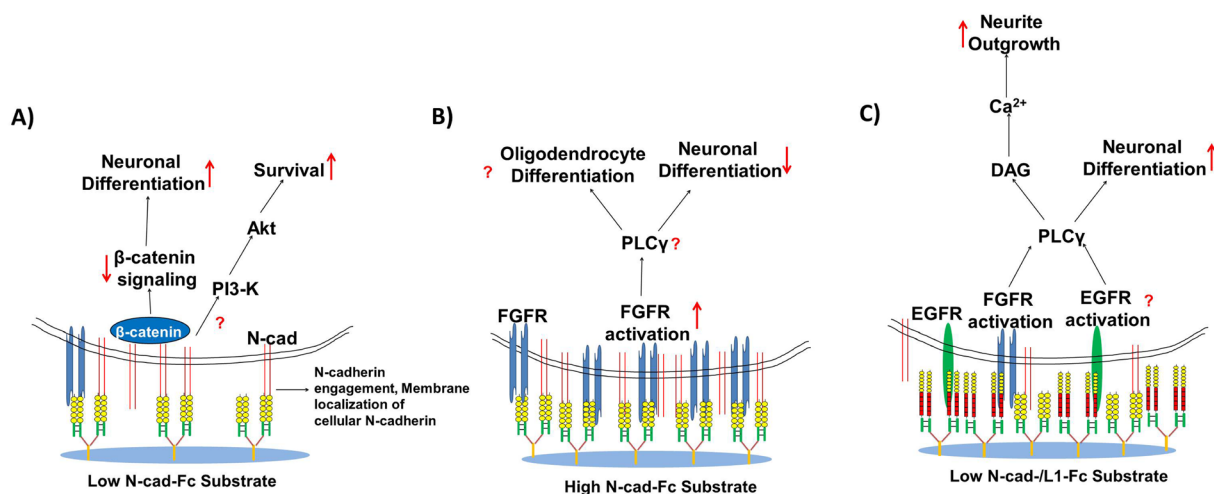


Figure 4.8. Proposed model for N-cadherin and L1 mediated H9-NSC behaviors. A) In the case of H9-NSCs cultured on low N-cad-Fc substrates, decreased β -catenin signaling might occur due to its sequestration at the cell membrane as a result of cellular N-cadherin engaging with substrate-bound N-cad-Fc. Because of the decrease in β -catenin signaling, H9-NSCs are more likely to differentiate into neurons versus H9-NSCs cultured on high N-cad-Fc presenting substrates where β -catenin did not appear to be localized at the cell membrane. Additionally, the higher degree of survival in H9-NSCs cultured on low N-cad-Fc presenting substrates possibly linked to the activation of the PI3-K/Akt anti-apoptotic signaling pathway, following N-cadherin engagement. B) The interaction of H9-NSCs with substrates presenting a higher density of N-cad-Fc perhaps leads to increased and sustained FGFR signaling and subsequent activation PLC γ , which is necessary for both oligodendrocyte and neuronal differentiation. Fewer neurons and more cells with a non-neuronal phenotype were observed in H9-NSCs cultured on high N-cad-Fc substrates, giving way to the possibility of a switch to oligodendroglial differentiation. C) The synergistic effects of N-cad-Fc and L1-Fc resulting in enhanced neuronal differentiation and neurite outgrowth may be the result of the different signaling pathways converging and amplifying differentiation and neurite outgrowth. N-cadherin activates FGFR, while L1 has been shown to activate FGFR and EGFR. The activation of both FGFR and EGFR signaling pathways can lead to the activation of PLC γ , which has been reported to be involved in neurite extension and neuronal differentiation.

The differential responses of H9-NSCs to varying concentrations of N-cad-Fc give some insight as to why synergistic effects were observed on certain substrates presenting both N-cad-Fc and L1-Fc. N-cad-Fc promoted adhesion, at varying concentrations, in contrast to L1-Fc substrates, indicating N-cad-Fc prompts the initial response of H9-NSCs and sets the stage for subsequent cell behaviors. Low N-cad-Fc alone resulted in a significant increase in MAP2+, but not neurofilament-M positive H9-NSCs compared to high

N-cad-Fc. By incorporating L1-Fc, the NSCs received an additional cue that further prompted differentiation and improved neuritogenesis. Previous work demonstrated that L1 increased neuronal differentiation of mouse neural stem cells^[87] and heterophilic interactions were possibly involved. While H9-NSCs do not express L1 (data not shown), L1 has been reported to participate in heterophilic interactions with cell surface receptors such as $\alpha_5\beta_1$ and $\alpha_v\beta_3$, as well as FGFR^[42,88]. Within our culture time period, H9-NSCs did not reach the post-mitotic stage, but they did exhibit features typical of maturing cells, as indicated by an increase in MAP2+ cells and longer neurites that were neurofilament-M positive. The combination of N-cad-Fc and L1-Fc enhanced neuronal differentiation and neuritogenesis, but survival of H9-NSCs cultured on very low or low N-cad-/L1-Fc substrates, resulted in less survival, but better than higher concentrations of N-cad-Fc combined with L1-Fc. The drop in cell survival when L1-Fc was presented on the substrate could be due to disruption in cell-cell or cell-substrate adherens junctions by L1-Fc, as L1 has been reported to disrupt E-cadherin formed junctions^[89] and disruption in N-cadherin junctions has been shown to increase cell death^[73,74]. Within the fibrous scaffolds, we observed less clustering in H9-NSCs grown on low N-cad-/L1-Fc compared to low N-cad-Fc, suggesting there was a slight interruption in cell-cell contacts. Our results of L1 and N-cadherin, combined, resulting in enhanced neurite outgrowth of differentiating H9-NSCs goes in line with previous work that demonstrated a synergistic effect between surface adsorb L1 and N-cadherin on neurite outgrowth of primary cortical neurons^[43]. To date, this is the first investigation into synergistic effects of these two cell adhesion molecules in promoting neuronal differentiation of H9-NSCs. We examined the role of FGFR activation and signaling in the cooperative effect of N-cad-Fc and L1-Fc on neuronal differentiation by inhibiting FGFR activation. However, we did not observe any differences between cells treated with an FGFR inhibitor and untreated cells, implying other receptors and signaling

pathways are likely responsible for the response, which deserves further mechanistic investigation. It is plausible that the presence of other L1-Fc activated pathways that converge on N-cadherin signaling, such as FGFR, resulting in enhanced neurite outgrowth and neuronal differentiation. Aside from FGFR, L1 has been implicated in direct interactions with epidermal growth factor receptor (EGF), as well as EGFR activation^[90,91]. EGFR activation within NSCs was previously shown to be involved in PLC γ signaling^[92,93], which results in transient calcium influxes that lead to neurite outgrowth. EGF was also shown to support neuronal survival and neurite outgrowth of cortical and cerebellar neurons^[94], as well as neuronal differentiation in PC12 cells that overexpressed EGFR^[95]. The same PLC γ signaling pathway is involved in neurite outgrowth mediated by N-cadherin and FGFR interactions, as well as FGFR and L1 interactions^[30,56]. A proposed model of N-cadherin and L1 interactions with FGFR and EGFR is depicted in Figure 4.8C.

Ultimately for cell transplantation, the behavior of H9-NSCs on three-dimensional scaffolds functionalized with N-cad-Fc and/or L1-Fc is of great interest. Within the fibrous scaffolds, we observed a synergistic effect on neurite outgrowth and neuronal differentiation of N-cad-Fc and L1-Fc when N-cad-Fc was low relative to the concentration of L1-Fc. Additionally, conditions where N-cad-Fc substrates allowed for a certain degree of cell-cell contact resulted in increased cell survival, with N-cad-Fc alone or in combination with L1-Fc. While surface bound N-cadherin disrupts cell-cell contacts, the fibrous architecture of the scaffolds allowed for the establishment of cell-cell contacts when the N-cad-Fc density was low, in contrast to 2-D thin films. Poly-D-lysine treated, electrospun, fibrous scaffolds were previously shown to promote increased cell-cell contacts, and subsequently viability, self-renewal, and directed differentiation of human embryonic stem cells^[96], demonstrating the benefit and ability of the fibrous architecture to mimic the endogenous microenvironment and foster cell interactions through microscale

confinement, in contrast to more planar scaffolds. However in the case of scaffolds functionalized with higher N-cadherin density, cell-cell contacts were disrupted by the interaction of cellular N-cadherin with substrate bound N-cadherin, resulting in less survival and neuronal differentiation of H9-NSCs. We also determined that a much lower concentration of N-cad-Fc, alone or co-presented with L1-Fc, could be combined with 3-D scaffolds promoting significant adhesion, neuronal differentiation, as well as neurite outgrowth of H9-NSCs, in contrast to 2-D films. These results point to the additive benefit of the topography of the fibrous scaffolds and biofunctionalization with N-cad-Fc and L1-Fc in promoting enhanced cell behaviors and further emphasize the importance of balancing concentration and presentation of biological cues with geometric properties of biomaterials so as to promote the desired cellular outcomes.

4.5. Summary and Conclusions

We investigated the effects of two dimensional polymer films and fibrous scaffolds functionalized with N-cadherin-Fc and/or L1-Fc in promoting enhanced behaviors of H9-NSCs such as neuronal differentiation, neurite outgrowth, and survival during oxidative stress. N-cadherin-coated substrates have been previously shown to promote neural differentiation, as well as maintenance and neural differentiation of neural stem cells. However, no studies have examined how varying concentrations of substrate presented N-cadherin-Fc affect neuronal differentiation, survival, and outgrowth of human embryonic stem cell-derived neural stem cells in 2-D and more importantly within 3-D, fibrous scaffolds. We showed as N-cadherin-Fc concentration increased, neuronal differentiation, neurite outgrowth, and survival of H9-NSCs decreased. In addition, we demonstrated that co-presentation of N-cadherin-Fc and L1-Fc enhances neuronal differentiation as well as neurite outgrowth, but only when N-cadherin-Fc was at a low concentration, relative to L1-

Fc. We presented the cell adhesion proteins from polymeric two dimensional thin films and fibrous scaffolds made from poly(DTE carbonate), in which important parameters such as degradation rate, stiffness, and protein deposition can be tailored for implantable devices for nervous system repair.

4.6. Supplemental Data

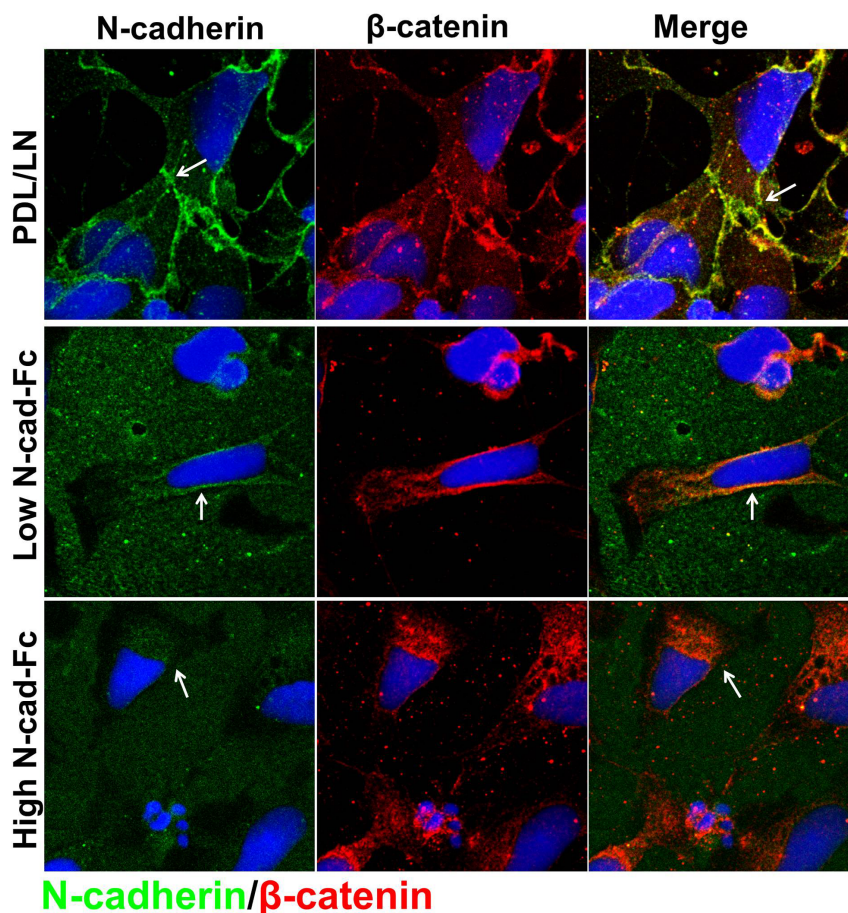


Figure 4.S1. Co-localization of N-cadherin and β -catenin in H9-NSCs cultured on N-cad-Fc substrates. After 24 hours, immunocytochemistry was used to determine the localization of N-cadherin (green) and β -catenin (red) in H9-NSCs cultured on PDL/LN (top), low N-cad-Fc, and high N-cad-Fc functionalized 2-D films. Hoechst 32258 was used to label nuclei (blue). In H9-NSCs cultured on PDL/LN substrates, N-cadherin was localized at cell-cell junctions, resulting in bright green bands around the cell membrane (white arrows). Co-localization of β -catenin was also observed at the cell membrane (white arrows, third column). A similar localization pattern was observed in H9-NSCs cultured on low-N-cad-Fc presenting 2-D films, in contrast to H9-NSCs cultured on high N-cad-Fc, which promoted a clustered localization of both N-cadherin and β -catenin away from the cell membrane. These results suggest that N-cadherin engagement between cellular N-cadherin and low N-cad-Fc substrates mimics cell-cell N-cadherin engagement and that the engagement is adequate in sequestering β -catenin.

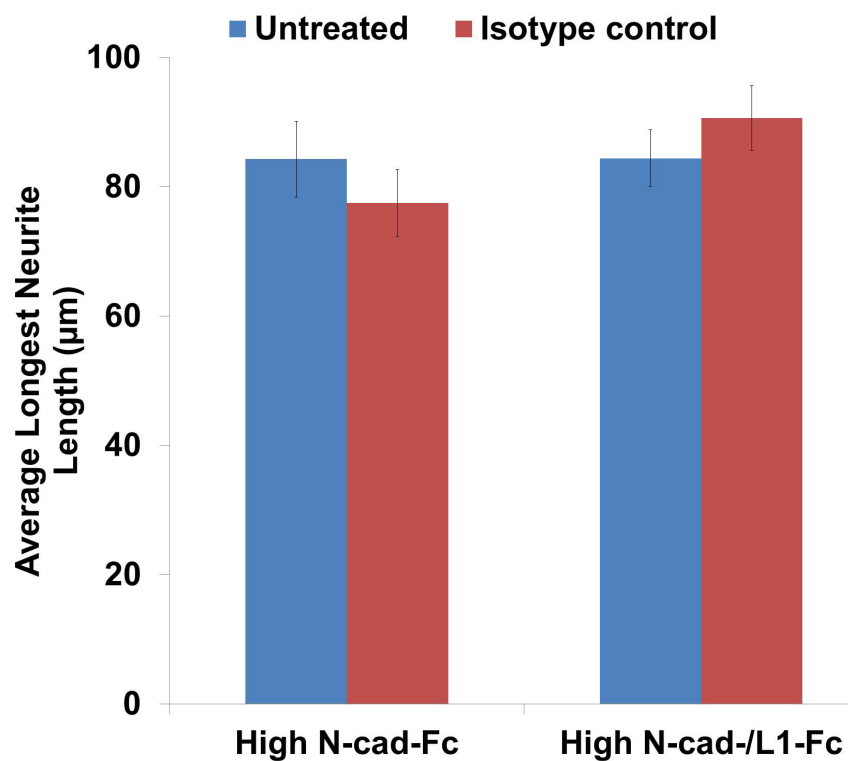


Figure 4.S2. Isotype control treatment of H9-NSCs for the N-cadherin antibody blocking studies. Similar to H9-NSCs treated with varying concentrations of anti-N-cadherin, H9-NSCs were treated with 100 µg/ml of sheep IgG isotype control to determine if interactions with sheep IgG had an influence on the cell behavior of H9-NSCs following treatment with sheep anti-N-cadherin. The longest neurite lengths of H9-NSCs treated with sheep IgG were comparable to that of untreated H9-NSCs.

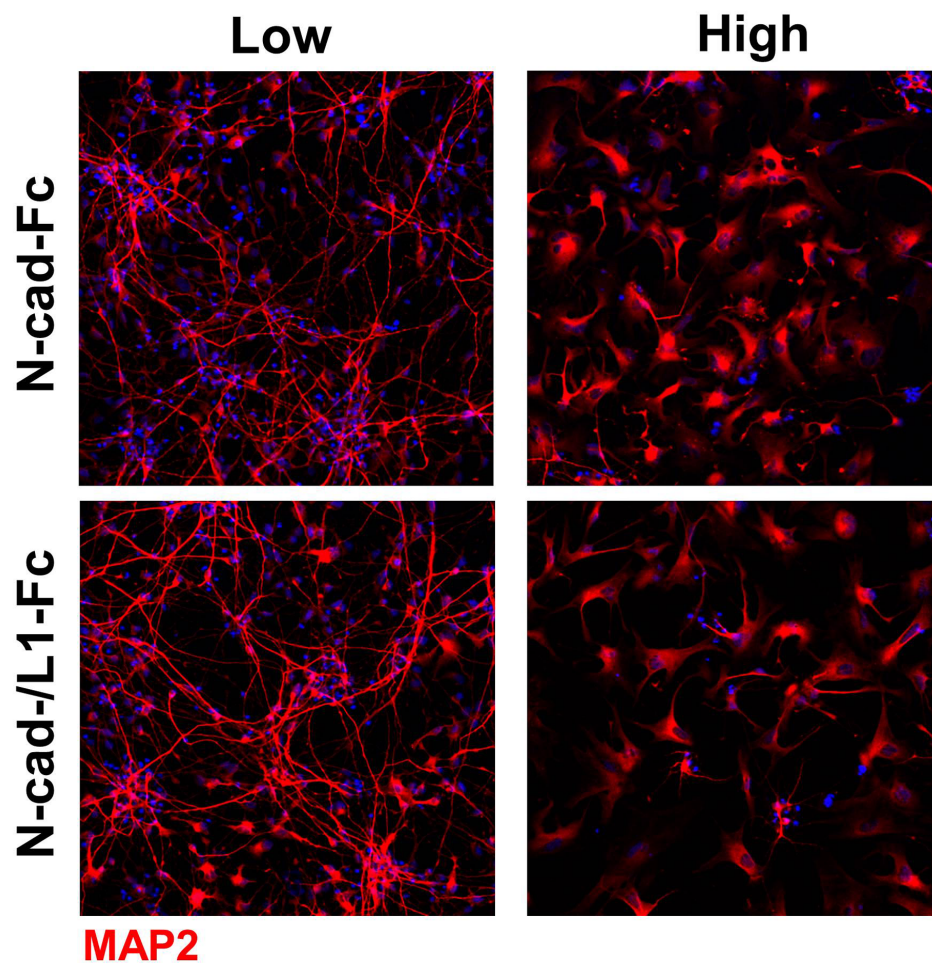


Figure 4.S3. MAP2 expression and morphology of H9-NSCs cultured on N-cad-Fc substrates after 2 weeks on 2-D films. After 14 days in culture, H9-NSCs positive for MAP2 (red) were identified using immunocytochemistry and nuclei were labeled with Hoechst 33258 (blue). H9-NSCs cultured on low N-cad-Fc and low N-cad-/L1-Fc 2-D films exhibited a large degree of cells possessing a neuronal morphology that were positive for MAP2. In contrast, a majority of H9-NSCs cultured on high N-cad-Fc and high N-cad-/L1-Fc exhibited a non-neuronal phenotype, consisting of cells that were larger in size.

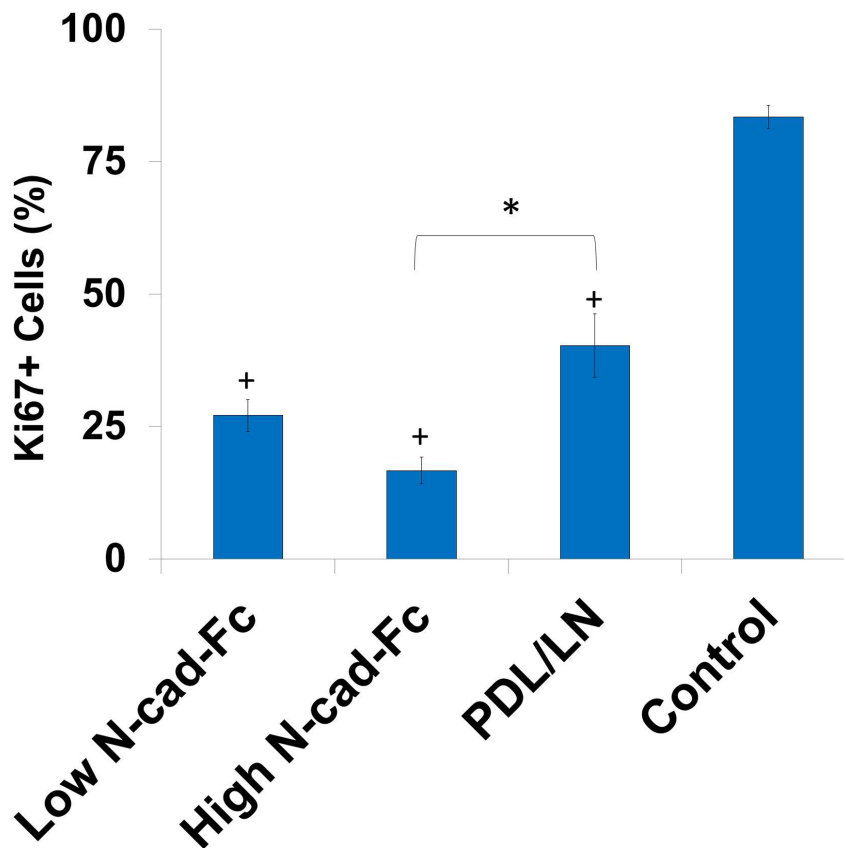


Figure 4.S4. Ki67 expression of H9-NSCs in response to N-cad-Fc substrates. After 7 days of culture in NDM, H9-NSCs Ki67 expression was determined using immunocytochemistry. High N-cad-Fc resulted in the lowest percentage of Ki67+ cells (17%), followed by low N-cad-Fc functionalized 2-D films (27%). PDL/laminin had a higher percentage of Ki67+ cells (40%), but lower than the control, H9-NSCs cultured in NPM, supplemented with bFGF (83%). (* denotes $p < 0.05$, + denotes $p < 0.05$ compared to control). NDM: neural differentiation medium, PDL: poly-D-lysine, LN: laminin, NPM: neural proliferation medium, bFGF: basic fibroblast growth factor

4.7. References

1. Gensel JC, DJ Donnelly and PG Popovich. (2011). Spinal cord injury therapies in humans: an overview of current clinical trials and their potential effects on intrinsic CNS macrophages. *Expert Opin Ther Targets* 15:505-18.
2. Jain KK. (2009). Cell therapy for CNS trauma. *Mol Biotechnol* 42:367-76.
3. Harrop JS, R Hashimoto, D Norvell, A Raich, B Aarabi, RG Grossman, JD Guest, CH Tator, J Chapman and MG Fehlings. (2012). Evaluation of clinical experience using cell-based therapies in patients with spinal cord injury: a systematic review. *J Neurosurg Spine* 17:230-46.
4. Zhang SC. (2003). Embryonic stem cells for neural replacement therapy: Prospects and challenges. *Journal of Hematotherapy & Stem Cell Research* 12:625-634.
5. Cao Q, XM Xu, WH Devries, GU Enzmann, P Ping, P Tsoulfas, PM Wood, MB Bunge and SR Whittemore. (2005). Functional recovery in traumatic spinal cord injury

- after transplantation of multilineurotrophin-expressing glial-restricted precursor cells. *J Neurosci* 25:6947-57.
6. Cao QL, RM Howard, JB Dennison and SR Whittemore. (2002). Differentiation of engrafted neuronal-restricted precursor cells is inhibited in the traumatically injured spinal cord. *Exp Neurol* 177:349-59.
 7. Cao QL, YP Zhang, RM Howard, WM Walters, P Tsoulfas and SR Whittemore. (2001). Pluripotent stem cells engrafted into the normal or lesioned adult rat spinal cord are restricted to a glial lineage. *Exp Neurol* 167:48-58.
 8. Cloutier F, MM Siegenthaler, G Nistor and HS Keirstead. (2006). Transplantation of human embryonic stem cell-derived oligodendrocyte progenitors into rat spinal cord injuries does not cause harm. *Regen Med* 1:469-79.
 9. Cummings BJ, N Uchida, SJ Tamaki, DL Salazar, M Hooshmand, R Summers, FH Gage and AJ Anderson. (2005). Human neural stem cells differentiate and promote locomotor recovery in spinal cord-injured mice. *Proc Natl Acad Sci U S A* 102:14069-74.
 10. Keirstead HS, T Ben-Hur, B Rogister, MT O'Leary, M Dubois-Dalcq and WF Blakemore. (1999). Polysialylated neural cell adhesion molecule-positive CNS precursors generate both oligodendrocytes and Schwann cells to remyelinate the CNS after transplantation. *J Neurosci* 19:7529-36.
 11. Keirstead HS, G Nistor, G Bernal, M Totoiu, F Cloutier, K Sharp and O Steward. (2005). Human embryonic stem cell-derived oligodendrocyte progenitor cell transplants remyelinate and restore locomotion after spinal cord injury. *J Neurosci* 25:4694-705.
 12. Mitsui T, JS Shumsky, AC Lepore, M Murray and I Fischer. (2005). Transplantation of neuronal and glial restricted precursors into contused spinal cord improves bladder and motor functions, decreases thermal hypersensitivity, and modifies intraspinal circuitry. *J Neurosci* 25:9624-36.
 13. Nistor GI, MO Totoiu, N Haque, MK Carpenter and HS Keirstead. (2005). Human embryonic stem cells differentiate into oligodendrocytes in high purity and myelinate after spinal cord transplantation. *Glia* 49:385-96.
 14. Hwang DH, HM Kim, YM Kang, IS Joo, CS Cho, BW Yoon, SU Kim and BG Kim. (2011). Combination of multifaceted strategies to maximize the therapeutic benefits of neural stem cell transplantation for spinal cord repair. *Cell transplantation* 20:1361-79.
 15. Kim BG, DH Hwang, SI Lee, EJ Kim and SU Kim. (2007). Stem cell-based cell therapy for spinal cord injury. *Cell transplantation* 16:355-64.
 16. Kim SU, HJ Lee and YB Kim. (2013). Neural stem cell-based treatment for neurodegenerative diseases. *Neuropathology : official journal of the Japanese Society of Neuropathology*.
 17. Lukovic D, V Moreno Manzano, M Stojkovic, SS Bhattacharya and S Erceg. (2012). Concise review: human pluripotent stem cells in the treatment of spinal cord injury. *Stem Cells* 30:1787-92.
 18. Nikolettou V and N Tavernarakis. (2012). Embryonic and induced pluripotent stem cell differentiation as a tool in neurobiology. *Biotechnology journal* 7:1156-68.
 19. Selvaraj V, P Jiang, O Chechneva, UG Lo and W Deng. (2012). Differentiating human stem cells into neurons and glial cells for neural repair. *Frontiers in bioscience : a journal and virtual library* 17:65-89.
 20. Cooke MJ, K Vulic and MS Shoichet. (2010). Design of biomaterials to enhance stem cell survival when transplanted into the damaged central nervous system. *Soft Matter* 6:4988-4998.

21. Kim H, MJ Cooke and MS Shoichet. (2012). Creating permissive microenvironments for stem cell transplantation into the central nervous system. *Trends in Biotechnology* 30:55-63.
22. Potter W, RE Kalil and WJ Kao. (2008). Biomimetic material systems for neural progenitor cell-based therapy. *Frontiers in bioscience : a journal and virtual library* 13:806-21.
23. Kwon YT, A Gupta, Y Zhou, M Nikolic and LH Tsai. (2000). Regulation of N-cadherin-mediated adhesion by the p35-Cdk5 kinase. *Current biology : CB* 10:363-72.
24. Gago N, V Avellana-Adalid, A Baron-Van Evercooren and M Schumacher. (2003). Control of cell survival and proliferation of postnatal PSA-NCAM(+) progenitors. *Molecular and cellular neurosciences* 22:162-78.
25. Wang TY, JS Forsythe, CL Parish and DR Nisbet. (2012). Biofunctionalisation of polymeric scaffolds for neural tissue engineering. *Journal of biomaterials applications* 27:369-90.
26. Cooke MJ, T Zahir, SR Phillips, DS Shah, D Athey, JH Lakey, MS Shoichet and SA Przyborski. (2010). Neural differentiation regulated by biomimetic surfaces presenting motifs of extracellular matrix proteins. *Journal of biomedical materials research. Part A* 93:824-32.
27. Haque A, XS Yue, A Motazedian, Y Tagawa and T Akaike. (2012). Characterization and neural differentiation of mouse embryonic and induced pluripotent stem cells on cadherin-based substrata. *Biomaterials* 33:5094-106.
28. Horne MK, DR Nisbet, JS Forsythe and CL Parish. (2010). Three-dimensional nanofibrous scaffolds incorporating immobilized BDNF promote proliferation and differentiation of cortical neural stem cells. *Stem Cells Dev* 19:843-52.
29. Ito Y, G Chen, Y Imanishi, T Morooka, E Nishida, Y Okabayashi and M Kasuga. (2001). Differential control of cellular gene expression by diffusible and non-diffusible EGF. *J Biochem* 129:733-7.
30. Doherty P and FS Walsh. (1996). CAM-FGF Receptor Interactions: A Model for Axonal Growth. *Molecular and cellular neurosciences* 8:99-111.
31. Horner PJ and FH Gage. (2000). Regenerating the damaged central nervous system. *Nature* 407:963-70.
32. Takeichi M. (2007). The cadherin superfamily in neuronal connections and interactions. *Nature Reviews Neuroscience* 8:11-20.
33. Skaper SD. (2012). Neuronal growth-promoting and inhibitory cues in neuroprotection and neuroregeneration. *Methods in molecular biology* 846:13-22.
34. Yue XS, Y Murakami, T Tamai, M Nagaoka, CS Cho, Y Ito and T Akaike. (2010). A fusion protein N-cadherin-Fc as an artificial extracellular matrix surface for maintenance of stem cell features. *Biomaterials* 31:5287-96.
35. Chen J, C Bernreuther, M Dihne and M Schachner. (2005). Cell adhesion molecule L1-transfected embryonic stem cells with enhanced survival support regrowth of corticospinal tract axons in mice after spinal cord injury. *J. Neurotrauma* 22:896-906.
36. Kenwrick S and P Doherty. (1998). Neural cell adhesion molecule L1: relating disease to function. *Bioessays* 20:668-75.
37. Loers G, S Chen, M Grumet and M Schachner. (2005). Signal transduction pathways implicated in neural recognition molecule L1 triggered neuroprotection and neuritogenesis. *Journal of neurochemistry* 92:1463-76.
38. Maness PF and M Schachner. (2007). Neural recognition molecules of the immunoglobulin superfamily: signaling transducers of axon guidance and neuronal migration. *Nat Neurosci* 10:19-26.

39. Moos M, R Tacke, H Scherer, D Teplow, K Fruh and M Schachner. (1988). Neural adhesion molecule L1 as a member of the immunoglobulin superfamily with binding domains similar to fibronectin. *Nature* 334:701-3.
40. Stallcup WB. (2000). The third fibronectin type III repeat is required for L1 to serve as an optimal substratum for neurite extension. *J Neurosci Res* 61:33-43.
41. Thelen K, V Kedar, AK Panicker, RS Schmid, BR Midkiff and PF Maness. (2002). The neural cell adhesion molecule L1 potentiates integrin-dependent cell migration to extracellular matrix proteins. *J Neurosci* 22:4918-31.
42. Kulahin N, S Li, V Kiselyov, E Bock and V Berezin. (2009). Identification of neural cell adhesion molecule L1-derived neuritogenic ligands of the fibroblast growth factor receptor. *J Neurosci Res* 87:1806-12.
43. Collazos-Castro JE, GR Hernandez-Labrado, JL Polo and C Garcia-Rama. (2013). N-Cadherin- and L1-functionalised conducting polymers for synergistic stimulation and guidance of neural cell growth. *Biomaterials* 34:3603-17.
44. Shi P, K Shen and LC Kam. (2007). Local presentation of L1 and N-cadherin in multicomponent, microscale patterns differentially direct neuron function in vitro. *Dev Neurobiol* 67:1765-76.
45. Moore RN, JF Cherry, V Mathur, R Cohen, M Grumet and PV Moghe. (2012). E-cadherin-expressing feeder cells promote neural lineage restriction of human embryonic stem cells. *Stem cells and development* 21:30-41.
46. Cherry JF, AL Carlson, FL Benarba, SD Sommerfeld, D Verma, G Loers, J Kohn, M Schachner and PV Moghe. (2012). Oriented, multimeric biointerfaces of the L1 cell adhesion molecule: an approach to enhance neuronal and neural stem cell functions on 2-D and 3-D polymer substrates. *Biointerphases* 7:22.
47. Tsuru A, M Mizuguchi, K Uyemura and S Takashima. (1996). Immunohistochemical expression of cell adhesion molecule L1 during development of the human brain. *Early human development* 45:93-101.
48. Marthiens V, I Kazanis, L Moss, K Long and C Ffrench-Constant. (2010). Adhesion molecules in the stem cell niche--more than just staying in shape? *Journal of cell science* 123:1613-22.
49. Noles SR and A Chenn. (2007). Cadherin inhibition of beta-catenin signaling regulates the proliferation and differentiation of neural precursor cells. *Molecular and cellular neurosciences* 35:549-58.
50. Rousso DL, CA Pearson, ZB Gaber, A Miquelajauregui, S Li, C Portera-Cailliau, EE Morrisey and BG Novitch. (2012). Foxp-mediated suppression of N-cadherin regulates neuroepithelial character and progenitor maintenance in the CNS. *Neuron* 74:314-30.
51. McCreedy DA and SE Sakiyama-Elbert. (2012). Combination therapies in the CNS: engineering the environment. *Neurosci Lett* 519:115-21.
52. Lee YS and TL Arinzeh. (2011). Electrospun Nanofibrous Materials for Neural Tissue Engineering. *Polymers* 3:413-426.
53. Mothe AJ, RY Tam, T Zahir, CH Tator and MS Shoichet. (2013). Repair of the injured spinal cord by transplantation of neural stem cells in a hyaluronan-based hydrogel. *Biomaterials* 34:3775-83.
54. Ertel SI and J Kohn. (1994). Evaluation of a series of tyrosine-derived polycarbonates as degradable biomaterials. *Journal of biomedical materials research* 28:919-30.
55. Meechaisue C, R Dubin, P Supaphol, VP Hoven and J Kohn. (2006). Electrospun mat of tyrosine-derived polycarbonate fibers for potential use as tissue scaffolding material. *Journal of biomaterials science. Polymer edition* 17:1039-56.

56. Williams EJ, J Furness, FS Walsh and P Doherty. (1994). Activation of the FGF receptor underlies neurite outgrowth stimulated by L1, N-CAM, and N-cadherin. *Neuron* 13:583-94.
57. Ma DK, K Ponnusamy, MR Song, GL Ming and H Song. (2009). Molecular genetic analysis of FGFR1 signalling reveals distinct roles of MAPK and PLCgamma1 activation for self-renewal of adult neural stem cells. *Molecular Brain* 2:16.
58. Numakawa T, T Matsumoto, Y Numakawa, M Richards, S Yamawaki and H Kunugi. (2011). Protective Action of Neurotrophic Factors and Estrogen against Oxidative Stress-Mediated Neurodegeneration. *Journal of toxicology* 2011:405194.
59. Kuhn HG PD. (2008). Detection and phenotypic characterization of adult neurogenesis. In: *Adult neurogenesis*. Gage FH KG, Hongjun S ed. Cold Spring Harbor Laboratory Press, Cold Spring Harbor, NY. pp 25-47.
60. Schnadelbach O, OW Blaschuk, M Symonds, BJ Gour, P Doherty and JW Fawcett. (2000). N-cadherin influences migration of oligodendrocytes on astrocyte monolayers. *Molecular and cellular neurosciences* 15:288-302.
61. Wilby MJ, EM Muir, J Fok-Seang, BJ Gour, OW Blaschuk and JW Fawcett. (1999). N-Cadherin inhibits Schwann cell migration on astrocytes. *Molecular and cellular neurosciences* 14:66-84.
62. Kawauchi T, K Sekine, M Shikanai, K Chihama, K Tomita, K Kubo, K Nakajima, Y Nabeshima and M Hoshino. (2010). Rab GTPases-dependent endocytic pathways regulate neuronal migration and maturation through N-cadherin trafficking. *Neuron* 67:588-602.
63. Reifsteck F, S Wee and BJ Wilkinson. (1987). Hydrophobicity-hydrophilicity of staphylococci. *Journal of medical microbiology* 24:65-73.
64. Jia Z, H Zhu, J Li, X Wang, H Misra and Y Li. (2012). Oxidative stress in spinal cord injury and antioxidant-based intervention. *Spinal Cord* 50:264-74.
65. Lelievre EC, C Plestant, C Boscher, E Wolff, RM Mege and H Birbes. (2012). N-cadherin mediates neuronal cell survival through Bim down-regulation. *PloS one* 7:e33206.
66. Loers G, SZ Chen, M Grumet and M Schachner. (2005). Signal transduction pathways implicated in neural recognition molecule L1 triggered neuroprotection and neuritogenesis. *Journal of neurochemistry* 92:1463-1476.
67. Ma W, T Tavakoli, E Derby, Y Serebryakova, MS Rao and MP Mattson. (2008). Cell-extracellular matrix interactions regulate neural differentiation of human embryonic stem cells. *BMC Dev Biol* 8:90.
68. Park S, KS Lee, YJ Lee, HA Shin, HY Cho, KC Wang, YS Kim, HT Lee, KS Chung, EY Kim and J Lim. (2004). Generation of dopaminergic neurons in vitro from human embryonic stem cells treated with neurotrophic factors. *Neurosci Lett* 359:99-103.
69. Brieva TA and PV Moghe. (2004). Exogenous cadherin microdisplay can interfere with endogenous signaling and reprogram gene expression in cultured hepatocytes. *Biotechnology and Bioengineering* 85:283-92.
70. Semler EJ, A Dasgupta and PV Moghe. (2005). Cytomimetic engineering of hepatocyte morphogenesis and function by substrate-based presentation of acellular E-cadherin. *Tissue engineering* 11:734-50.
71. Wang L, Z Li, C Wang, Y Yang, L Sun, W Yao, X Cai, G Wu, F Zhou and X Zha. (2009). E-cadherin decreased human breast cancer cells sensitivity to staurosporine by up-regulating Bcl-2 expression. *Archives of biochemistry and biophysics* 481:116-22.
72. Hofmann C, F Obermeier, M Artinger, M Hausmann, W Falk, J Schoelmerich, G Rogler and J Grossmann. (2007). Cell-cell contacts prevent anoikis in primary human colonic epithelial cells. *Gastroenterology* 132:587-600.

73. Ando K, K Uemura, A Kuzuya, M Maesako, M Asada-Utsugi, M Kubota, N Aoyagi, K Yoshioka, K Okawa, H Inoue, J Kawamata, S Shimohama, T Arai, R Takahashi and A Kinoshita. (2011). N-cadherin regulates p38 MAPK signaling via association with JNK-associated leucine zipper protein: implications for neurodegeneration in Alzheimer disease. *The Journal of biological chemistry* 286:7619-28.
74. Tran NL, DG Adams, RR Vaillancourt and RL Heimark. (2002). Signal transduction from N-cadherin increases Bcl-2. Regulation of the phosphatidylinositol 3-kinase/Akt pathway by homophilic adhesion and actin cytoskeletal organization. *The Journal of biological chemistry* 277:32905-14.
75. Lee HJ, J Park, OJ Yoon, HW Kim, Y Lee do, H Kim do, WB Lee, NE Lee, JV Bonventre and SS Kim. (2011). Amine-modified single-walled carbon nanotubes protect neurons from injury in a rat stroke model. *Nature nanotechnology* 6:121-5.
76. Otero JJ, W Fu, L Kan, AE Cuadra and JA Kessler. (2004). Beta-catenin signaling is required for neural differentiation of embryonic stem cells. *Development* 131:3545-57.
77. Lilien J and J Balsamo. (2005). The regulation of cadherin-mediated adhesion by tyrosine phosphorylation/dephosphorylation of beta-catenin. *Current opinion in cell biology* 17:459-65.
78. Yap AS, WM Brieher and BM Gumbiner. (1997). Molecular and functional analysis of cadherin-based adherens junctions. *Annual review of cell and developmental biology* 13:119-46.
79. Nelson WJ and R Nusse. (2004). Convergence of Wnt, beta-catenin, and cadherin pathways. *Science* 303:1483-7.
80. Zhang J, GJ Woodhead, SK Swaminathan, SR Noles, ER McQuinn, AJ Pisarek, AM Stocker, CA Mutch, N Funatsu and A Chenn. (2010). Cortical neural precursors inhibit their own differentiation via N-cadherin maintenance of beta-catenin signaling. *Developmental cell* 18:472-9.
81. Woodhead GJ, CA Mutch, EC Olson and A Chenn. (2006). Cell-autonomous beta-catenin signaling regulates cortical precursor proliferation. *The Journal of neuroscience : the official journal of the Society for Neuroscience* 26:12620-30.
82. Cajanek L, D Ribeiro, I Liste, CL Parish, V Bryja and E Arenas. (2009). Wnt/beta-catenin signaling blockade promotes neuronal induction and dopaminergic differentiation in embryonic stem cells. *Stem Cells* 27:2917-27.
83. Blumcke I, AJ Becker, S Normann, V Hans, BM Riederer, S Krajewski, OD Wiestler and G Reifenberger. (2001). Distinct expression pattern of microtubule-associated protein-2 in human oligodendrogliomas and glial precursor cells. *J Neuropathol Exp Neurol* 60:984-93.
84. Skaper SD, L Facci, G Williams, EJ Williams, FS Walsh and P Doherty. (2004). A dimeric version of the short N-cadherin binding motif HAVDI promotes neuronal cell survival by activating an N-cadherin/fibroblast growth factor receptor signalling cascade. *Molecular and cellular neurosciences* 26:17-23.
85. Suyama K, I Shapiro, M Guttman and RB Hazan. (2002). A signaling pathway leading to metastasis is controlled by N-cadherin and the FGF receptor. *Cancer cell* 2:301-14.
86. Williams EJ, G Williams, FV Howell, SD Skaper, FS Walsh and P Doherty. (2001). Identification of an N-cadherin motif that can interact with the fibroblast growth factor receptor and is required for axonal growth. *J Biol Chem* 276:43879-86.
87. Dihne M, C Bernreuther, M Sibbe, W Paulus and M Schachner. (2003). A new role for the cell adhesion molecule L1 in neural precursor cell proliferation, differentiation, and transmitter-specific subtype generation. *J Neurosci* 23:6638-50.

88. Felding-Habermann B, S Silletti, F Mei, CH Siu, PM Yip, PC Brooks, DA Cheresch, TE O'Toole, MH Ginsberg and AM Montgomery. (1997). A single immunoglobulin-like domain of the human neural cell adhesion molecule L1 supports adhesion by multiple vascular and platelet integrins. *J Cell Biol* 139:1567-81.
89. Shtutman M, E Levina, P Ohouo, M Baig and IB Roninson. (2006). Cell adhesion molecule L1 disrupts E-cadherin-containing adherens junctions and increases scattering and motility of MCF7 breast carcinoma cells. *Cancer research* 66:11370-80.
90. Islam R, LV Kristiansen, S Romani, L Garcia-Alonso and M Hortsch. (2004). Activation of EGF receptor kinase by L1-mediated homophilic cell interactions. *Molecular biology of the cell* 15:2003-12.
91. Yoon H, JK Min, DG Lee, DG Kim, SS Koh and HJ Hong. (2012). L1 cell adhesion molecule and epidermal growth factor receptor activation confer cisplatin resistance in intrahepatic cholangiocarcinoma cells. *Cancer letters* 316:70-6.
92. Wahl MI, TO Daniel and G Carpenter. (1988). Antiphosphotyrosine recovery of phospholipase C activity after EGF treatment of A-431 cells. *Science* 241:968-70.
93. Meisenhelder J, PG Suh, SG Rhee and T Hunter. (1989). Phospholipase C-gamma is a substrate for the PDGF and EGF receptor protein-tyrosine kinases in vivo and in vitro. *Cell* 57:1109-22.
94. Yamada M, T Ikeuchi and H Hatanaka. (1997). The neurotrophic action and signalling of epidermal growth factor. *Progress in neurobiology* 51:19-37.
95. Traverse S, K Seedorf, H Paterson, CJ Marshall, P Cohen and A Ullrich. (1994). EGF triggers neuronal differentiation of PC12 cells that overexpress the EGF receptor. *Current biology : CB* 4:694-701.
96. Carlson AL, CA Florek, JJ Kim, T Neubauer, JC Moore, RI Cohen, J Kohn, M Grumet and PV Moghe. (2012). Microfibrous substrate geometry as a critical trigger for organization, self-renewal, and differentiation of human embryonic stem cells within synthetic 3-dimensional microenvironments. *FASEB journal : official publication of the Federation of American Societies for Experimental Biology* 26:3240-51.

Chapter 5

Dissertation Summary and Future Directions

5.1. Dissertation Summary

The field of neural tissue engineering aims to combine cells, biomaterials, and bioactive factors to replace lost cells, support spared neural tissue, and promote integration of transplanted cells with native tissue following injury to the central nervous system or the onset of neurodegenerative diseases. Several approaches have been investigated for potential cell sources for cell transplantation therapy, the type and configuration of the biomaterials, as well as the biological cues that would recapitulate the endogenous microenvironment that promotes neural cell development and function. An ideal design of transplantable cell/bioactive scaffolds would 1) provide a permissive growth substrate for transplanted cells to integrate with this host tissue and 2) encourage the host tissue to grow beyond the site of injury, reconnect to targets, and reestablish cell functions for restoration of motor function. While the field has made considerable progress in identifying cell sources and testing their efficacy in promoting regeneration of injured tissue and functional recovery, several challenges still exist, such as increasing survival and function of transplanted cells. Bioactive, biomaterial scaffolds have gained much attention as an approach to address problems associated with cell survival following transplantation into injured or diseased neural tissue^[1-3].

The goal of this thesis was to design and optimize three-dimensional, implantable bioactive scaffolds, through examining the effects of protein presentation and the combined effects of neural cell adhesion proteins on H9 human embryonic stem cell-derived neural stem cells (H9-NSCs). The findings of the thesis demonstrate the ability to modulate neural cell behaviors such as neurite outgrowth, survival, and differentiation by altering protein

presentation as well as the combining two key neural adhesion proteins necessary for normal nervous system development. Specifically, utilizing protein A to present the extracellular domain of L1, fused with the Fc region of human IgG, promoted improved efficacy of L1-Fc as demonstrated by enhanced neurite outgrowth, as well as neuronal differentiation of H9-NSCs. These results further reveal the importance of protein orientation in designing biomimetic constructs for neural tissue engineering and substrates for cell transplantation therapy. For the first time, the effects of L1, functionalized polymeric fibrous scaffolds on differentiation behaviors of human neural stem cells were identified. Additionally, work from this thesis detected differential responses of H9-NSCs to varying concentrations of N-cadherin, as well as the combination of N-cadherin and L1. These differences were manifested in changes in neuronal differentiation, neurite outgrowth, and survival. Previous studies have investigated the use of N-cadherin as an artificial extracellular matrix for neuronal cells, as well as stem cells^[4-6], but have not investigated and identified optimal dosing conditions for promoting neuronal differentiation of human embryonic derived-neural stem cells. For the first time, it has been determined the density of surface presented N-cadherin-Fc influences neuronal differentiation efficiency of H9, human embryonic stem cell (hESC)-derived neural stem cells (H9-NSCs). Another insight highlighted in this work is the synergy between N-cadherin and L1 in enhancing neuronal differentiation and neurite outgrowth of hESC-derived NSCs, further emphasizing the importance and benefit of presenting multiple biomolecules, which are involved in different processes of neural development, for the design of biomimetics for neural tissue engineering. While other groups have shown differential and synergistic effects between L1 and N-cadherin^[7,8], none have examined the combined effects of the two proteins on hESC-NSCs behaviors. Moreover, this work demonstrated the feasibility of translating specific orientations of L1-Fc and N-cadherin-Fc

onto both aligned and randomly oriented electrospun scaffolds, setting the stage for use of these cellularized, bioactive-scaffold constructs within *in vivo* models of spinal cord injury, traumatic brain injury, or neurodegenerative disease models.

As reviewed in Chapter 1, cell replacement therapy is a promising approach for treatment of spinal cord injury, traumatic brain injury, and neurodegenerative disorders such as Alzheimer's and Parkinson's disease. The transplantation of neuronal cells, combined with a supportive, three-dimensional bioactive scaffold, would be ideal as the supportive structure of the scaffold in providing anchorage for the transplanted cells and improved cell survival and integration of endogenous tissue. The work from this thesis establishes that electrospun scaffolds, biofunctionalized with L1-Fc, N-cadherin-Fc, alone or in combination promote and support neuronal differentiation, neurite outgrowth, and survival of neural stem cells derived from hESCs *in vitro*.

5.2. Future Directions

5.2.1. Identifying the Molecular Basis of L1/N-cadherin Functionalized Substrates in Modulating NSC Behaviors

The work performed in Chapter 4 highlighted the synergistic effects of L1-Fc and N-cadherin Fc in promoting neuronal differentiation and neurite outgrowth of hESC-NSCs, when combined at a specific ratio. One receptor that we hypothesized to be involved in this synergistic effect was the fibroblast growth factor receptor (FGFR). We postulated FGFR was a likely candidate due to several studies demonstrating that L1 and N-cadherin mediated outgrowth of neuronal cells is dependent on FGFR activation^[9,10]. Kulahin et al identified two motifs within the third and fifth fibronectin type III repeats of L1, one of which binds to the acidic domain within FGFR^[11] and a motif within the fourth domain of N-cadherin that has been shown to interact with FGFR^[12]. In order to elucidate the role of

FGFR in the response of hESC-NSCs to the different N-cadherin presenting substrates, as well as the synergistic effect of L1 and N-cadherin in neuronal differentiation and neurite outgrowth of H9-NSCs, we used a FGFR inhibitor, PD173074, as this inhibitor has been shown to reduce neurite outgrowth mediated by N-cadherin and L1^[12]. Findings of studies outlined in Chapter 4 suggest that 1) FGFR signaling acts as a regulator of neuronal differentiation observed in H9-NSCs cultured on N-cadherin presenting substrates and 2) FGFR signaling plays less of a role or may not be solely responsible for synergistic effect between L1-Fc and N-cadherin-Fc. Additional studies need to be performed to better understand the involvement of FGFR signaling pathways involved in the response of H9-NSCs to N-cadherin-Fc and L1-Fc substrates. Small interfering RNA sequences (siRNA) are often used to knockdown gene expression and this technique would be useful in modifying H9-NSC FGFR gene expression to further understand how FGFR impacts neuronal differentiation of H9-NSCs. Additionally, to truly understand the mechanism of action of FGFR signaling, the use of pharmacological inhibitors to block PLC γ , P13K, and MAPK (MEK/ERK) signaling cascades would be necessary^[13,14]. Epidermal growth factor receptor (EGFR) signaling also activates PLC γ ^[15,16] signaling, similar to FGFR. Reports have demonstrated the involvement of EGF and EGFR in neuronal differentiation and neurite outgrowth^[17,18], and EGFR has been shown to interact with L1^[19,20]. Inhibition of EGFR function through the use of siRNA or pharmacological inhibitors would better elucidate the role of EGFR in neuronal differentiation and neurite outgrowth mediated by N-cad-/L1-Fc functionalized substrates.

5.2.2. Improvement in Neuronal Yield and Alternative Cell Sources for Cell Transplantation

The degree of neuronal differentiation was limited in the studies performed, with relatively low efficiency in neuronal differentiation and lack of differentiation of hESC-NSCs into different neuronal subtypes. This is in part due to relatively short culture periods. We used 7 days as an endpoint to investigate early on how L1 and N-cadherin substrates influenced the development of hESC-NSCs *in vitro*. Therefore, significantly longer culture periods are necessary for more robust differentiation, as demonstrated in other studies^[21]. Additionally, very few factors were present in our culture system. The differentiation medium used for culturing the cells only consisted of neuralbasal medium, B-27 supplement, and the neurotrophic factor, BDNF. We selected this simple formulation because soluble BDNF does not interrupt the trilineage potential of NSCs^[22], thereby enabling us to better discern how the L1-Fc and N-cadherin-Fc substrates influenced neural stem cell differentiation. Within the culture time period of our studies, there were no signs of subtype specific neuronal differentiation. Therefore, longer culture periods are necessary to properly characterize neuronal subtypes that may arise after growth of H9-NSCs on the various L1-Fc and N-cad-Fc substrates. Many groups have developed protocols for achieving high neuronal yields as well as protocols to direct differentiation into specific neuronal subtypes such as GABAergic^[23], dopaminergic^[24], and motor neurons^[25], using specific combinations of growth factors. Culturing H9-NSCs on L1 and/or N-cadherin functionalized scaffolds in combination with a cocktail of growth factors, small molecules, or morphogens would be better suited for directed, subtype specific differentiation NSCs.

Another interesting approach would be to combine the L1-Fc biofunctionalized scaffolds with hESC-NSCs that overexpress L1, possibly leading to a mature and functional bioactive scaffold/cell construct. Chen et al. found that L1-overexpressing mouse embryonic stem cells transplanted into the contused mouse spinal cord showed better survival and promoted regrowth of the corticospinal tract axons^[26]. Another study,

demonstrated the ability of Schwann cells, engineered to express L1 on the cell surface and in a soluble form, promoted early functional recovery and myelination in a mouse contusion spinal cord injury model^[27]. More recently, He et al transplanted neural stem cells that both expressed L1 on the cell surface and secreted a trimeric form of L1 and found these cells enhanced motor function, reduced the glial scar volume, prevented axonal degeneration, and improved myelination^[28]. All of these studies illustrate the benefit of having neural cells express L1 or the benefit of presenting a soluble form of L1 to the harsh environment of the injured spinal cord. Combining neural stem cells that secrete soluble L1 with scaffolds biofunctionalized with L1 and/or N-cadherin, might further improve survival of transplanted cells, as well as provide structural support, which could mediate better integration of transplanted cells at the injury site, as this has been demonstrated when primary neural cells were transplanted within scaffolds into the injured spinal cord^[29-31]. Conceivably cells engineered to overexpress of L1 or a trimeric form, at the cell surface and/or as a soluble factor, in combination with L1-biofunctionalized scaffolds could be another avenue to explore for cell transplantation therapy.

Current differentiation procedures for neuronal differentiation of human embryonic stem cells can be time-consuming. As a result, research efforts have focused on directly converting H9-hESCs and human induced pluripotent stem cells (iPSCs) into induced neurons (iNs) using a combination of defined transcription factors^[32]. Neuronal cells produced with this method expressed β -III-tubulin and MAP2 after 8 days and fired spontaneous action potentials after only 6 days. More recently a single factor has been shown to generate iNs in under two weeks, which formed pre- and post-synaptic connections and integrated into existing neuronal networks following transplantation into mouse brain^[33]. L1-/N-cadherin-Fc biofunctionalized fibrous scaffolds would be advantageous substrates for iNs *in vitro* studies for development and disease models and

for *in vivo* models as these substrates have the potential to promote synapse formation, provide physical support and a permissive substrate for neurite extensions, foster cell-cell contacts, and promote survival following transplantation. Differentiation procedures involving the combination transcription factors reprogramming to generate iNs and morphogens or growth factors would have to be put in place in order to generate the appropriate neuronal subtype. Research is currently underway in our laboratory to generate motor neurons using transcription factor-reprogramming combined with sonic hedgehog and retinoic acid.

5.2.3. Alternative Approach for Tethering L1-Fc and N-cadherin-Fc

The approach used to immobilize L1-Fc and N-cadherin-Fc involved the use of protein A. While this presentation scheme results in an orientation of both proteins that is physiologically relevant and improved bioactivity, protein A was merely adsorbed to the surfaces of the two-dimensional films and electrospun scaffolds. Over time, protein A could desorb from the surface resulting loss of the bioactive cues^[3]. Additionally, as protein A is the derivative of the bacteria *Staphylococcus aureus*, an adverse host response is possible^[34]. Using Fc binding peptides, shown to have an equivalent affinity for Fc as protein A^[35], or protein A mimetic peptides^[36] in place of protein A is one approach to circumventing adverse that might arise from using protein A. Although protein A peptide mimics could address unfavorable reactions in response to protein A, this does not address the issue of desorption over time. Thus, a more stable functionalization scheme would be useful.

Tethering L1 and N-cadherin to scaffolds via the biotin-streptavidin interaction would be an advantageous approach as the stable, biotin-streptavidin bond represents the strongest non-covalent bond and dissociation of the complex is very slow^[37,38], addressing issues regarding desorption of proteins over time. Streptavidin has four biotin binding sites

and the biotin-streptavidin complex is widely utilized for clinical diagnostics and cancer therapeutics^[38], demonstrating its translatability. In collaboration with the laboratory of Dr. Joachim Kohn, we have demonstrated the feasibility of tethering biotin-modified L1-Fc, via streptavidin, to the surface of polymers also modified with biotin. Following modification of L1-Fc with biotin, there was no loss in L1-Fc function and we observed an increase in the surface density of L1-Fc and enhanced neurite outgrowth of primary spinal cord neurons compared to conventional adsorption of L1-Fc. Another benefit afforded by this system is the ability to tether different beneficial peptides, proteins, and growth factors, allowing for the design of a bioactive scaffold that aims to account for the multitude of factors necessary to promote adhesion, appropriate neuronal differentiation and maturation, neurite outgrowth, and survival of neural stem cells both *in vitro* and *in vivo*. Further work is required to identify the combination of factors required to promote the desired phenotypic outcomes *in vitro* for use in *in vivo* injury models. In regards to L1 and N-cadherin, the work from this thesis provides new insights into the nature of configurations, concentrations, and combinations of these two cell adhesion molecules that are useful for promoting increased neuronal differentiation of H9-NSCs.

5.2.4. L1 and N-Cadherin-Derived Peptide Biofunctionalized Substrates for Neural Tissue Engineering

Protein mimetics offer several advantages over protein fragments. For example, peptide mimics can be designed such that modifications for covalent linkage do not interrupt with bioactivity, which is more likely with larger protein fragments. Additionally, the use of high quantities of peptides is more cost-effective than that of larger protein fragments. Moreover, biofunctionalizing biomaterials with specific, key active sequences could result in high local concentrations of protein-derived active sites, resulting in

enhanced cellular responses. Peptides derived from functional motifs within L1 and N-cadherin have been identified and investigated for their influence in neural cell behaviors such as neurite outgrowth, as well as adhesion. L1 peptides derived from specific regions within the third and fifth fibronectin III repeats were shown to promote neurite outgrowth of rat cerebellar neurons^[11]. Additionally, the L1 peptide used for studies detailed in Chapter 2 has been shown to possess neuritogenic properties^[39]. Motifs that mediate N-cadherin homophilic interactions were identified within the first extracellular domain of N-cadherin^[40,41], as well as regions within the fourth extracellular domain that facilitates N-cadherin/FGF receptor mediated neurite outgrowth^[12]. Future work could include the design of a system in which the various L1 and N-cadherin mimetics are incorporated onto the surface of electrospun scaffolds, and their ability in promoting adhesion, neuronal differentiation, and neurite outgrowth of hESCs could be evaluated. Different approaches could be used to tether the peptides to the surface such as covalently linking the peptides to the surface of the material or using the biotin/streptavidin polymeric system to immobilize the peptides. In either case, careful attention would need to be given to peptide modifications when designing the coupling scheme for linking the sequence to the scaffold surface to ensure proper orientation of the peptide, for maximal bioactivity.

5.2.5. Transplantation of H9-NSCs within L1-/N-cadherin-Fc Functionalized Scaffolds for *in vivo* Models

The next step would be to investigate how well biomaterials, functionalized with L1, N-cadherin, or a combination of the two, using low N-cadherin-Fc and L1-Fc, promote survival and integration of H9-derived neurons into a spinal cord injury model (SCI). Several studies have utilized hemi-section or complete transection SCI models due to the ease of scaffold transplantation and the ability to discern how well the transplanted device

promotes regeneration of damaged tissue^[42-45]. However, the contusion model represents a more clinically relevant model, as this type of injury most closely mimics the crush and fracture injury that occurs in humans^[46,47]. In collaboration with researchers from the Keck Center for Collaborative Neuroscience at Rutgers University, we envision that the electrospun scaffolds, biofunctionalized with N-cadherin-Fc and/or L1-Fc, with or without hESC-NSCs would be introduced into a contusion model. In order to transplant the electrospun scaffolds, a myelotomy would be performed 10 days after the initial injury and the scaffolds would be inserted into the empty area using a procedure previously described, where electrospun scaffolds were biofunctionalized with GDNF and primary cortical neural stem cells were seeded into the scaffolds prior to transplanting into a contusion SCI model^[48]. Initial studies could aim to assess histological outcomes such as survival and integration of H9-NSCs and regeneration of host tissue within the transplanted scaffold, while later studies could aim to evaluate recovery of motor functions.

5.3. References

1. Cooke MJ, K Vulic and MS Shoichet. (2010). Design of biomaterials to enhance stem cell survival when transplanted into the damaged central nervous system. *Soft Matter* 6:4988-4998.
2. McCreedy DA and SE Sakiyama-Elbert. (2012). Combination therapies in the CNS: engineering the environment. *Neurosci Lett* 519:115-21.
3. Kim H, MJ Cooke and MS Shoichet. (2012). Creating permissive microenvironments for stem cell transplantation into the central nervous system. *Trends in Biotechnology* 30:55-63.
4. Bixby JL and R Zhang. (1990). Purified N-cadherin is a potent substrate for the rapid induction of neurite outgrowth. *The Journal of cell biology* 110:1253-60.
5. Haque A, XS Yue, A Motazedian, Y Tagawa and T Akaike. (2012). Characterization and neural differentiation of mouse embryonic and induced pluripotent stem cells on cadherin-based substrata. *Biomaterials* 33:5094-106.
6. Yue XS, Y Murakami, T Tamai, M Nagaoka, CS Cho, Y Ito and T Akaike. (2010). A fusion protein N-cadherin-Fc as an artificial extracellular matrix surface for maintenance of stem cell features. *Biomaterials* 31:5287-96.

7. Collazos-Castro JE, GR Hernandez-Labrado, JL Polo and C Garcia-Rama. (2013). N-Cadherin- and L1-functionalised conducting polymers for synergistic stimulation and guidance of neural cell growth. *Biomaterials* 34:3603-17.
8. Shi P, K Shen and LC Kam. (2007). Local presentation of L1 and N-cadherin in multicomponent, microscale patterns differentially direct neuron function in vitro. *Dev Neurobiol* 67:1765-76.
9. Doherty P and FS Walsh. (1996). CAM-FGF Receptor Interactions: A Model for Axonal Growth. *Molecular and cellular neurosciences* 8:99-111.
10. Williams EJ, J Furness, FS Walsh and P Doherty. (1994). Activation of the FGF receptor underlies neurite outgrowth stimulated by L1, N-CAM, and N-cadherin. *Neuron* 13:583-94.
11. Kulahin N, S Li, V Kiselyov, E Bock and V Berezin. (2009). Identification of neural cell adhesion molecule L1-derived neuritogenic ligands of the fibroblast growth factor receptor. *J Neurosci Res* 87:1806-12.
12. Williams EJ, G Williams, FV Howell, SD Skaper, FS Walsh and P Doherty. (2001). Identification of an N-cadherin motif that can interact with the fibroblast growth factor receptor and is required for axonal growth. *J Biol Chem* 276:43879-86.
13. Kirschbaum K, M Kriebel, EU Kranz, O Potz and H Volkmer. (2009). Analysis of non-canonical fibroblast growth factor receptor 1 (FGFR1) interaction reveals regulatory and activating domains of neurofascin. *The Journal of biological chemistry* 284:28533-42.
14. Webber CA, YY Chen, CL Hehr, J Johnston and S McFarlane. (2005). Multiple signaling pathways regulate FGF-2-induced retinal ganglion cell neurite extension and growth cone guidance. *Molecular and cellular neurosciences* 30:37-47.
15. Meisenhelder J, PG Suh, SG Rhee and T Hunter. (1989). Phospholipase C-gamma is a substrate for the PDGF and EGF receptor protein-tyrosine kinases in vivo and in vitro. *Cell* 57:1109-22.
16. Wahl MI, TO Daniel and G Carpenter. (1988). Antiphosphotyrosine recovery of phospholipase C activity after EGF treatment of A-431 cells. *Science* 241:968-70.
17. Traverse S, K Seedorf, H Paterson, CJ Marshall, P Cohen and A Ullrich. (1994). EGF triggers neuronal differentiation of PC12 cells that overexpress the EGF receptor. *Current biology : CB* 4:694-701.
18. Yamada M, T Ikeuchi and H Hatanaka. (1997). The neurotrophic action and signalling of epidermal growth factor. *Progress in neurobiology* 51:19-37.
19. Islam R, LV Kristiansen, S Romani, L Garcia-Alonso and M Hortsch. (2004). Activation of EGF receptor kinase by L1-mediated homophilic cell interactions. *Molecular biology of the cell* 15:2003-12.
20. Yoon H, JK Min, DG Lee, DG Kim, SS Koh and HJ Hong. (2012). L1 cell adhesion molecule and epidermal growth factor receptor activation confer cisplatin resistance in intrahepatic cholangiocarcinoma cells. *Cancer letters* 316:70-6.
21. Yuan SH, J Martin, J Elia, J Flippin, RI Paramban, MP Hefferan, JG Vidal, Y Mu, RL Killian, MA Israel, N Emre, S Marsala, M Marsala, FH Gage, LS Goldstein and CT Carson. (2011). Cell-surface marker signatures for the isolation of neural stem cells, glia and neurons derived from human pluripotent stem cells. *PloS one* 6:e17540.
22. Horne MK, DR Nisbet, JS Forsythe and CL Parish. (2010). Three-dimensional nanofibrous scaffolds incorporating immobilized BDNF promote proliferation and differentiation of cortical neural stem cells. *Stem Cells Dev* 19:843-52.
23. Carri AD, M Onorati, MJ Lelos, V Castiglioni, A Faedo, R Menon, S Camnasio, R Vuono, P Spaiardi, F Talpo, M Toselli, G Martino, RA Barker, SB Dunnett, G Biella and E

- Cattaneo. (2013). Developmentally coordinated extrinsic signals drive human pluripotent stem cell differentiation toward authentic DARPP-32+ medium-sized spiny neurons. *Development* 140:301-12.
24. Kriks S, JW Shim, J Piao, YM Ganat, DR Wakeman, Z Xie, L Carrillo-Reid, G Auyeung, C Antonacci, A Buch, L Yang, MF Beal, DJ Surmeier, JH Kordower, V Tabar and L Studer. (2011). Dopamine neurons derived from human ES cells efficiently engraft in animal models of Parkinson's disease. *Nature* 480:547-51.
 25. Nizzardo M, C Simone, M Falcone, F Locatelli, G Riboldi, GP Comi and S Corti. (2010). Human motor neuron generation from embryonic stem cells and induced pluripotent stem cells. *Cellular and molecular life sciences : CMLS* 67:3837-47.
 26. Chen J, C Bernreuther, M Dihne and M Schachner. (2005). Cell adhesion molecule L1-transfected embryonic stem cells with enhanced survival support regrowth of corticospinal tract axons in mice after spinal cord injury. *J. Neurotrauma* 22:896-906.
 27. Lavdas AA, J Chen, F Papastefanaki, S Chen, M Schachner, R Matsas and D Thomaidou. (2010). Schwann cells engineered to express the cell adhesion molecule L1 accelerate myelination and motor recovery after spinal cord injury. *Exp Neurol* 221:206-16.
 28. He X, M Knepper, C Ding, J Li, S Castro, M Siddiqui and M Schachner. (2012). Promotion of spinal cord regeneration by neural stem cell-secreted trimerized cell adhesion molecule L1. *PloS one* 7:e46223.
 29. Teng YD, EB Lavik, X Qu, KI Park, J Ourednik, D Zurakowski, R Langer and EY Snyder. (2002). Functional recovery following traumatic spinal cord injury mediated by a unique polymer scaffold seeded with neural stem cells. *Proceedings of the National Academy of Sciences of the United States of America* 99:3024-9.
 30. Hurtado A, LD Moon, V Maquet, B Blits, R Jerome and M Oudega. (2006). Poly (D,L-lactic acid) macroporous guidance scaffolds seeded with Schwann cells genetically modified to secrete a bi-functional neurotrophin implanted in the completely transected adult rat thoracic spinal cord. *Biomaterials* 27:430-42.
 31. Rauch MF, SR Hynes, J Bertram, A Redmond, R Robinson, C Williams, H Xu, JA Madri and EB Lavik. (2009). Engineering angiogenesis following spinal cord injury: a coculture of neural progenitor and endothelial cells in a degradable polymer implant leads to an increase in vessel density and formation of the blood-spinal cord barrier. *The European journal of neuroscience* 29:132-45.
 32. Pang ZP, N Yang, T Vierbuchen, A Ostermeier, DR Fuentes, TQ Yang, A Citri, V Sebastiano, S Marro, TC Sudhof and M Wernig. (2011). Induction of human neuronal cells by defined transcription factors. *Nature* 476:220-3.
 33. Zhang Y, C Pak, Y Han, H Ahlenius, Z Zhang, S Chanda, S Marro, C Patzke, C Acuna, J Covy, W Xu, N Yang, T Danko, L Chen, M Wernig and TC Sudhof. (2013). Rapid single-step induction of functional neurons from human pluripotent stem cells. *Neuron* 78:785-98.
 34. Atkins KL, JD Burman, ES Chamberlain, JE Cooper, B Poutrel, S Bagby, AT Jenkins, EJ Feil and JM van den Elsen. (2008). *S. aureus* IgG-binding proteins SpA and Sbi: host specificity and mechanisms of immune complex formation. *Molecular immunology* 45:1600-11.
 35. Jeong YJ, HJ Kang, KH Bae, MG Kim and SJ Chung. (2010). Efficient selection of IgG Fc domain-binding peptides fused to fluorescent protein using *E. coli* expression system and dot-blotting assay. *Peptides* 31:202-6.

36. Li R, V Dowd, DJ Stewart, SJ Burton and CR Lowe. (1998). Design, synthesis, and application of a protein A mimetic. *Nature biotechnology* 16:190-5.
37. Chivers CE, AL Koner, ED Lowe and M Howarth. (2011). How the biotin-streptavidin interaction was made even stronger: investigation via crystallography and a chimaeric tetramer. *The Biochemical journal* 435:55-63.
38. Hamblett KJ, BB Kegley, DK Hamlin, MK Chyan, DE Hyre, OW Press, DS Wilbur and PS Stayton. (2002). A streptavidin-biotin binding system that minimizes blocking by endogenous biotin. *Bioconjugate chemistry* 13:588-98.
39. Appel F, J Holm, JF Conscience, F von Bohlen und Halbach, A Faissner, P James and M Schachner. (1995). Identification of the border between fibronectin type III homologous repeats 2 and 3 of the neural cell adhesion molecule L1 as a neurite outgrowth promoting and signal transducing domain. *J Neurobiol* 28:297-312.
40. Blaschuk OW, R Sullivan, S David and Y Pouliot. (1990). Identification of a Cadherin Cell-Adhesion Recognition Sequence. *Developmental Biology* 139:227-229.
41. Williams E, G Williams, BJ Gour, OW Blaschuk and P Doherty. (2000). A novel family of cyclic peptide antagonists suggests that N-cadherin specificity is determined by amino acids that flank the HAV motif. *Journal of Biological Chemistry* 275:4007-4012.
42. Zamani F, MA Tehran, M Latifi, MA Shokrgozar and A Zaminy. (2013). Promotion of spinal cord axon regeneration by 3D nanofibrous core-sheath scaffolds. *Journal of biomedical materials research. Part A*.
43. Hatami M, NZ Mehrjardi, S Kiani, K Hemmesi, H Azizi, A Shahverdi and H Baharvand. (2009). Human embryonic stem cell-derived neural precursor transplants in collagen scaffolds promote recovery in injured rat spinal cord. *Cytherapy* 11:618-30.
44. Olson HE, GE Rooney, L Gross, JJ Nesbitt, KE Galvin, A Knight, B Chen, MJ Yaszemski and AJ Windebank. (2009). Neural stem cell- and Schwann cell-loaded biodegradable polymer scaffolds support axonal regeneration in the transected spinal cord. *Tissue engineering. Part A* 15:1797-805.
45. Gao M, P Lu, B Bednark, D Lynam, JM Conner, J Sakamoto and MH Tuszynski. (2013). Templated agarose scaffolds for the support of motor axon regeneration into sites of complete spinal cord transection. *Biomaterials* 34:1529-36.
46. Kalderon N, M Muruganandham, JA Koutcher and M Potuzak. (2007). Therapeutic strategy for acute spinal cord contusion injury: cell elimination combined with microsurgical intervention. *PloS one* 2:e565.
47. Stokes BT and LB Jakeman. (2002). Experimental modelling of human spinal cord injury: a model that crosses the species barrier and mimics the spectrum of human cytopathology. *Spinal Cord* 40:101-9.
48. Wang TY, JS Forsythe, DR Nisbet and CL Parish. (2012). Promoting engraftment of transplanted neural stem cells/progenitors using biofunctionalised electrospun scaffolds. *Biomaterials* 33:9188-97.